Effect of size and charge on Hückel and Baird aromaticity in [*N*]annulenes

Louis Van Nyvel[a], Mercedes Alonso[a,*] and Miquel Solà[b,*]

[a] Department of General Chemistry (ALGC), Vrije Universiteit Brussel (VUB), Pleinlaan 2, 1050 Brussels, Belgium. e-mail: mercedes.alonso.giner@vub.be

[b] Institut de Química Computacional i Catàlisi (IQCC) and Departament de Química, Universitat de Girona, C/ Maria Aurèlia Capmany, 69, 17003-Girona, Catalonia, Spain. e-mail: miquel.sola@udg.edu

TABLE OF CONTENTS

Aromaticity Indices

Structural indices

The harmonic oscillator model of aromaticity (HOMA) was introduced by Kruszewski and Krygowski.[1] In their Equation (1), they utilise a variety of different parameters. One is the empirical normalisation constant α_j, which ensures that HOMA values fall between -1 and 1. An α_j value of 257.7 is typical for a C-C bond.[2] In addition, an optimal bond distance r_{opt} is included. It represents the distance for which a minimum amount of energy is needed to transform a bond into either a single or double bond.[4] However, the use of reference values precludes the applicability of this structural index to all types of bonds. Finally, it is necessary to consider the number of bonds n within the ring, as well as the distance $r_{A_i,A_{i+1}}$ between two consecutive atoms, A_i and A_{i+1}.[2,3] In essence, HOMA will ultimately demonstrate the difference between this bond distance and the previously cited reference values.[4] In general, values of approximately 1, 0, and -1 are indicative of aromatic, nonaromatic, and antiaromatic structures, respectively.[2]

$$\text{HOMA} = 1 - \frac{1}{n}\sum_{i=1}^{n} \alpha_j \left(r_{opt} - r_{A_i,A_{i+1}}\right)^2 \tag{1}$$

The bond-length alternation (BLA) is an alternative structural index. Using Equation 2, the average bond length alternation between two consecutive bonds can be determined.[5,6] Additionally, the total number of bonds n within the ring must be considered. The version of BLA used in this work is the revised version, which has been optimised for use with rings that possess an odd number of atoms.[5,7] The presence of large BLA values is indicative of antiaromatic structures, whereas values close to zero are suggestive of aromatic and potential nonaromatic structures.[6]

$$\text{BLA} = \frac{1}{2n}\sum_{i=1}^{n} \left| r_{A_i,A_{i+1}} - r_{A_{i+1},A_{i+2}} \right| \tag{2}$$

Electronic indices

Most of the electronic indices employ the electron delocalisation index (DI), $\delta(A,B)$, to predict aromaticity. This index was originally proposed by Bader *et al.*,[8] with subsequent refinements made by Poater and colleagues.[9] The DI can be used to determine the bond order of a given bond and represents the number of electrons shared by two atoms.[2,4] Typically, an aromatic bond has a DI value around 1.5, with single, double, and triple bonds exhibiting values around 1, 2, and 3 respectively.

$$\delta(A,B) = -2\int_{\Omega_A}\int_{\Omega_B} \rho_{XC}(r_1,r_2)\, dr_1\, dr_2 = -2cov(N_A,N_B) \tag{3}$$

In order to ascertain $\delta(A,B)$, the double integral of the negative exchange-correlation density $\rho_{XC}(r_1,r_2)$ over the atomic basins Ω_A and Ω_B must be determined (Equation 3).[10] The exchange-correlation density is defined as the difference between the uncorrelated ($\rho(\mathbf{r}_1)\rho(\mathbf{r}_2)$) and correlated ($\rho(\mathbf{r}_1,\mathbf{r}_2)$) parts of the pair density.[10] The basins are obtained by partitioning the molecule into different atomic basins based on the Quantum Theory of Atoms-in-Molecules (QTAIM) approach.[10,11]

Matito and colleagues devised the aromatic fluctuation index (FLU), which is the electronic equivalent of HOMA.[2] Instead of bond distances, the electron delocalisation $\delta(A_i,A_{i-1})$ and valence $\delta(A_i)$ of each atom in the ring is employed.[2] Once again, a reference value ($\delta_{ref}(A_i,A_{i-1})$) is used, which limits its applicability. In the case of a C-C bond, benzene is taken as the reference.[6] Furthermore, the α term was incorporated into Equation 4 to guarantee that the initial term is always greater than 1.[2] To enforce this, the valence, which corresponds to the number of valence electrons of the atom, of two consecutive atoms is considered, as illustrated in Equation 5.[2] Aromatic structures exhibit FLU values close to zero, whereas large values indicate non- and antiaromatic structures.[2,4]

$$\text{FLU} = \frac{1}{n}\sum_{i=1}^{n}\left[\left(\frac{\delta(A_i)}{\delta(A_{i-1})}\right)^{\alpha}\left(\frac{\delta(A_i,A_{i-1}) - \delta_{ref}(A_i,A_{i-1})}{\delta_{ref}(A_i,A_{i-1})}\right)\right]^2 \tag{4}$$

$$\alpha = \begin{cases} 1, & \delta(A_{i-1}) \leq \delta(A_i) \\ -1, & \delta(A_i) < \delta(A_{i-1}) \end{cases} \tag{5}$$

The bond-order alternation (BOA) is the electronic equivalent of BLA.[4,6] Both indices employ similar equations, with an average calculated in both cases. However, in this instance, the delocalisation index of successive bonds is used instead of bond distances.[4,6,7] Once again, the revised version, optimised for use with rings containing an odd number of atoms, was selected.[5] BOA's predictions are analogous to those of BLA.

$$\mathrm{BOA} = \frac{1}{2n}\sum_{i=1}^{n}\left|\delta(A_i,A_{i+1}) - \delta(A_{i+1},A_{i+2})\right| \tag{6}$$

One of the multicenter indices, designed by Giambiagi and colleagues, is I_{ring},[12] which provides information about electrons that are shared between multiple centers/atoms.[10] In Equation 7, the atomic overlap matrix of molecular orbitals i and j $(S_{ij}(A) = \int_A dr\phi_i^*(r)\phi_j(r))$ is utilised to predict the aromaticity.[6,10,13] Notably, the sequence of atoms is crucial for I_{ring}, as the orbitals must overlap with two neighbouring atoms to create a circular pattern reminiscent of cyclic delocalisation.[13]

$$I_{ring} = 2^N \sum_{i_1 i_2 \ldots i_n}^{occ} S_{i_1 i_2}(A_1) S_{i_2 i_3}(A_2) \ldots S_{i_n i_1}(A_n) \tag{7}$$

The multicenter index (MCI) eliminates the constraint present in I_{ring} and encompasses all possible n! permutations $P(A)$ of the atoms in the ring.[6,10,13,14] This approach is therefore not limited to the cyclic delocalisation but also incorporates cross-ring delocalisation, which may have a significant contribution to the aromaticity in some species otherwise invisible to I_{ring}.[4,6,13] Both I_{ring} and MCI employ the same criteria for predicting the type of aromaticity. Large positive and negative values corresponding to aromatic and antiaromatic rings, respectively, while results around zero indicate nonaromatic ones. Importantly, both criteria should be used on ring structures possessing between 3 to 16 atoms.[13]

$$\mathrm{MCI} = \frac{1}{2N}\sum_{P(A)} I_{ring}(A) \tag{8}$$

The examination of multicenter delocalisation in large rings (n > 10) is not possible with I_{ring} and MCI due to the presence of a significant numerical error.[13] However, Matito identified a solution by employing the same theoretical framework as the *para*-delocalisation index, namely that the delocalisation of *para*-localised atoms is greater than those of *meta*-localised ones.[13] The proposed index, AV1245, represents the average delocalisation between four multicenters and provides information about the ease with which electrons can move through the conjugated structure, or in other words, are shared between bonds.[6,13] However, the implementation of an average masks outliers, both large and small, and thus can obscure important information about the overall aromaticity of the structure.[6] By utilising the absolute value of the AV1245 segment with the lowest value, named AV_{min}, it is possible to identify the segment that impede free movement of electrons through the molecule.[5,6] The large outcomes of AV1245 and AV_{min} are indicative of aromatic structures. For non- and antiaromatic rings, the values are approximately zero. However, it is important to note that the values of both indices will decrease as the size of the structure increases.[6]

Szczepanik and colleagues have developed an electronic index that enables the visualisation of electron delocalisation at a global or local level.[15,16] Of the various electron density of delocalised bonds (EDDB) functions, the $EDDB_H(r)$ was selected since it does not consider the hydrogen atoms present in the system, yet still provides a comprehensive overview of the global aromaticity.[16]

For a single-determinantal wavefunction, the $EDDB_H(r)$ function can be obtained by utilising Equations 9 and 10.[16] In the former equation, $\chi_\nu(r)$ represents the natural atomic orbitals (NAO), while D^{Ω_H} is the density matrix whose trace represents a measurement of the global aromaticity, given that it contains the population of delocalised electrons throughout the system.[16]

$$EDDB_H(r) = \sum_{\mu\nu} \chi_\mu^\dagger(r) D_{\mu,\nu}^{\Omega_H} \chi_\nu(r) \tag{9}$$

The components of the D^{Ω_H} matrix are comprised of several matrices (Equation 10). The P^σ matrix contains the σ spin-resolved charge and bond-order (CBO), while the $C_{a,b}^{\sigma}$ matrix is responsible for the linear coefficients of the appropriately orthogonalised σ spin-resolved two-center bond-order orbitals (2cBO) of the chemical bond X_a-X_b after applying a diagonalisation of the off-diagonal block of the P^σ matrix.[16] The diagonal of $\lambda_{a,b}^{\sigma}$ contains the eigenvalues of the 2cBO, which can be interpreted as the occupation numbers of the orbitals.[16] The $\varepsilon_{a,b}^{\Omega_H}$ is also a diagonal matrix consisting of the σ-spin bond-conjugation factors.[16] In the case of a conjugated bond, at least one element of the diagonal will be close to 1, whereas in the case of a localised bond, the majority of elements will be close to 0.[16] The final matrix is the Ω_H, which encompasses all possible atomic pairs ($n(n-1)/2$) within an n-atomic system, irrespective of their bonding status.[16]

$$D^{\Omega_H} = 2 \sum_{\sigma=\alpha,\beta} P^{\sigma} \left[\sum_{a,b}^{\Omega_H} C_{a,b}^{\sigma} \varepsilon_{a,b}^{\Omega_{H'}\sigma} \left(\lambda_{a,b}^{\sigma}\right)^2 C_{a,b}^{\sigma\,\dagger} \right] P^{\sigma} \quad (10)$$

Furthermore, it is possible to decompose the $EDDB_H(r)$ function into the contributions of the different symmetry components (σ, π, etc.).[16] By diagonalising the density matrix from Equation 10, the occupation numbers of the natural orbitals for bond delocalisation (NOBD) eigenfunctions can be obtained.[16] By using these occupation numbers, for example, the percentage of π-aromaticity can be determined, providing information on where the electrons are delocalised.[16]

Magnetic indices

The magnetic indices were designed to investigate the response of a molecule to the presence of an external magnetic field (B_{ext}) perpendicular to the molecular plane.[17] The application of such a magnetic field results in the π-electrons within the ring moving in a circular motion, thereby generating a diatropic ring current (J_d) outside the ring moving clockwise, and a paratropic (J_p) one inside moving counter clockwise, at all times.[18] These currents generate an induced magnetic field (B_{ind}), which is opposite to the external magnetic field in the case of the diatropic current while the paratropic current strengthens the external field.[18]

The nucleus independent chemical shift (NICS) is a method that establishes the aromaticity of a ring by capturing the magnetic shielding of a ghost atom (Bq), since this is influenced by the induced magnetic field.[19-21] The choice of this type of atom is based on its status as an innocent observer, as it lacks a nucleus that could affect the measurement.[17,21] Which would be the case when lithium or helium was selected.[17,21] within the NICS method, different variations exist depending on the position of the ghost atom and the tensor components considered.[20] In NICS(0), the Bq atom is placed in the center of the ring.[20] However, this position is susceptible to unnegligible σ-contributions.[20] In order to address this issue, the Bq atom was relocated 1Å above the center of the ring (NICS(1)).[20] A further approach to study only the π-contributions is to combine the gauge-independent atomic orbitals (GIAO) method with the out-of-plane tensor ($NICS(1)_{zz}$).[20,22] Finally, after performing an NMR calculation, the negative of the magnetic shielding of the ghost atom is taken to ascertain the aromaticity.[18,20,23] Typically, large positive and negative values of NICS can be found for aromatic and antiaromatic rings, respectively.

The gauge including magnetically induced current (GIMIC) method, which determines the magnetically induced current density by multiplying the current susceptibility and the strength of the external magnetic field,[18] is another magnetic index. As with the NICS method, the GIAO approach is also employed. By applying this method, the current density is made independent of the magnetic field, and the basis set conversion can be improved.[18,24] The aromaticity of a molecule is established by calculating the strength of the current density using a numerical integration.[18] This strength is comprised of two contributions: a diatropic (+) and a paratropic (-) one.[18] The sign of the sum of these contributions allows the dominant ring current to be identified and linked to the aromaticity. Aromatic systems possess a dominant diatropic ring current, while antiaromatic compounds a paratropic ring current.[18] It is important to note that nonaromatic molecules also possess both diatropic and paratropic contributions, but these cancel each other out when summed.[18]

Reactivity index

The relative hardness ($\Delta\eta$) is obtained by taking the difference between the lowest unoccupied molecular orbital (LUMO) and highest occupied molecular orbital (HOMO) orbital energies (ε) of the indene (**A**) and isoindene (**C**) structures (Equation 11) from the ISE_{II} method (Figure 1).[25]

$$\Delta\eta = \eta_A - \eta_C = \left(\varepsilon_{LUMO_A} - \varepsilon_{HOMO_A}\right) - \left(\varepsilon_{LUMO_C} - \varepsilon_{HOMO_C}\right) \quad (11)$$

De Proft and Geerlings have previously demonstrated that determining $\Delta\eta$ by utilising the methyl-methylene structures, derived from the ISE_I method, is an effective way of acquiring the aromaticity.[25] In their paper, they report that, in accordance with the maximum hardness principle, the methyl derivative is expected to be harder than the methylene, which should also indicate aromatic structures.[25] Applying the same reasoning to the ISE_{II} isomers, we expect the indene to be harder than the isoindene isomer when indicating the presence of an aromatic macrocycle, and vice versa.

Annulene structures

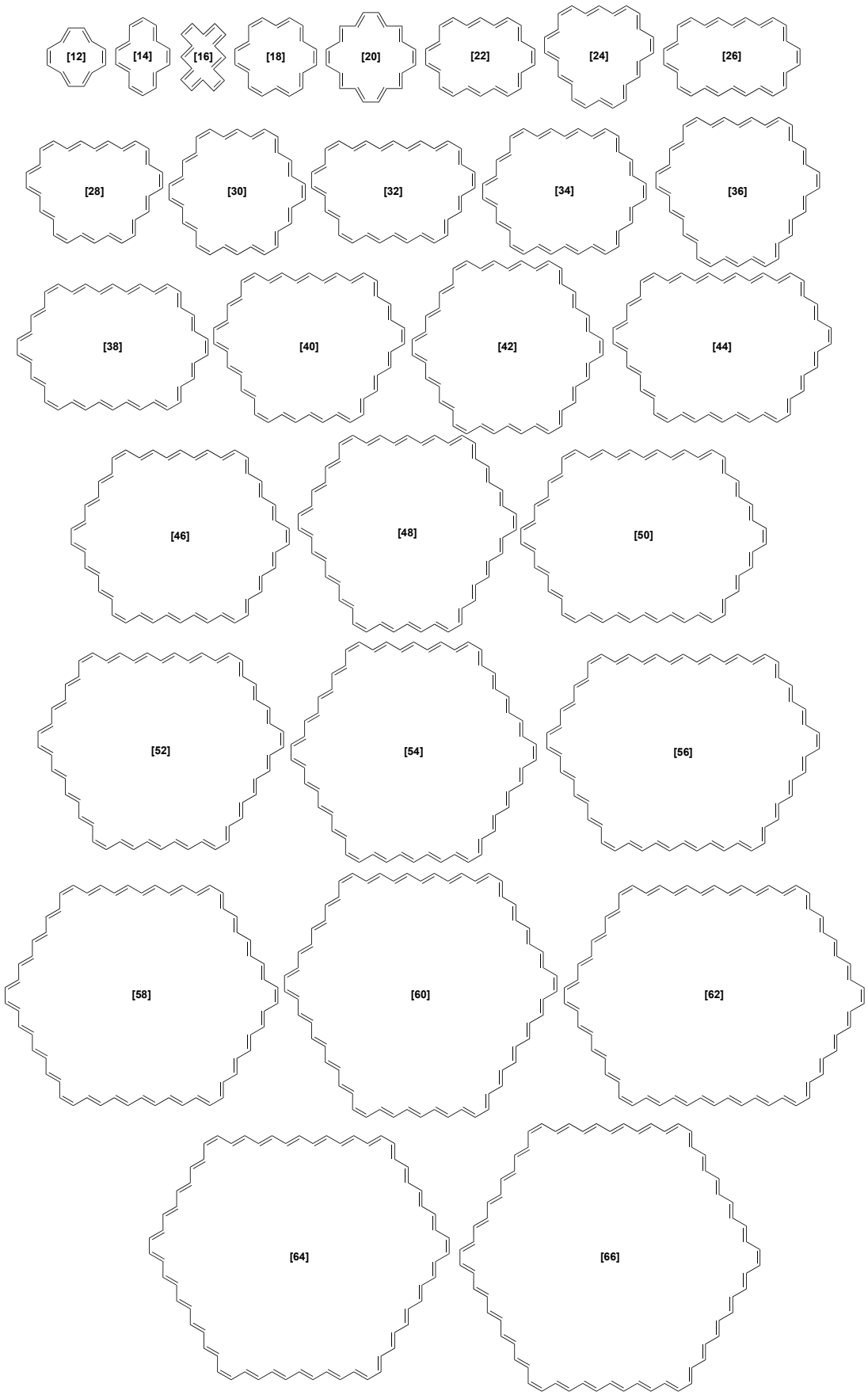

Figure S1: The test bed for the examination of the Hückel and Baird rules in [4*n*] and [4*n*+2] annulenes (*N* = 12-66, even).

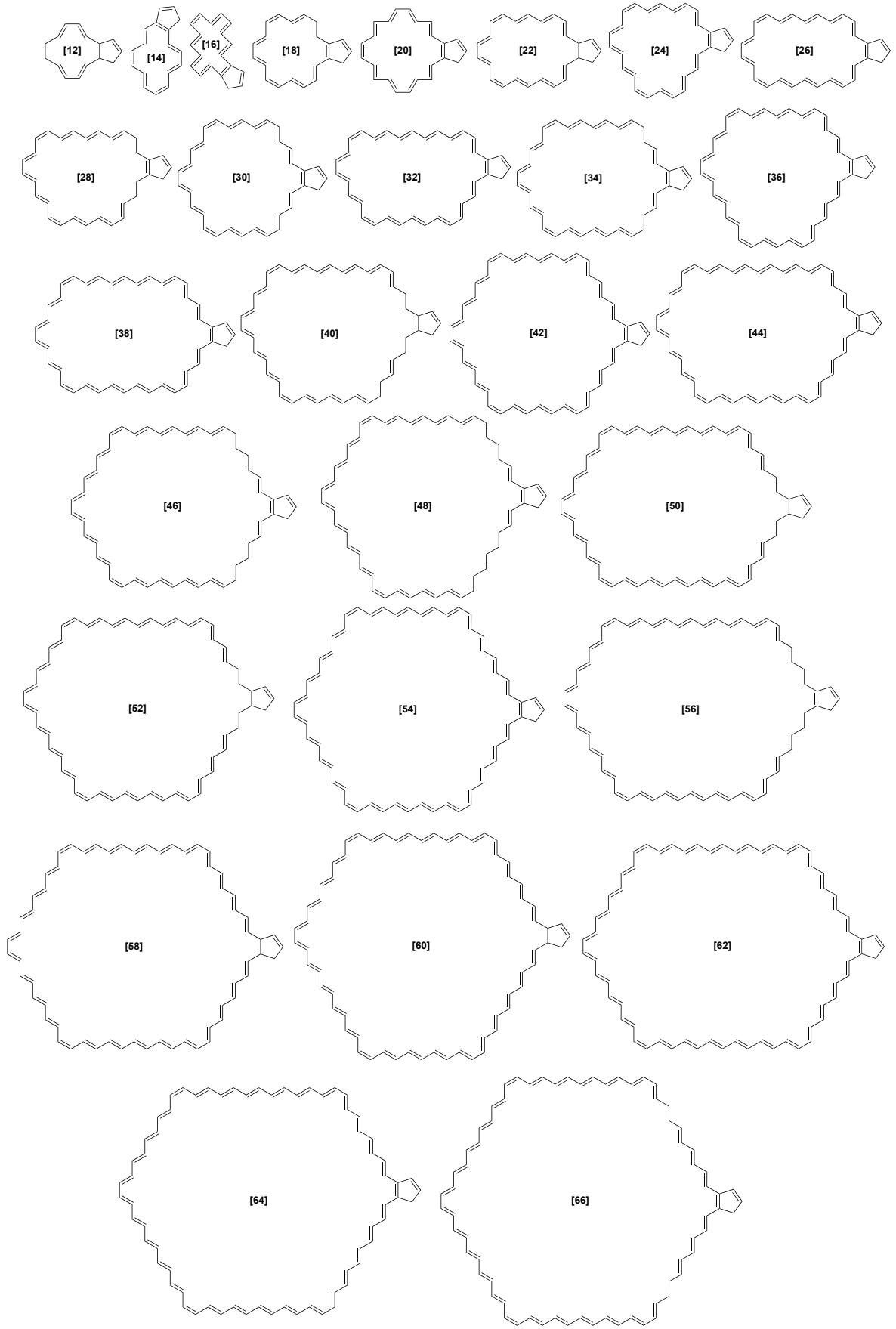

Figure S2: The geometries of the indene isomers **A** of the ISE_{II} method to obtain the ASE results.

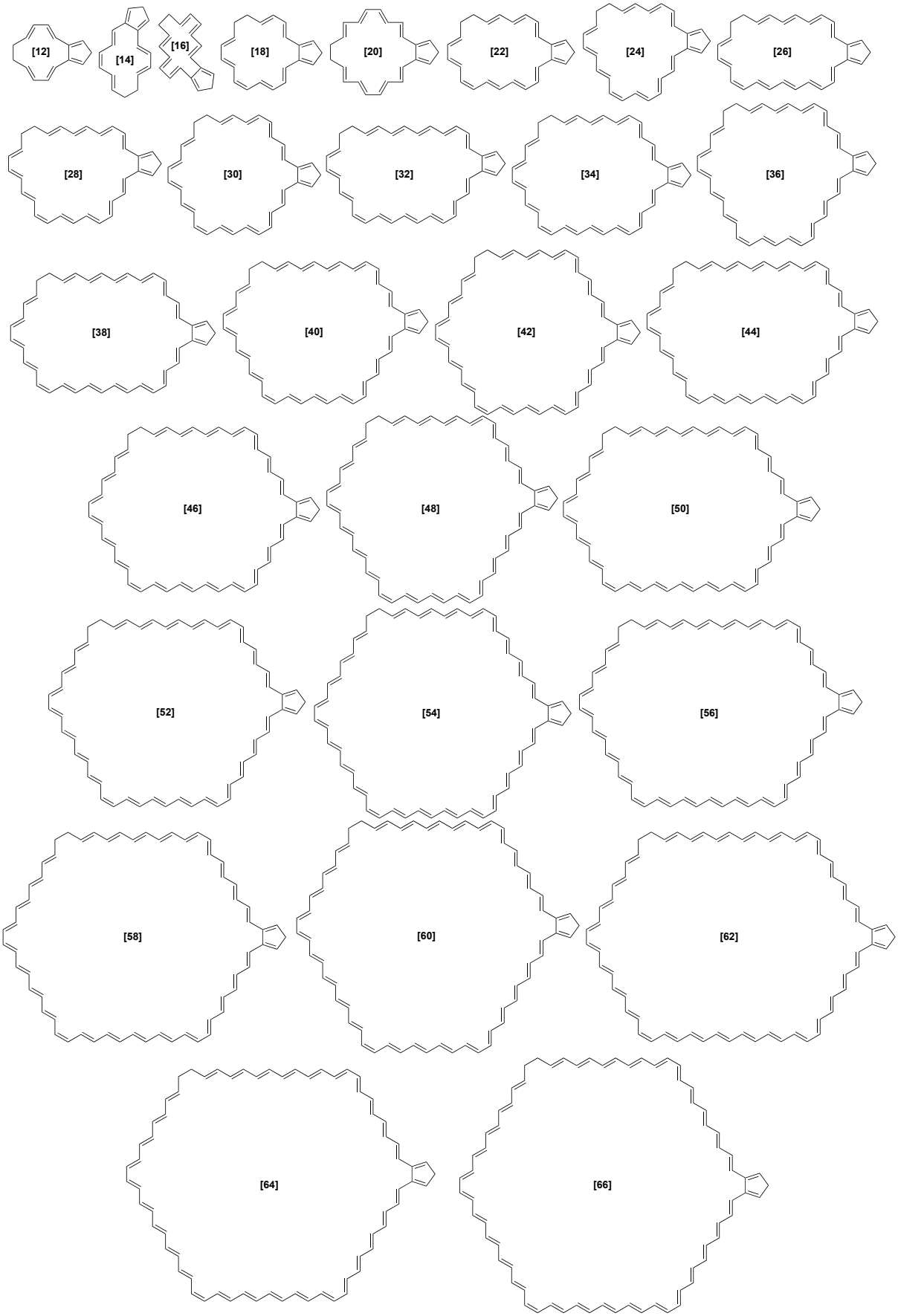

Figure S3: The geometries of the dihydro isoindene derivatives **B** in the ISE_{II} method needed to implement the *anti-syn* corrections for the evaluation of the ASE.

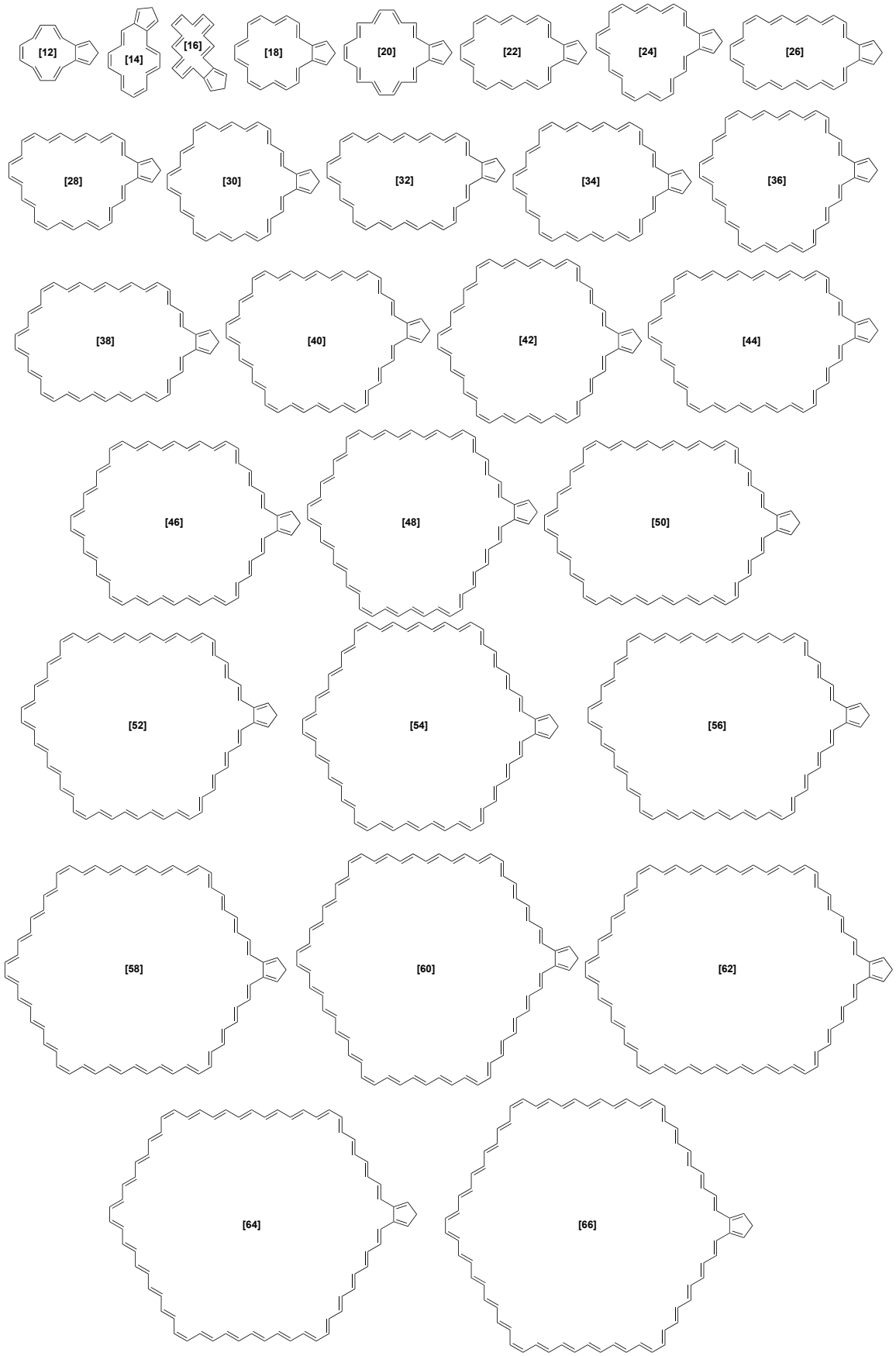

Figure S4: The geometries of the isoindene isomers **C** of the ISE_{II} method to obtain the ASE results.

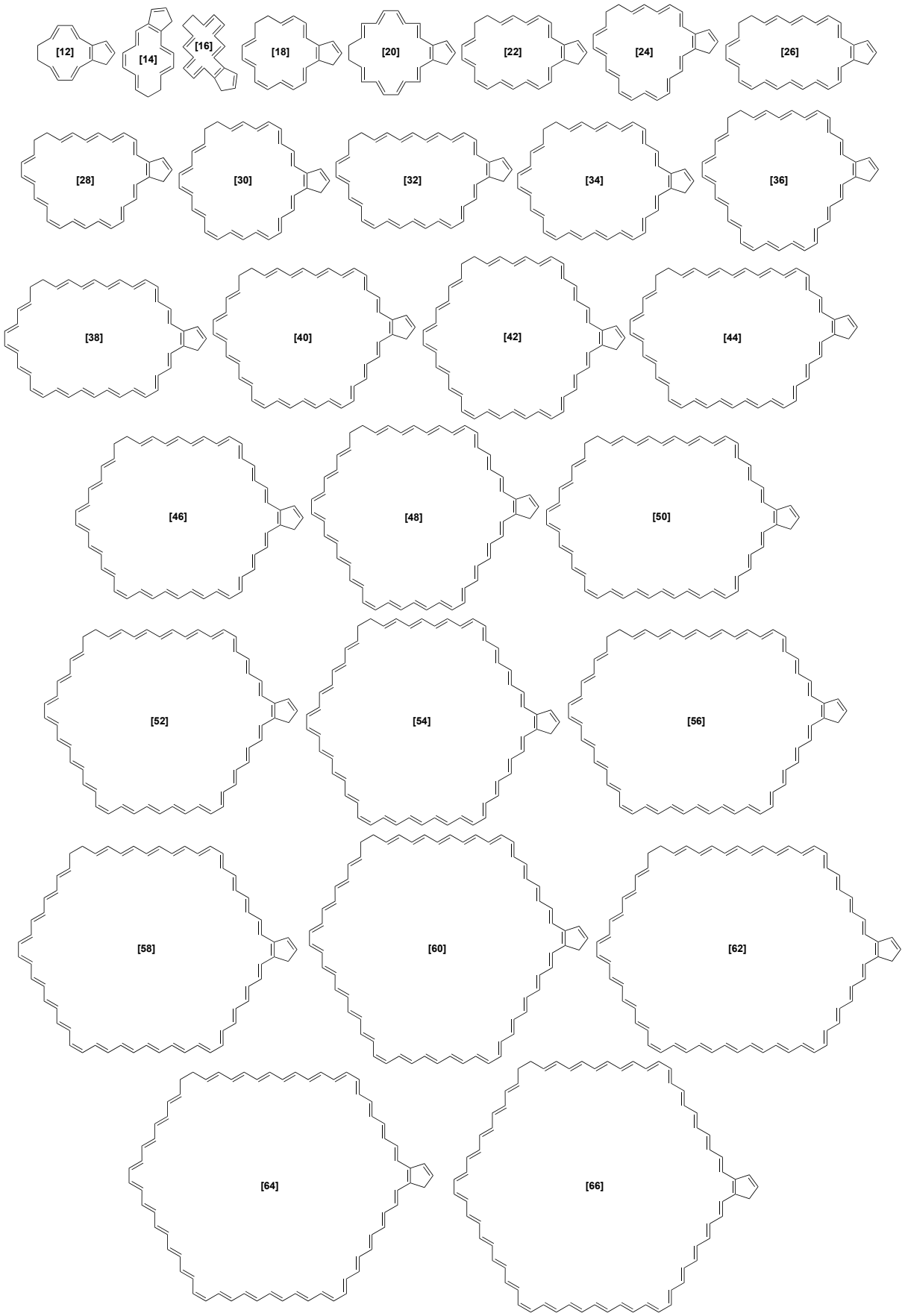

Figure S5: The geometries of the dihydro indene derivatives **D** in the ISE_{II} method needed to implement the *anti-syn* corrections for the evaluation of the ASE.

Influence of the level of theory on the evaluation of aromaticity indices

ASE

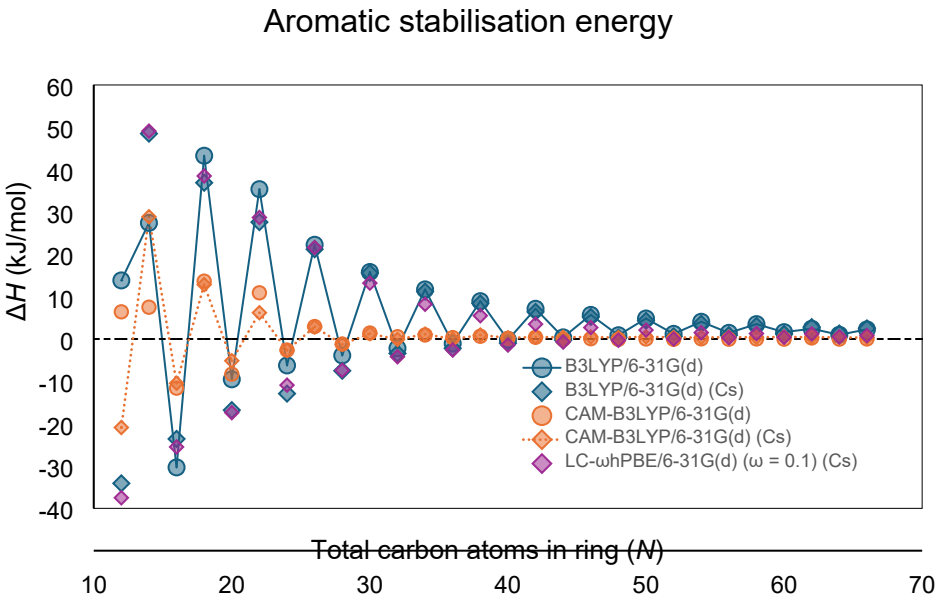

Figure S6: Influence of the level of theory on the ASE of closed-shell [*N*]annulenes (*N* = 12-66). The molecular geometries were constrained to C_s symmetry and optimised at the B3LYP/6-31G(d), CAM-B3LYP/6-31G(d), and LC-ωhPBE/6-31G(d) levels of theory (data taken from ref. [26]). Additionaly, the molecular geometries were reoptimised using B3LYP/6-31G(d) and CAM-B3LYP/6-31G(d) without symmetry constraint to determine the influence of planarity on the evaluation of stabilization energies.

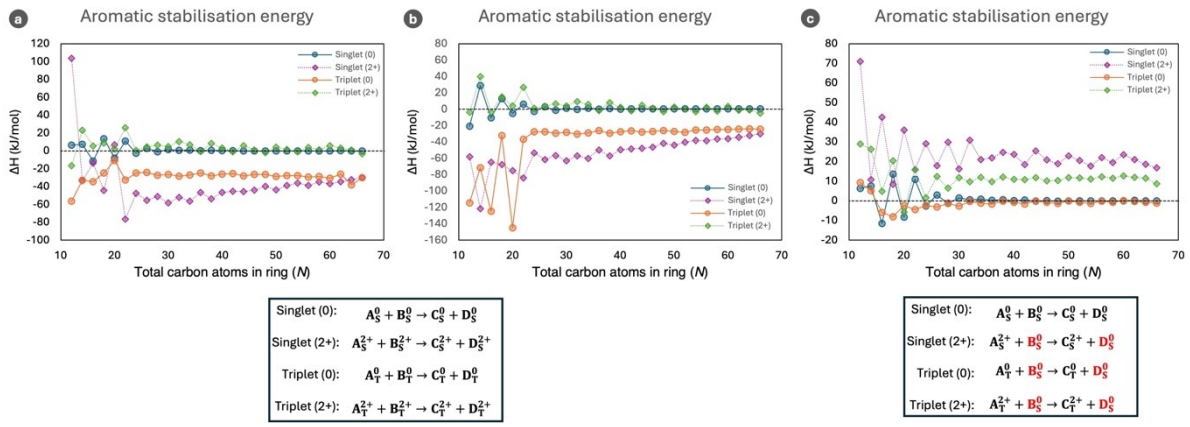

Figure S7: ASEs of the neutral closed-shell and triplet [*N*]annulenes as well as the triplet and singlet dicationic counterparts (*N* =12-66) computed at the (U)CAM-B3LYP/6-31G(d). A) The structures to evaluate the ASE values were not subjected to any constraints. The geometries of **A**, **B**, **C**, and **D** do not contain any imaginary frequencies. B) All the structures in the ASE calculations are enforced to be planar. Consequently, several geometries contain one or more imaginary frequencies. C) The electronic energy and ZPVE of the **B** and **D** structures employed in the ISE_{II} method exhibit C_s symmetry. By contrast, the structure of **A** and **C** were optimised without any constraints.

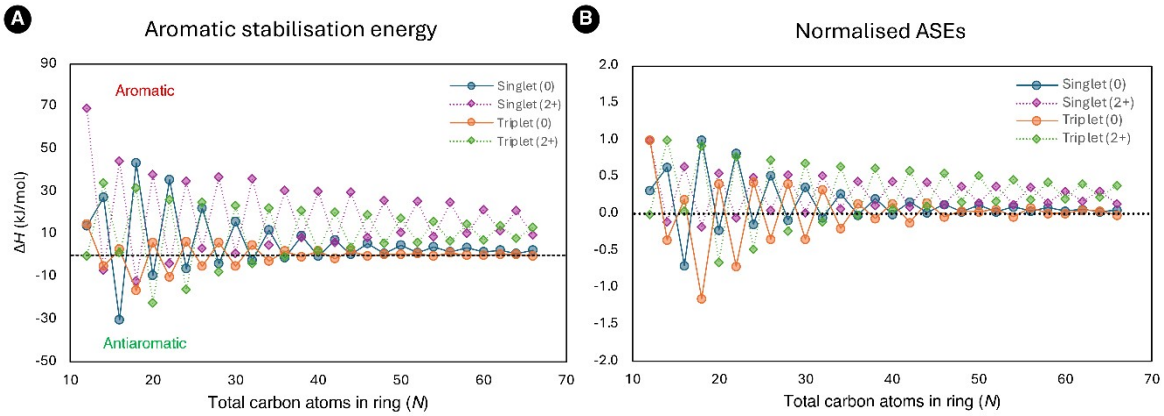

Figure S8: ASE results of the neutral closed-shell and triplet [*N*]annulenes as well as the triplet and singlet dicationic counterparts computed at the B3LYP/6-31G(d). A) The electronic energy and ZPVE of the **B** and **D** structures employed in the ISE_{II} method were derived from ref. [26] and exhibit C_s symmetry. By contrast, the structure of **A** and **C** were optimised without any constraints. B) The normalized ASE values for all the series. The highest positive ASE value is set to be equal to 1 for each series.

HOMA

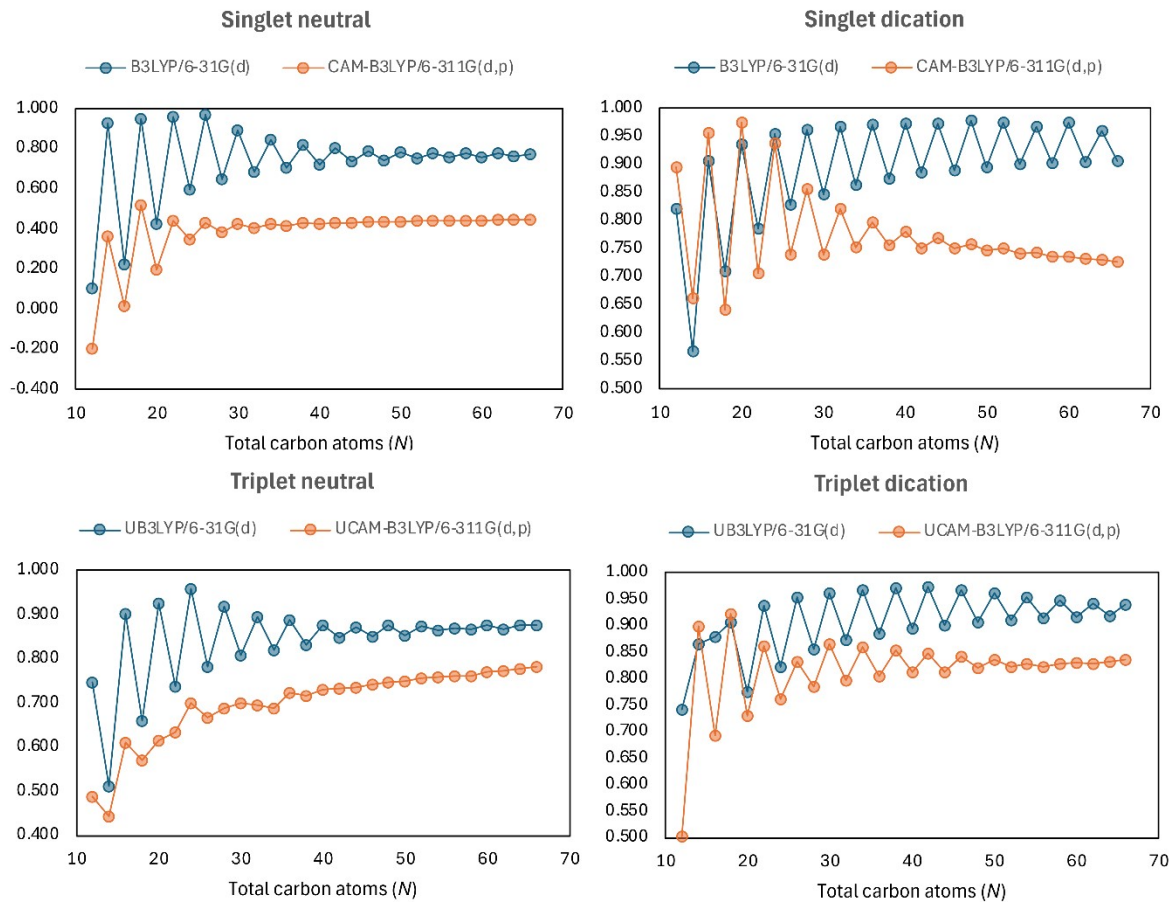

Figure S9: The evolution of the structural index HOMA of neutral and charged annulenes in the singlet and triplet states (*N* = 12-66) obtained with two different levels of theory with functionals including a different percentage of Hartree Fock exchange: B3LYP (19%) and CAM-B3LYP (19-65%). Note that different scales are used to illustrate better the differences for neutral/charged singlet and triplet annulenes.

Table S1: The HOMA index of the [*N*]annulenes (*N*=12-66) with distinct charges and multiplicities obtained using two different level of theory.

	(U)B3LYP/6-31G(d)				(U)CAM-B3LYP/6-311G(d,p)			
N	**Singlet (0)**	**Singlet (2+)**	**Triplet (0)**	**Triplet (2+)**	**Singlet (0)**	**Singlet (2+)**	**Triplet (0)**	**Triplet (2+)**
12	0.105	0.821	0.746	0.743	-0.194	0.895	0.488	0.504
14	0.929	0.568	0.513	0.865	0.365	0.661	0.443	0.899
16	0.225	0.906	0.902	0.878	0.015	0.955	0.610	0.693
18	0.946	0.709	0.660	0.906	0.518	0.642	0.572	0.922
20	0.427	0.936	0.925	0.775	0.197	0.974	0.616	0.731
22	0.960	0.785	0.738	0.938	0.443	0.706	0.635	0.861
24	0.597	0.953	0.958	0.823	0.348	0.938	0.701	0.762
26	0.967	0.828	0.783	0.953	0.430	0.739	0.667	0.833
28	0.650	0.962	0.918	0.855	0.383	0.856	0.688	0.786
30	0.892	0.847	0.809	0.962	0.425	0.740	0.700	0.866
32	0.683	0.966	0.895	0.874	0.405	0.821	0.696	0.797
34	0.846	0.864	0.821	0.967	0.426	0.752	0.689	0.859
36	0.706	0.971	0.887	0.886	0.417	0.796	0.723	0.806
38	0.819	0.875	0.833	0.970	0.430	0.756	0.717	0.854
40	0.722	0.973	0.876	0.895	0.425	0.780	0.729	0.812
42	0.801	0.886	0.848	0.973	0.432	0.751	0.733	0.848
44	0.734	0.973	0.872	0.902	0.431	0.768	0.735	0.813
46	0.790	0.890	0.851	0.968	0.435	0.750	0.742	0.842
48	0.743	0.977	0.876	0.907	0.435	0.759	0.747	0.820
50	0.784	0.895	0.852	0.962	0.438	0.747	0.749	0.836
52	0.750	0.975	0.873	0.911	0.439	0.750	0.756	0.822
54	0.779	0.900	0.866	0.953	0.440	0.741	0.759	0.829
56	0.755	0.967	0.868	0.914	0.441	0.743	0.761	0.823
58	0.777	0.902	0.868	0.947	0.442	0.736	0.762	0.829
60	0.759	0.975	0.877	0.916	0.443	0.736	0.770	0.831
62	0.776	0.903	0.868	0.943	0.444	0.731	0.772	0.829
64	0.762	0.959	0.877	0.918	0.445	0.730	0.777	0.832
66	0.774	0.906	0.875	0.939	0.446	0.726	0.781	0.836

BLA

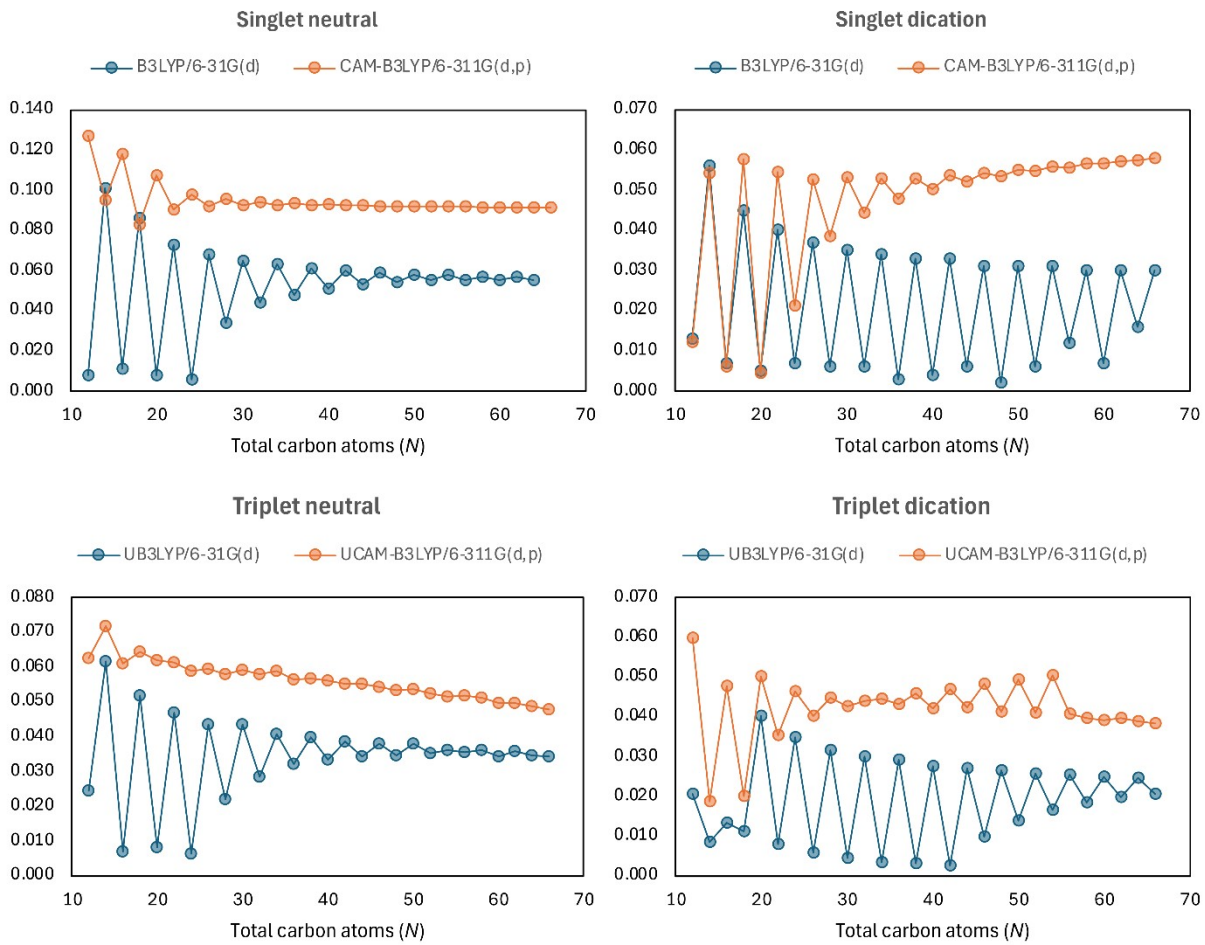

Figure S10: The evolution of the structural index BLA of neutral and charged annulenes in the singlet and triplet states (*N* = 12-66) obtained with two different levels of theory with functionals including a different percentage of Hartree Fock exchange: B3LYP (19%) and CAM-B3LYP (19-65%). Note that different scales are used to illustrate better the differences for neutral/charged singlet and triplet annulenes.

Table S2: The BLA index of the [*N*]annulenes (*N* = 12-66) with distinct charges and multiplicities obtained using two different level of theory.

	(U)B3LYP/6-31G(d)				(U)CAM-B3LYP/6-311G(d,p)			
N	**Singlet (0)**	**Singlet (2+)**	**Triplet (0)**	**Triplet (2+)**	**Singlet (0)**	**Singlet (2+)**	**Triplet (0)**	**Triplet (2+)**
12	0.104	0.013	0.024	0.021	0.127	0.012	0.062	0.060
14	0.008	0.056	0.062	0.008	0.095	0.054	0.072	0.019
16	0.101	0.007	0.007	0.013	0.118	0.006	0.061	0.048
18	0.011	0.045	0.052	0.011	0.083	0.058	0.064	0.020
20	0.086	0.005	0.008	0.040	0.107	0.004	0.062	0.050
22	0.008	0.040	0.047	0.008	0.090	0.054	0.061	0.035
24	0.073	0.007	0.006	0.035	0.098	0.021	0.059	0.046
26	0.006	0.037	0.044	0.006	0.092	0.053	0.060	0.040
28	0.068	0.006	0.022	0.032	0.096	0.038	0.058	0.045
30	0.034	0.035	0.043	0.004	0.092	0.053	0.059	0.043
32	0.065	0.006	0.028	0.030	0.094	0.044	0.058	0.044
34	0.044	0.034	0.041	0.004	0.092	0.053	0.059	0.045
36	0.063	0.003	0.032	0.029	0.093	0.048	0.056	0.043
38	0.048	0.033	0.040	0.003	0.092	0.053	0.057	0.046
40	0.061	0.004	0.033	0.027	0.093	0.050	0.056	0.042
42	0.051	0.033	0.038	0.003	0.092	0.054	0.055	0.047
44	0.060	0.006	0.034	0.027	0.092	0.052	0.055	0.042
46	0.053	0.031	0.038	0.010	0.092	0.054	0.054	0.048
48	0.059	0.002	0.034	0.026	0.092	0.053	0.053	0.041
50	0.054	0.031	0.038	0.014	0.092	0.055	0.054	0.049
52	0.058	0.006	0.035	0.026	0.092	0.055	0.052	0.041
54	0.055	0.031	0.036	0.016	0.092	0.056	0.051	0.050
56	0.058	0.012	0.036	0.025	0.092	0.056	0.052	0.041
58	0.055	0.030	0.036	0.018	0.092	0.056	0.051	0.039
60	0.057	0.007	0.034	0.025	0.092	0.057	0.050	0.039
62	0.055	0.030	0.036	0.020	0.091	0.057	0.050	0.040
64	0.057	0.016	0.034	0.025	0.091	0.057	0.049	0.039
66	0.055	0.030	0.034	0.021	0.091	0.058	0.048	0.038

FLU

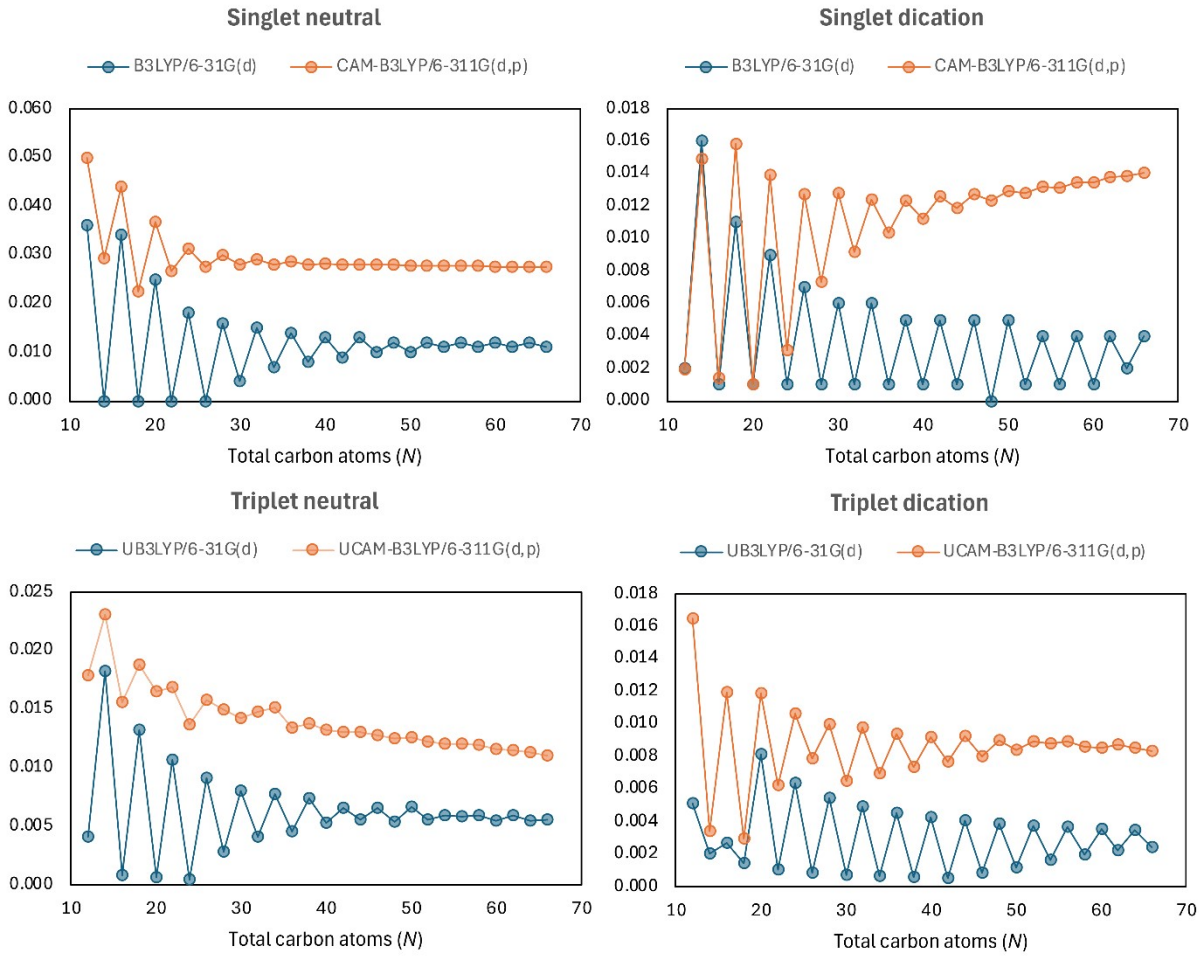

Figure S11: The evolution of the electronic index FLU of neutral and charged annulenes in the singlet and triplet states (N = 12-66) obtained with two different levels of theory with functionals including a different percentage of Hartree Fock exchange: B3LYP (19%) and CAM-B3LYP (19-65%). Note that different scales are used to illustrate better the differences for neutral/charged singlet and triplet annulenes.

Table S3: The FLU index of the [*N*]annulenes (*N* = 12-66) with distinct charges and multiplicities obtained using two different level of theory.

	(U)B3LYP/6-31G(d)				(U)CAM-B3LYP/6-311G(d,p)			
N	**Singlet (0)**	**Singlet (2+)**	**Triplet (0)**	**Triplet (2+)**	**Singlet (0)**	**Singlet (2+)**	**Triplet (0)**	**Triplet (2+)**
12	0.036	0.002	0.004	0.005	0.050	0.002	0.018	0.016
14	0.000	0.016	0.018	0.002	0.029	0.015	0.023	0.003
16	0.034	0.001	0.001	0.003	0.044	0.001	0.016	0.012
18	0.000	0.011	0.013	0.001	0.023	0.016	0.019	0.003
20	0.025	0.001	0.001	0.008	0.037	0.001	0.016	0.012
22	0.000	0.009	0.011	0.001	0.027	0.014	0.017	0.006
24	0.018	0.001	0.000	0.006	0.031	0.003	0.014	0.011
26	0.000	0.007	0.009	0.001	0.028	0.013	0.016	0.008
28	0.016	0.001	0.003	0.005	0.030	0.007	0.015	0.010
30	0.004	0.006	0.008	0.001	0.028	0.013	0.014	0.007
32	0.015	0.001	0.004	0.005	0.029	0.009	0.015	0.010
34	0.007	0.006	0.008	0.001	0.028	0.012	0.015	0.007
36	0.014	0.001	0.005	0.005	0.029	0.010	0.013	0.009
38	0.008	0.005	0.007	0.001	0.028	0.012	0.014	0.007
40	0.013	0.001	0.005	0.004	0.028	0.011	0.013	0.009
42	0.009	0.005	0.007	0.001	0.028	0.013	0.013	0.008
44	0.013	0.001	0.006	0.004	0.028	0.012	0.013	0.009
46	0.010	0.005	0.007	0.001	0.028	0.013	0.013	0.008
48	0.012	0.000	0.005	0.004	0.028	0.012	0.013	0.009
50	0.010	0.005	0.007	0.001	0.028	0.013	0.013	0.008
52	0.012	0.001	0.006	0.004	0.028	0.013	0.012	0.009
54	0.011	0.004	0.006	0.002	0.028	0.013	0.012	0.009
56	0.012	0.001	0.006	0.004	0.028	0.013	0.012	0.009
58	0.011	0.004	0.006	0.002	0.028	0.013	0.012	0.009
60	0.012	0.001	0.005	0.004	0.028	0.013	0.012	0.009
62	0.011	0.004	0.006	0.002	0.028	0.014	0.012	0.009
64	0.012	0.002	0.005	0.004	0.028	0.014	0.011	0.009
66	0.011	0.004	0.006	0.002	0.028	0.014	0.011	0.008

BOA

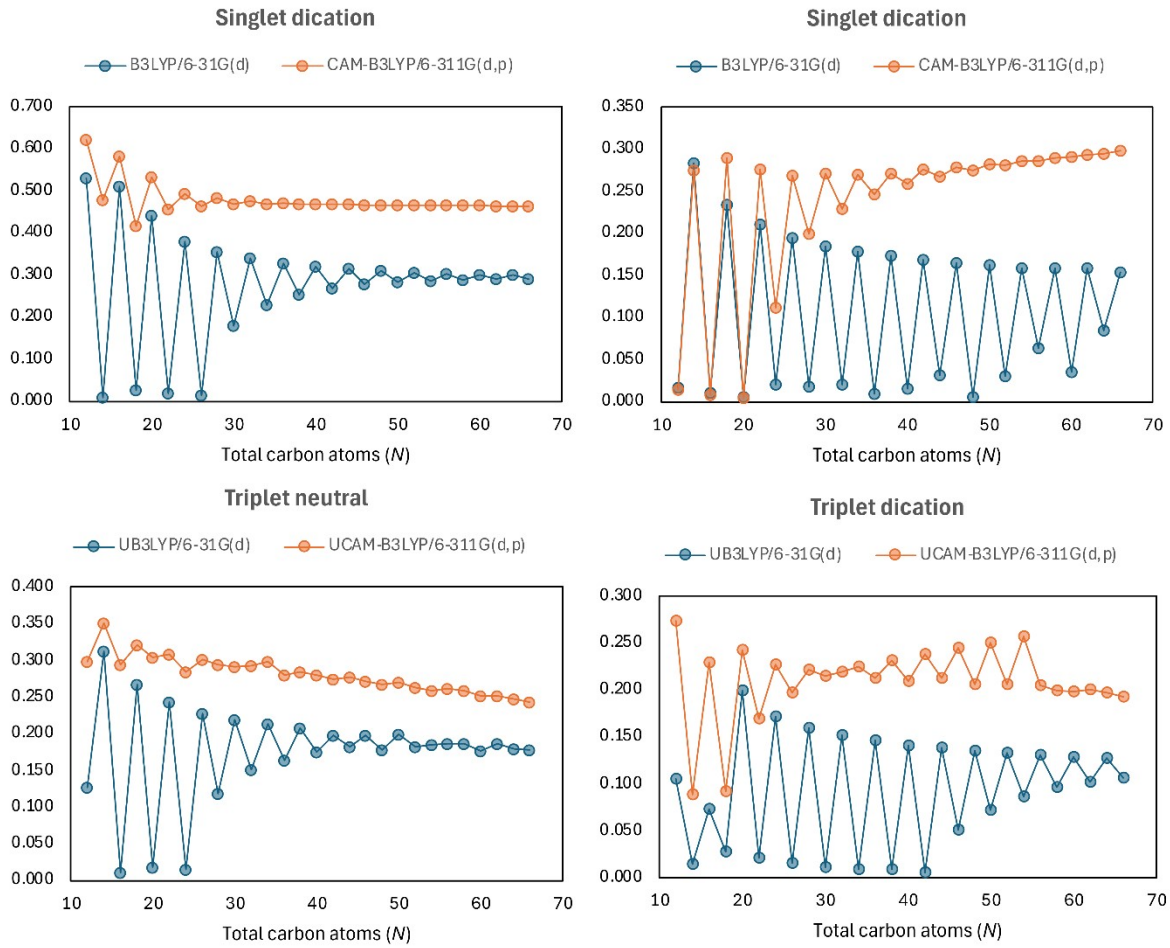

Figure S12: The evolution of the electronic index BOA of neutral and charged annulenes in the singlet and triplet states (*N* = 12-66) obtained with two different levels of theory with functionals including a different percentage of Hartree Fock exchange: B3LYP (19%) and CAM-B3LYP (19-65%). Note that different scales are used to illustrate better the differences for neutral/charged singlet and triplet annulenes.

Table S4: The electronic BOA index of the [*N*]annulenes (*N* = 12-66) with distinct charges and multiplicities obtained using two different level of theory.

	(U)B3LYP/6-31G(d)				(U)CAM-B3LYP/6-311G(d,p)			
N	**Singlet (0)**	**Singlet (2+)**	**Triplet (0)**	**Triplet (2+)**	**Singlet (0)**	**Singlet (2+)**	**Triplet (0)**	**Triplet (2+)**
12	0.529	0.017	0.127	0.106	0.620	0.014	0.298	0.273
14	0.008	0.283	0.313	0.015	0.477	0.275	0.351	0.088
16	0.509	0.011	0.011	0.073	0.582	0.008	0.294	0.229
18	0.025	0.234	0.268	0.028	0.417	0.290	0.321	0.091
20	0.441	0.006	0.018	0.199	0.533	0.004	0.305	0.242
22	0.019	0.210	0.244	0.021	0.456	0.276	0.308	0.169
24	0.378	0.020	0.015	0.172	0.493	0.112	0.285	0.227
26	0.014	0.194	0.228	0.016	0.463	0.268	0.301	0.197
28	0.355	0.018	0.119	0.159	0.482	0.199	0.294	0.221
30	0.179	0.185	0.220	0.012	0.467	0.271	0.291	0.214
32	0.339	0.021	0.151	0.152	0.475	0.229	0.294	0.219
34	0.228	0.178	0.214	0.009	0.468	0.270	0.299	0.224
36	0.328	0.009	0.164	0.146	0.472	0.246	0.280	0.213
38	0.252	0.174	0.208	0.009	0.467	0.271	0.285	0.231
40	0.320	0.016	0.176	0.141	0.469	0.259	0.280	0.210
42	0.267	0.169	0.197	0.006	0.467	0.276	0.275	0.238
44	0.314	0.031	0.182	0.138	0.468	0.268	0.277	0.212
46	0.277	0.165	0.197	0.051	0.466	0.278	0.272	0.244
48	0.309	0.006	0.177	0.135	0.467	0.274	0.267	0.206
50	0.282	0.163	0.200	0.072	0.466	0.282	0.270	0.250
52	0.305	0.030	0.182	0.133	0.466	0.281	0.264	0.206
54	0.286	0.159	0.186	0.086	0.465	0.286	0.259	0.256
56	0.302	0.064	0.187	0.131	0.465	0.286	0.261	0.205
58	0.288	0.159	0.187	0.096	0.465	0.290	0.259	0.199
60	0.300	0.035	0.177	0.129	0.464	0.291	0.251	0.198
62	0.290	0.159	0.187	0.102	0.464	0.294	0.252	0.200
64	0.299	0.085	0.179	0.128	0.464	0.295	0.247	0.197
66	0.291	0.154	0.178	0.107	0.464	0.298	0.243	0.193

AV1245

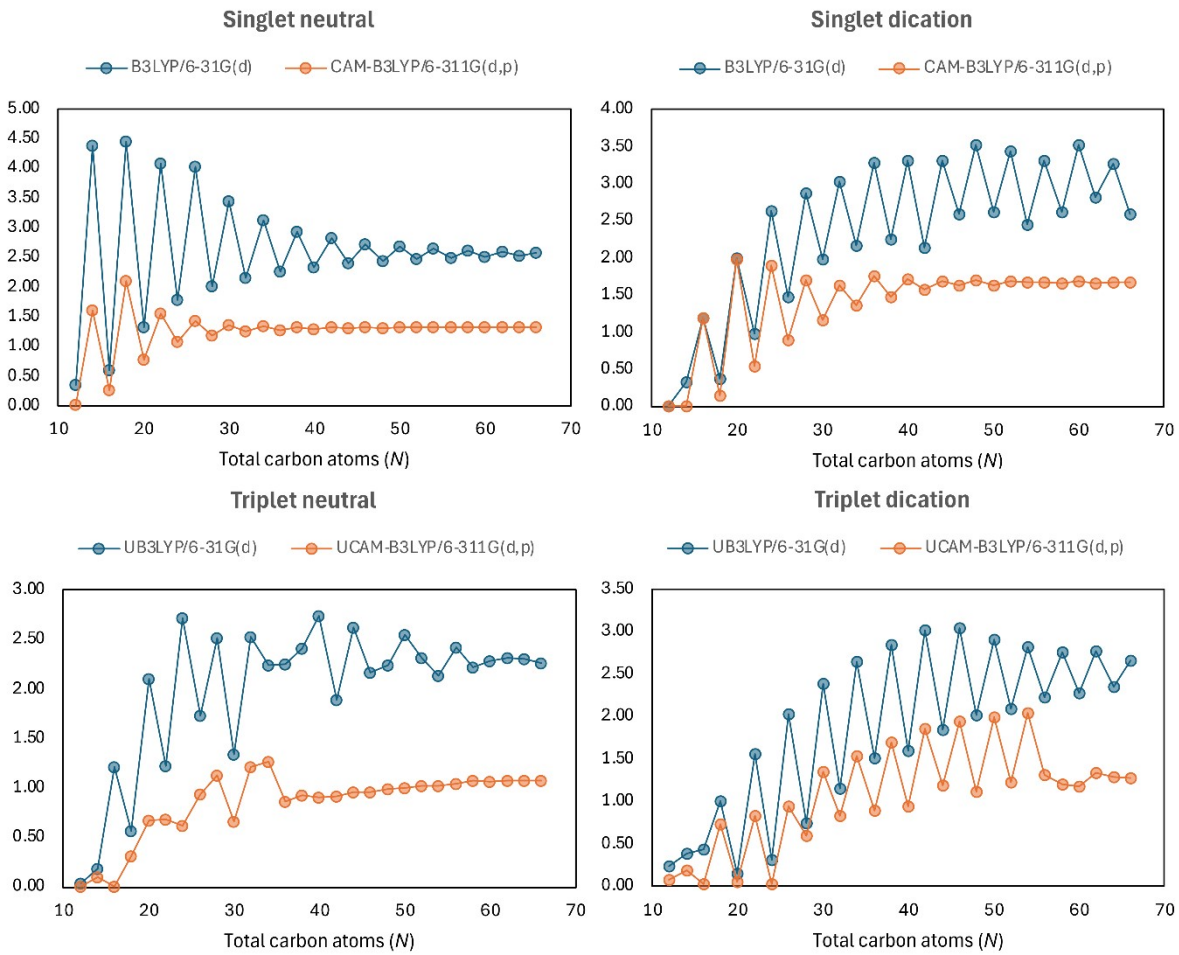

Figure S13: The evolution of the electronic index AV1245 of neutral and charged annulenes in the singlet and triplet states (*N* = 12-66) obtained with two different levels of theory with functionals including a different percentage of Hartree Fock exchange: B3LYP (19%) and CAM-B3LYP (19-65%). Note that different scales are used to illustrate better the differences for neutral/charged singlet and triplet annulenes.

Table S5: The electronic AV1245 index of the [*N*]annulenes (*N*=12-66) with distinct charges and multiplicities obtained using two different level of theory.

	(U)B3LYP/6-31G(d)				(U)CAM-B3LYP/6-311G(d,p)			
N	**Singlet (0)**	**Singlet (2+)**	**Triplet (0)**	**Triplet (2+)**	**Singlet (0)**	**Singlet (2+)**	**Triplet (0)**	**Triplet (2+)**
12	1.12	-0.42	-0.05	0.63	0.34	0.38	0.19	0.23
14	4.62	1.35	0.98	0.70	1.80	1.06	0.89	0.53
16	0.99	1.45	1.53	0.91	0.58	1.40	1.16	0.25
18	4.57	1.78	1.51	1.16	2.31	1.70	1.27	0.97
20	1.65	2.38	2.42	0.68	1.02	2.29	1.57	0.53
22	4.41	2.31	2.07	1.79	1.84	2.14	1.68	1.24
24	2.28	2.94	2.97	1.32	1.40	2.74	2.04	0.98
26	4.32	2.69	2.47	2.29	1.74	2.45	1.95	1.47
28	2.51	3.24	3.10	1.81	1.52	2.82	2.12	1.36
30	3.84	2.94	2.78	2.67	1.69	2.59	2.23	1.68
32	2.66	3.43	3.17	2.17	1.59	2.87	2.24	1.62
34	3.54	3.12	2.93	2.94	1.68	2.72	2.25	1.90
36	2.76	3.57	3.27	2.44	1.63	2.90	2.43	1.82
38	3.37	3.26	3.07	3.15	1.68	2.80	2.42	2.07
40	2.83	3.66	3.30	2.66	1.65	2.90	2.49	1.97
42	3.25	3.35	3.22	3.30	1.68	2.83	2.53	2.20
44	2.88	3.72	3.34	2.83	1.67	2.91	2.55	2.07
46	3.18	3.43	3.27	3.37	1.68	2.86	2.59	2.31
48	2.92	3.79	3.41	2.96	1.68	2.90	2.63	2.17
50	3.14	3.48	3.31	3.40	1.69	2.87	2.63	2.38
52	2.95	3.82	3.43	3.07	1.68	2.89	2.67	2.23
54	3.11	3.53	3.42	3.42	1.69	2.87	2.70	2.44
56	2.97	3.82	3.44	3.15	1.69	2.88	2.71	2.29
58	3.09	3.56	3.45	3.44	1.69	2.86	2.73	2.33
60	2.99	3.87	3.51	3.23	1.69	2.87	2.76	2.35
62	3.07	3.59	3.47	3.45	1.70	2.85	2.77	2.36
64	3.00	3.83	3.52	3.28	1.70	2.85	2.80	2.39
66	3.06	3.61	3.53	3.47	1.70	2.84	2.82	2.42

AV_{min}

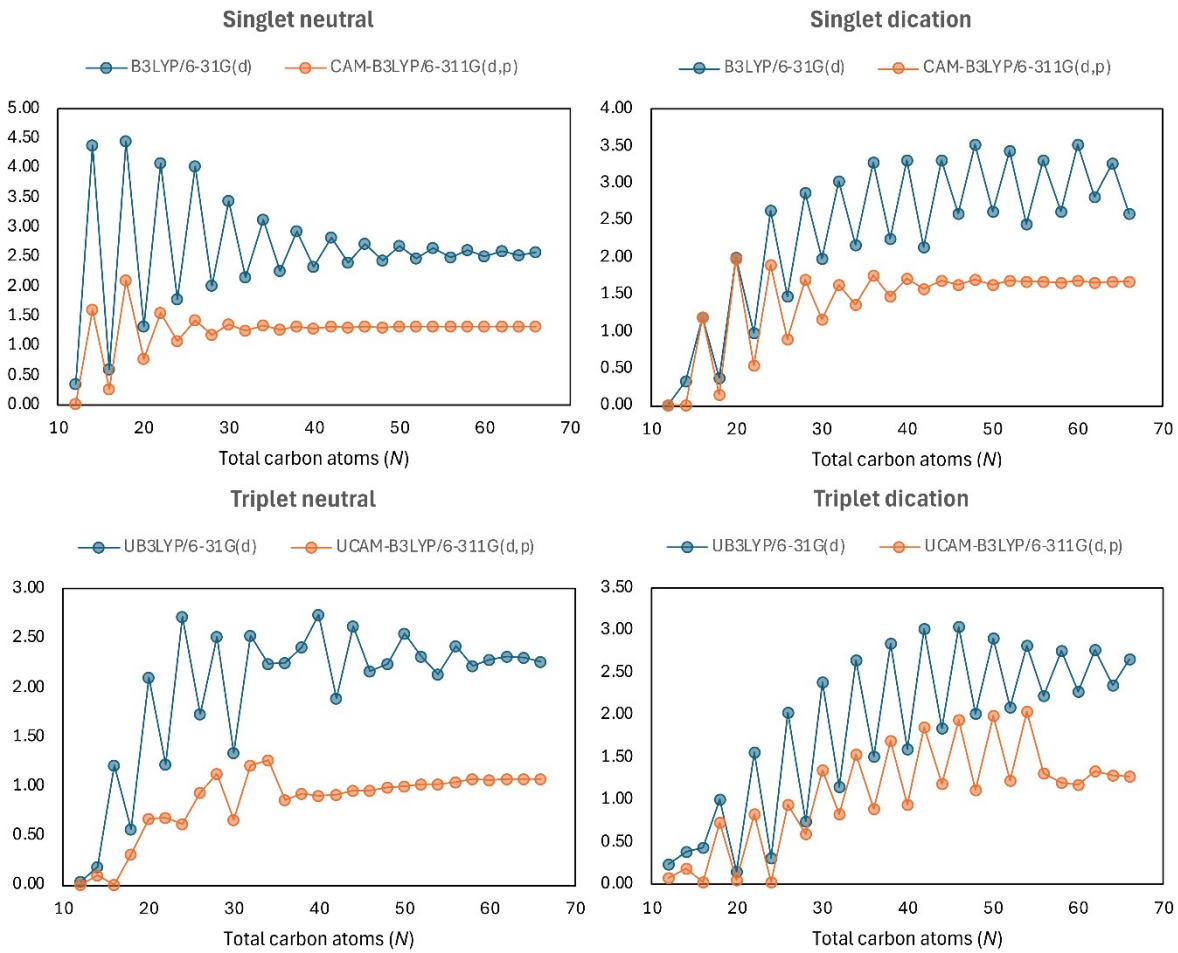

Figure S14: The evolution of the electronic index AV_{min} of neutral and charged annulenes in the singlet and triplet states (*N* = 12-66) obtained with two different levels of theory with functionals including a different percentage of Hartree Fock exchange: B3LYP (19%) and CAM-B3LYP (19-65%).

Table S6: The electronic AV_{min} index of the [*N*]annulenes (*N*=12-66) with distinct charges and multiplicities obtained using two different level of theory.

	(U)B3LYP/6-31G(d)				(U)CAM-B3LYP/6-311G(d,p)			
N	**Singlet (0)**	**Singlet (2+)**	**Triplet (0)**	**Triplet (2+)**	**Singlet (0)**	**Singlet (2+)**	**Triplet (0)**	**Triplet (2+)**
12	0.36	0.01	0.04	0.24	0.02	0.01	0.01	0.08
14	4.39	0.34	0.19	0.40	1.61	0.01	0.10	0.20
16	0.61	1.19	1.21	0.44	0.27	1.20	0.00	0.03
18	4.46	0.37	0.56	1.01	2.10	0.15	0.31	0.74
20	1.33	2.00	2.10	0.16	0.78	1.99	0.67	0.06
22	4.08	0.99	1.23	1.56	1.55	0.54	0.68	0.83
24	1.78	2.64	2.72	0.32	1.08	1.91	0.62	0.03
26	4.03	1.48	1.74	2.04	1.43	0.90	0.94	0.95
28	2.01	2.87	2.51	0.75	1.18	1.71	1.13	0.60
30	3.45	1.98	1.34	2.39	1.37	1.17	0.67	1.36
32	2.16	3.03	2.52	1.16	1.25	1.63	1.22	0.83
34	3.12	2.17	2.24	2.65	1.34	1.36	1.26	1.54
36	2.27	3.28	2.25	1.51	1.28	1.76	0.86	0.89
38	2.93	2.26	2.41	2.85	1.33	1.48	0.92	1.70
40	2.34	3.32	2.74	1.61	1.30	1.71	0.91	0.94
42	2.82	2.14	1.90	3.03	1.33	1.57	0.92	1.86
44	2.40	3.32	2.63	1.85	1.31	1.69	0.96	1.19
46	2.73	2.59	2.17	3.05	1.33	1.63	0.96	1.94
48	2.44	3.53	2.24	2.02	1.32	1.71	0.99	1.12
50	2.68	2.62	2.55	2.91	1.33	1.63	1.00	2.00
52	2.47	3.44	2.31	2.10	1.32	1.69	1.03	1.23
54	2.65	2.45	2.14	2.82	1.33	1.67	1.03	2.05
56	2.49	3.31	2.42	2.23	1.32	1.68	1.05	1.31
58	2.62	2.62	2.22	2.76	1.33	1.67	1.08	1.21
60	2.51	3.53	2.29	2.29	1.32	1.69	1.07	1.18
62	2.60	2.82	2.31	2.77	1.33	1.66	1.07	1.34
64	2.52	3.27	2.31	2.36	1.33	1.68	1.08	1.29
66	2.59	2.59	2.26	2.67	1.33	1.68	1.08	1.28

NICS(1)$_{zz}$

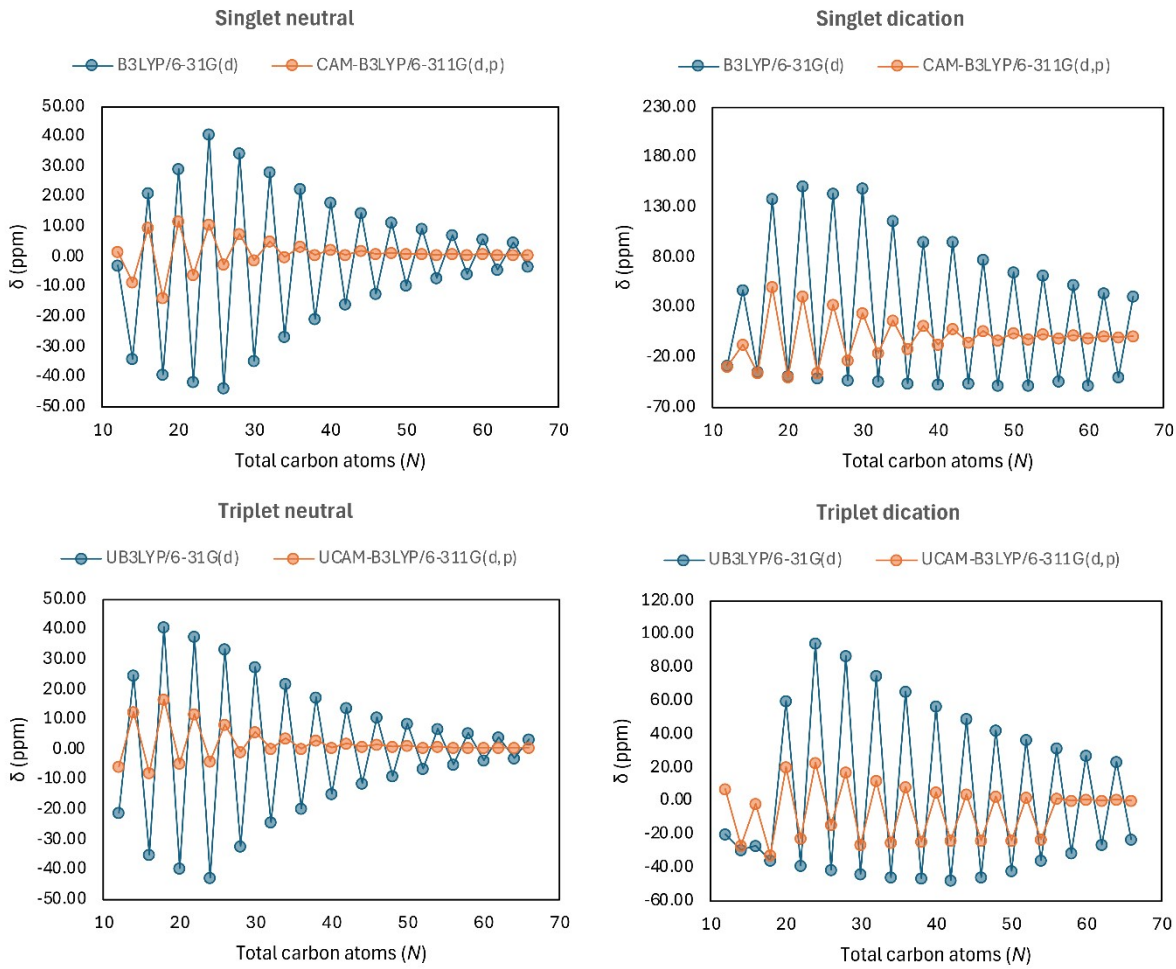

Figure S15: The evolution of the magnetic index NICS(1)$_{zz}$ (in ppm) of neutral and charged annulenes in the singlet and triplet states (N = 12-66) obtained with two different levels of theory with functionals including a different percentage of Hartree Fock exchange: B3LYP (19%) and CAM-B3LYP (19-65%). Note that different scales are used to illustrate better the differences for neutral/charged singlet and triplet annulenes.

Table S7: The magnetic NICS(1)$_{zz}$ index (ppm) of the [*N*]annulenes (*N*=12-66) with distinct charges and multiplicities obtained using two different level of theory.

	(U)B3LYP/6-31G(d)				(U)CAM-B3LYP/6-311G(d,p)			
N	**Singlet (0)**	**Singlet (2+)**	**Triplet (0)**	**Triplet (2+)**	**Singlet (0)**	**Singlet (2+)**	**Triplet (0)**	**Triplet (2+)**
12	-2.94	-28.19	-21.10	-19.54	1.61	-29.31	-5.59	7.27
14	-34.08	47.33	24.97	-28.96	-8.51	-7.34	12.76	-26.74
16	21.31	-34.14	-35.00	-26.71	9.84	-35.06	-7.84	-1.44
18	-39.05	138.62	41.05	-35.43	-13.50	50.89	16.89	-32.43
20	29.24	-38.97	-39.33	60.13	11.73	-39.88	-4.46	20.60
22	-41.71	151.16	37.64	-38.82	-5.86	41.09	11.91	-22.21
24	40.81	-40.66	-42.50	94.80	10.79	-35.43	-3.89	22.87
26	-43.63	144.11	33.53	-41.32	-2.48	32.68	8.55	-14.19
28	34.69	-42.72	-32.17	87.09	7.52	-22.77	-0.84	17.70
30	-34.58	149.47	27.62	-43.71	-0.98	23.97	6.11	-25.72
32	28.29	-43.89	-24.13	75.28	5.37	-15.36	0.36	12.28
34	-26.56	116.78	21.98	-45.13	0.05	17.17	3.95	-24.63
36	22.53	-45.90	-19.61	66.14	3.53	-11.28	0.53	8.35
38	-20.53	95.17	17.44	-46.19	0.65	12.10	2.99	-23.97
40	18.13	-46.58	-14.70	56.92	2.55	-7.16	0.85	5.80
42	-15.83	95.33	14.00	-47.12	0.76	8.91	2.07	-23.67
44	14.62	-46.36	-11.07	49.30	1.94	-4.51	0.99	4.07
46	-12.11	78.11	11.01	-45.27	0.85	6.17	1.59	-23.42
48	11.60	-48.19	-8.57	42.83	1.43	-3.11	0.90	2.84
50	-9.34	65.13	8.71	-41.45	0.87	4.31	1.29	-23.23
52	9.27	-47.52	-6.43	37.01	1.15	-1.81	0.86	2.06
54	-7.15	61.92	6.92	-35.64	0.78	3.28	1.01	-22.99
56	7.42	-43.63	-4.71	32.06	0.97	-0.99	0.81	1.55
58	-5.48	53.01	5.44	-30.72	0.72	2.31	0.85	0.25
60	5.96	-47.51	-3.63	27.75	0.85	-0.55	0.70	1.16
62	-4.17	44.74	4.29	-26.20	0.67	1.67	0.75	0.38
64	4.68	-39.12	-2.67	23.95	0.68	-0.19	0.64	0.91
66	-3.16	41.07	3.39	-22.58	0.59	1.33	0.63	0.40

GIMIC

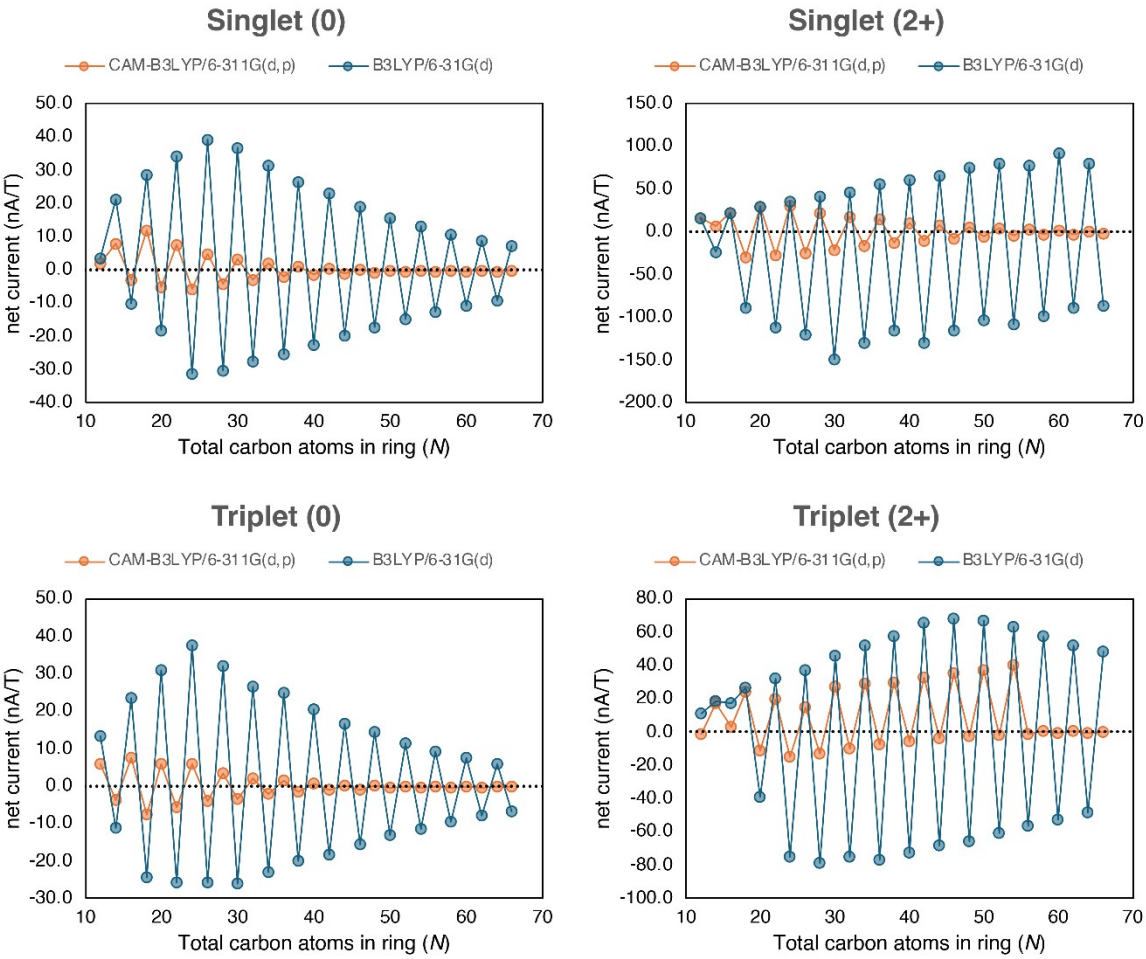

Figure S16: The evolution of the net ring current strength (in nA/T) from GIMIC calculations of neutral and charged annulenes in the singlet and triplet states (*N* = 12-66) obtained with two different levels of theory with functionals including a different percentage of Hartree Fock exchange: B3LYP (19%) and CAM-B3LYP (19-65%). Note that different scales are used to illustrate better the differences for neutral/charged singlet and triplet annulenes.

Table S8: The net ring current strength (in nA/T) from GIMIC calculations of the [*N*]annulenes (*N*=12-66) with distinct charges and multiplicities, obtained using two different level of theory.

	(U)B3LYP/6-31G(d)				(U)CAM-B3LYP/6-311G(d,p)			
N	**Singlet (0)**	**Singlet (2+)**	**Triplet (0)**	**Triplet (2+)**	**Singlet (0)**	**Singlet (2+)**	**Triplet (0)**	**Triplet (2+)**
12	3.6	16.1	13.3	10.9	2.1	16.6	5.9	-1.2
14	21.1	-23.3	-11.1	18.3	7.8	6.4	-3.8	17.1
16	-10.1	22.3	23.6	17.2	-3.0	22.6	7.5	3.0
18	28.7	-88.0	-24.5	26.3	12.0	-29.1	-7.7	24.1
20	-18.1	29.5	31.0	-38.9	-5.0	29.5	6.0	-11.3
22	34.3	-111.6	-25.8	32.1	7.5	-27.1	-5.6	19.5
24	-31.2	35.9	37.5	-75.2	-5.7	31.2	6.0	-15.2
26	39.2	-120.0	-25.9	37.3	4.9	-24.1	-4.0	14.5
28	-30.3	41.8	32.0	-78.7	-4.3	23.0	3.3	-13.3
30	36.8	-148.3	-26.2	45.9	3.2	-20.9	-3.6	27.2
32	-27.4	46.9	26.5	-75.3	-3.0	17.5	2.0	-9.8
34	31.5	-129.1	-23.1	52.1	2.0	-16.5	-2.2	28.7
36	-25.3	55.7	24.8	-76.7	-2.1	14.7	1.4	-7.5
38	26.6	-115.3	-19.9	57.7	1.2	-12.6	-1.6	29.9
40	-22.4	61.7	20.4	-72.4	-1.5	10.6	0.6	-5.5
42	23.0	-129.5	-18.3	65.7	0.6	-10.1	-1.1	33.0
44	-19.6	66.2	16.7	-68.0	-1.0	7.6	0.2	-3.8
46	19.1	-115.2	-15.5	68.3	0.3	-7.4	-0.9	35.1
48	-17.2	75.6	14.3	-65.6	-0.8	6.2	0.1	-2.8
50	15.8	-103.5	-13.0	66.9	0.0	-5.4	-0.6	37.2
52	-14.8	80.2	11.5	-61.0	-0.6	4.1	-0.1	-2.0
54	13.2	-107.2	-11.5	62.8	-0.2	-4.2	-0.5	39.9
56	-12.7	78.5	9.1	-56.3	-0.5	2.8	-0.2	-1.4
58	10.8	-98.0	-9.6	57.7	-0.2	-3.1	-0.5	0.6
60	-10.7	92.1	7.6	-52.9	-0.4	2.2	-0.2	-1.0
62	8.8	-88.1	-8.0	52.2	-0.2	-2.3	-0.4	0.3
64	-9.1	80.6	5.9	-48.5	-0.4	1.3	-0.3	-0.8
66	7.2	-86.6	-6.9	48.3	-0.3	-1.7	-0.3	0.1

Relative hardness

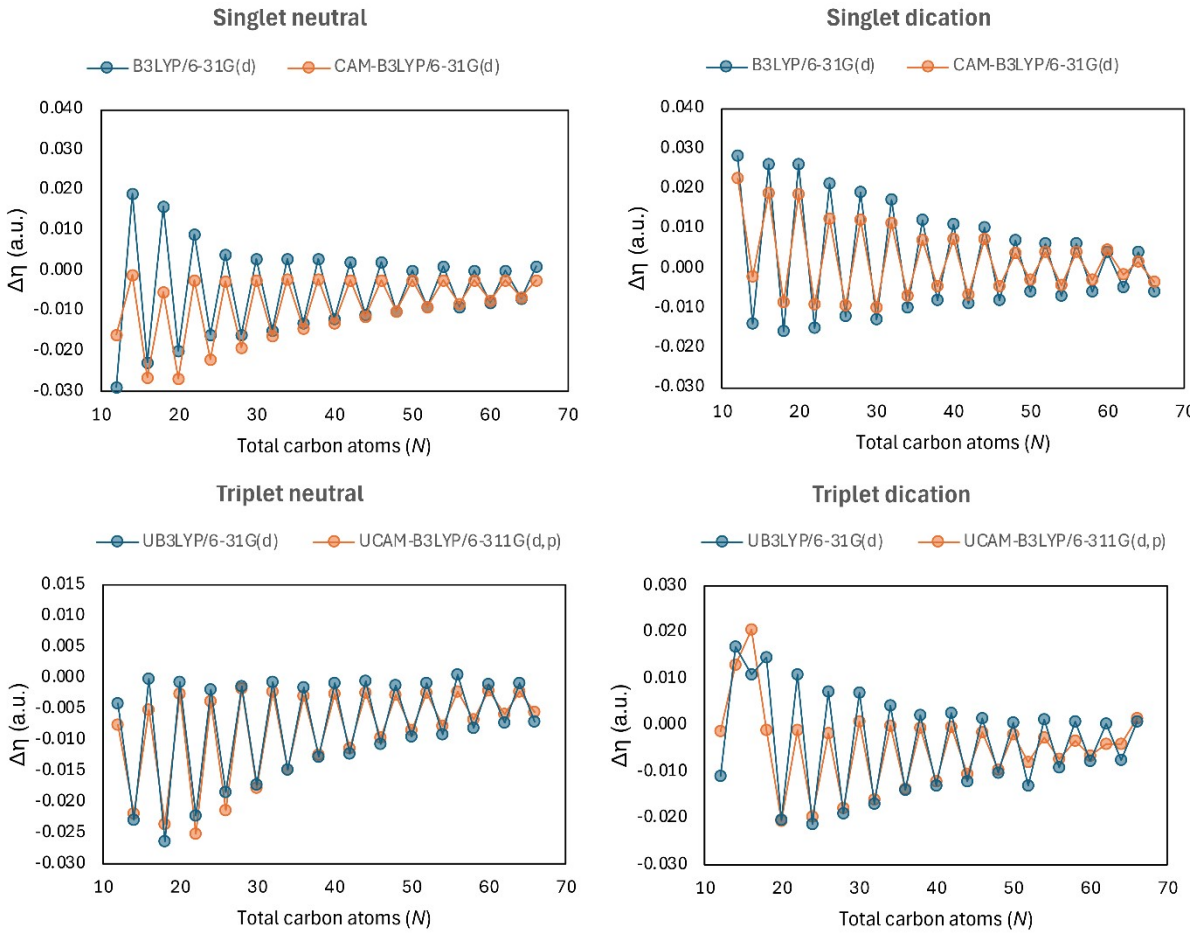

Figure S17: The evolution of the reactivity index $\Delta\eta$ (in hartrees) of neutral and charged annulenes in the singlet and triplet states (N = 12-66) obtained with two different levels of theory with functionals including a different percentage of Hartree Fock exchange: B3LYP (19%) and CAM-B3LYP (19-65%). Note that different scales are used to illustrate better the differences for neutral/charged singlet and triplet annulenes.

Table S9: The relative hardness (in hartrees) of the [*N*]annulenes (*N* = 12-66) with distinct charges and multiplicities obtained using two different level of theory.

	(U)B3LYP/6-31G(d)				(U)CAM-B3LYP/6-31G(d)			
N	**Singlet (0)**	**Singlet (2+)**	**Triplet (0)**	**Triplet (2+)**	**Singlet (0)**	**Singlet (2+)**	**Triplet (0)**	**Triplet (2+)**
12	-0.029	0.028	-0.004	-0.011	-0.016	0.022	-0.008	-0.001
14	0.019	-0.014	-0.023	0.017	-0.001	-0.002	-0.022	0.013
16	-0.023	0.026	0.000	0.011	-0.027	0.019	-0.005	0.020
18	0.016	-0.016	-0.026	0.014	-0.005	-0.009	-0.024	-0.001
20	-0.020	0.026	-0.001	-0.020	-0.027	0.018	-0.003	-0.021
22	0.009	-0.015	-0.022	0.011	-0.002	-0.009	-0.025	-0.001
24	-0.016	0.021	-0.002	-0.021	-0.022	0.012	-0.004	-0.020
26	0.004	-0.012	-0.018	0.007	-0.003	-0.009	-0.021	-0.002
28	-0.016	0.019	-0.001	-0.019	-0.019	0.012	-0.002	-0.018
30	0.003	-0.013	-0.017	0.007	-0.003	-0.010	-0.018	0.001
32	-0.015	0.017	-0.001	-0.017	-0.016	0.011	-0.002	-0.016
34	0.003	-0.010	-0.015	0.004	-0.002	-0.007	-0.015	0.000
36	-0.013	0.012	-0.002	-0.014	-0.014	0.007	-0.003	-0.014
38	0.003	-0.008	-0.013	0.002	-0.002	-0.005	-0.012	-0.001
40	-0.012	0.011	-0.001	-0.013	-0.013	0.007	-0.003	-0.012
42	0.002	-0.009	-0.012	0.003	-0.003	-0.007	-0.011	0.000
44	-0.011	0.010	-0.001	-0.012	-0.011	0.007	-0.002	-0.011
46	0.002	-0.008	-0.011	0.001	-0.002	-0.005	-0.010	-0.002
48	-0.010	0.007	-0.001	-0.010	-0.010	0.004	-0.003	-0.010
50	0.000	-0.006	-0.010	0.001	-0.002	-0.003	-0.008	-0.002
52	-0.009	0.006	-0.001	-0.013	-0.009	0.004	-0.002	-0.008
54	0.001	-0.007	-0.009	0.001	-0.002	-0.004	-0.008	-0.003
56	-0.009	0.006	0.000	-0.009	-0.008	0.004	-0.002	-0.007
58	0.000	-0.006	-0.008	0.001	-0.002	-0.003	-0.007	-0.003
60	-0.008	0.004	-0.001	-0.008	-0.007	0.004	-0.002	-0.007
62	0.000	-0.005	-0.007	0.000	-0.002	-0.002	-0.006	-0.004
64	-0.007	0.004	-0.001	-0.008	-0.007	0.002	-0.002	-0.004
66	0.001	-0.006	-0.007	0.001	-0.002	-0.003	-0.006	0.002

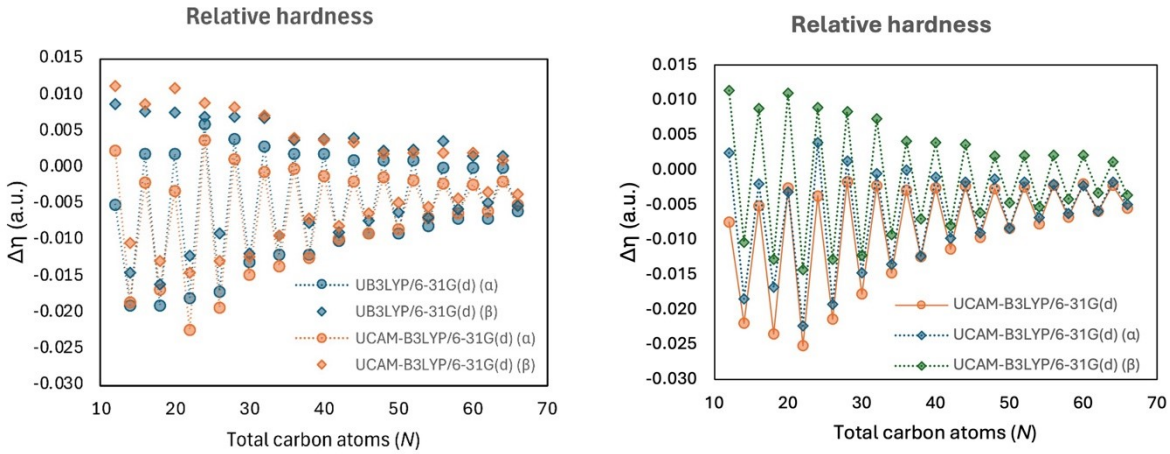

Figure S18: The relative hardness of the triplet neutral [N]annulenes (N=12-66) computed considering the frontier orbital energies of the α- and β-electrons.

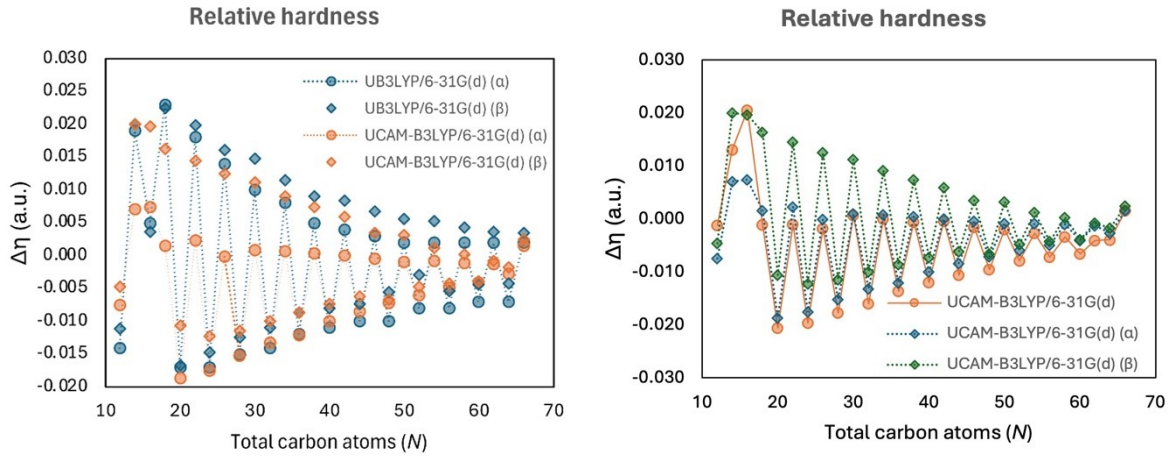

Figure S19: The relative hardness of the triplet charged [N]annulenes (*N* = 12-66) computed considering the frontier orbital energies of the α- and β-electrons as well as different levels of theory.

Error in the QTAIM integrations

Table S10: The error and the total Laplacian of the QTAIM integrations at the (U)B3LYP/6-31G(d) level of theory provided by the ESI-3D calculations.

	(U)B3LYP/6-31G(d)							
	Singlet (0)		Singlet (2+)		Triplet (0)		Triplet (2+)	
N	**Error(S)**	**Laplacian**	**Error(S)**	**Laplacian**	**Error(S)**	**Laplacian**	**Error(S)**	**Laplacian**
12	0.0031	0.0020	0.0050	0.0018	0.0054	0.0019	0.0060	0.0016
14	0.0019	0.0014	0.0044	0.0011	0.0068	0.0016	0.0034	0.0014
16	0.0032	0.0018	0.0052	0.0017	0.0049	0.0015	0.0108	0.0037
18	0.0020	0.0017	0.0050	0.0017	0.0051	0.0018	0.0031	0.0008
20	0.0056	0.0024	0.0094	0.0032	0.0052	0.0016	0.0095	0.0029
22	0.0034	0.0021	0.0062	0.0018	0.0053	0.0019	0.0047	0.0016
24	0.0034	0.0023	0.0067	0.0023	0.0077	0.0020	0.0060	0.0018
26	0.0042	0.0024	0.0067	0.0025	0.0088	0.0023	0.0069	0.0020
28	0.0047	0.0021	0.0077	0.0021	0.0096	0.0019	0.0105	0.0026
30	0.0055	0.0025	0.0115	0.0034	0.0125	0.0030	0.0104	0.0027
32	0.0114	0.0037	0.0209	0.0046	0.0214	0.0048	0.0198	0.0040
34	0.0110	0.0054	0.0125	0.0034	0.0209	0.0059	0.0194	0.0060
36	0.0066	0.0030	0.0124	0.0029	0.0106	0.0021	0.0150	0.0033
38	0.0080	0.0042	0.0186	0.0039	0.0159	0.0043	0.0137	0.0035
40	0.0082	0.0036	0.0145	0.0030	0.0129	0.0028	0.0153	0.0036
42	0.0083	0.0036	0.0185	0.0044	0.0150	0.0032	0.0169	0.0040
44	0.0091	0.0037	0.0159	0.0034	0.0192	0.0045	0.0181	0.0036
46	0.0094	0.0039	0.0183	0.0043	0.0183	0.0034	0.0176	0.0034
48	0.0103	0.0037	0.0190	0.0037	0.0206	0.0041	0.0208	0.0034
50	0.0099	0.0035	0.0183	0.0040	0.0219	0.0042	0.0208	0.0041
52	0.0113	0.0043	0.0216	0.0043	0.0229	0.0039	0.0281	0.0051
54	0.0118	0.0045	0.0228	0.0041	0.0226	0.0044	0.0216	0.0047
56	0.0126	0.0047	0.0220	0.0040	0.0288	0.0053	0.0245	0.0045
58	0.0121	0.0045	0.0266	0.0049	0.0263	0.0047	0.0242	0.0047
60	0.0148	0.0051	0.0246	0.0050	0.0252	0.0044	0.0253	0.0042
62	0.0142	0.0053	0.0270	0.0051	0.0285	0.0048	0.0288	0.0053
64	0.0167	0.0056	0.0279	0.0057	0.0267	0.0048	0.0319	0.0055
66	0.0165	0.0063	0.0259	0.0047	0.0302	0.0047	0.0309	0.0052

Table S11: The error and the total Laplacian of the QTAIM integrations at the (U)CAM-B3LYP/6-311G(d,p) level of theory provided by the ESI-3D calculations.

	(U)CAM-B3LYP/6-311G(d,p)							
	Singlet (0)		Singlet (2+)		Triplet (0)		Triplet (2+)	
N	Error(S)	Laplacian	Error(S)	Laplacian	Error(S)	Laplacian	Error(S)	Laplacian
12	0.0032	0.0019	0.0024	0.0022	0.0046	0.0017	0.0030	0.0013
14	0.0028	0.0020	0.0043	0.0018	0.0065	0.0021	0.0073	0.0018
16	0.0042	0.0025	0.0040	0.0020	0.0082	0.0022	0.0095	0.0025
18	0.0021	0.0014	0.0030	0.0019	0.0059	0.0017	0.0037	0.0014
20	0.0040	0.0032	0.0045	0.0025	0.0103	0.0026	0.0102	0.0028
22	0.0034	0.0020	0.0034	0.0016	0.0084	0.0027	0.0073	0.0020
24	0.0047	0.0027	0.0041	0.0022	0.0072	0.0021	0.0089	0.0023
26	0.0047	0.0024	0.0061	0.0030	0.0131	0.0028	0.0093	0.0023
28	0.0057	0.0027	0.0066	0.0028	0.0111	0.0029	0.0093	0.0025
30	0.0060	0.0028	0.0071	0.0037	0.0126	0.0028	0.0110	0.0025
32	0.0078	0.0030	0.0154	0.0044	0.0125	0.0029	0.0120	0.0028
34	0.0121	0.0048	0.0079	0.0038	0.0264	0.0062	0.0149	0.0032
36	0.0079	0.0035	0.0069	0.0028	0.0123	0.0033	0.0145	0.0028
38	0.0104	0.0043	0.0079	0.0032	0.0186	0.0037	0.0147	0.0031
40	0.0095	0.0037	0.0066	0.0032	0.0173	0.0036	0.0156	0.0037
42	0.0105	0.0040	0.0078	0.0032	0.0172	0.0033	0.0170	0.0036
44	0.0121	0.0043	0.0091	0.0041	0.0201	0.0041	0.0181	0.0036
46	0.0114	0.0039	0.0105	0.0048	0.0189	0.0042	0.0192	0.0036
48	0.0135	0.0048	0.0102	0.0037	0.0211	0.0036	0.0222	0.0045
50	0.0136	0.0044	0.0113	0.0043	0.0248	0.0044	0.0220	0.0040
52	0.0135	0.0049	0.0124	0.0044	0.0255	0.0048	0.0264	0.0047
54	0.0140	0.0049	0.0129	0.0044	0.0250	0.0047	0.0244	0.0046
56	0.0149	0.0047	0.0127	0.0046	0.0289	0.0051	0.0327	0.0051
58	0.0137	0.0045	0.0142	0.0049	0.0281	0.0045	0.0284	0.0054
60	0.0197	0.0059	0.0152	0.0053	0.0276	0.0050	0.0316	0.0052
62	0.0190	0.0057	0.0157	0.0058	0.0293	0.0041	0.0336	0.0050
64	0.0209	0.0065	0.0183	0.0061	0.0292	0.0056	0.0331	0.0051
66	0.0197	0.0061	0.0171	0.0054	0.0330	0.0048	0.0334	0.0050

Correlation plots between the B3LYP and CAM-B3LYP indices of aromaticity

Table S12: Correlation coefficients (R^2) between the aromaticity indices computed using B3LYP and CAM-B3LYP for all the [N]annulenes with N = 12-66 (112 systems). $R^2 > 0.60$ are indicated in green.

index	R^2
HOMA	0.60
BLA	0.51
FLU	0.58
BOA	0.50
AV1245	0.68
AV_{min}	0.75
GIMIC	0.50
$NICS(1)_{zz}$	0.60
Δη	0.81
ASE	0.59

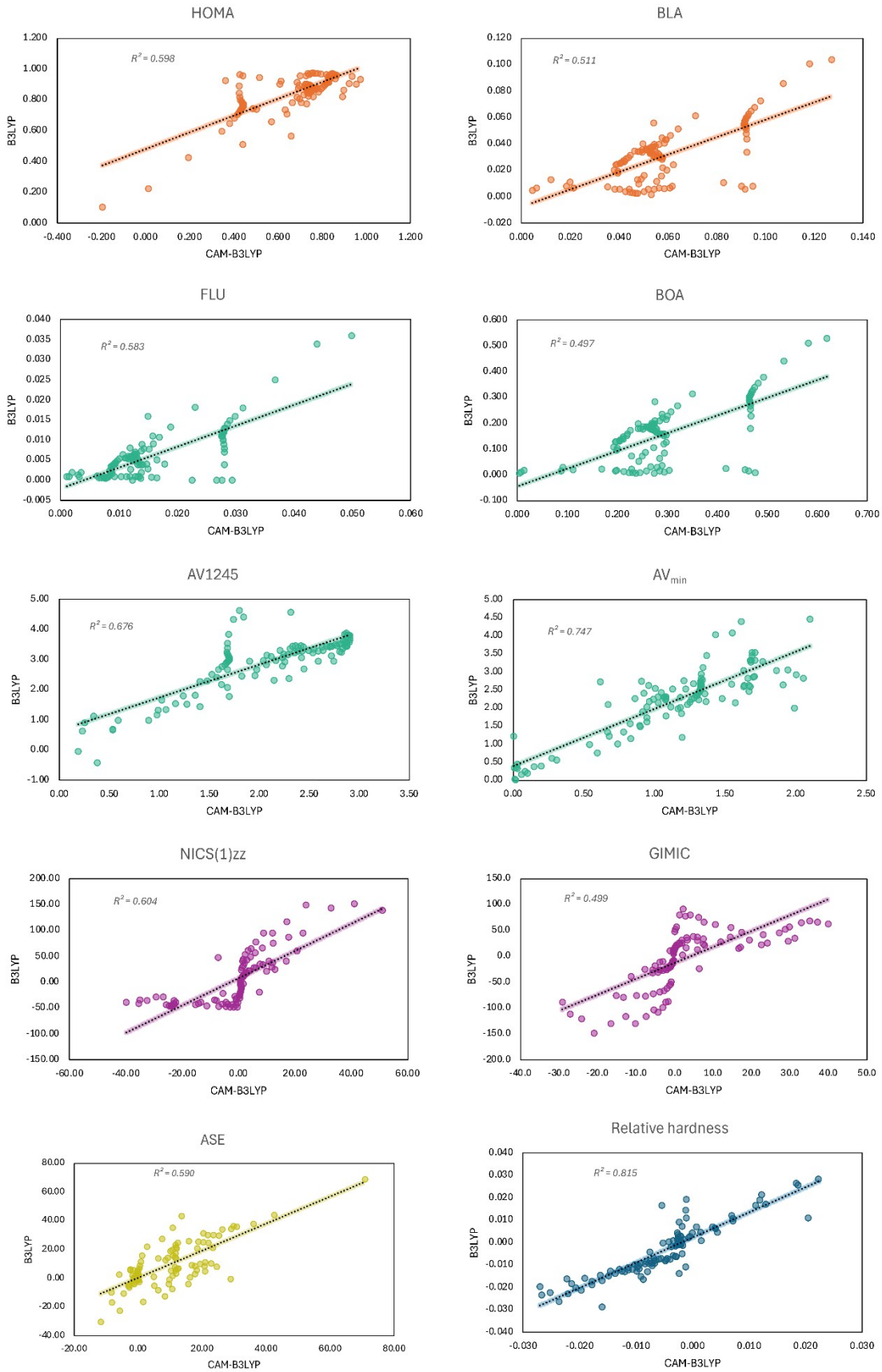

Figure S20: The correlation plots between the aromaticity indices evolution of the neutral and charged [N]annulenes in the singlet and triplet states (N = 12-66) computed with B3LYP and CAM-B3LYP (112 systems).

B3LYP aromaticity results

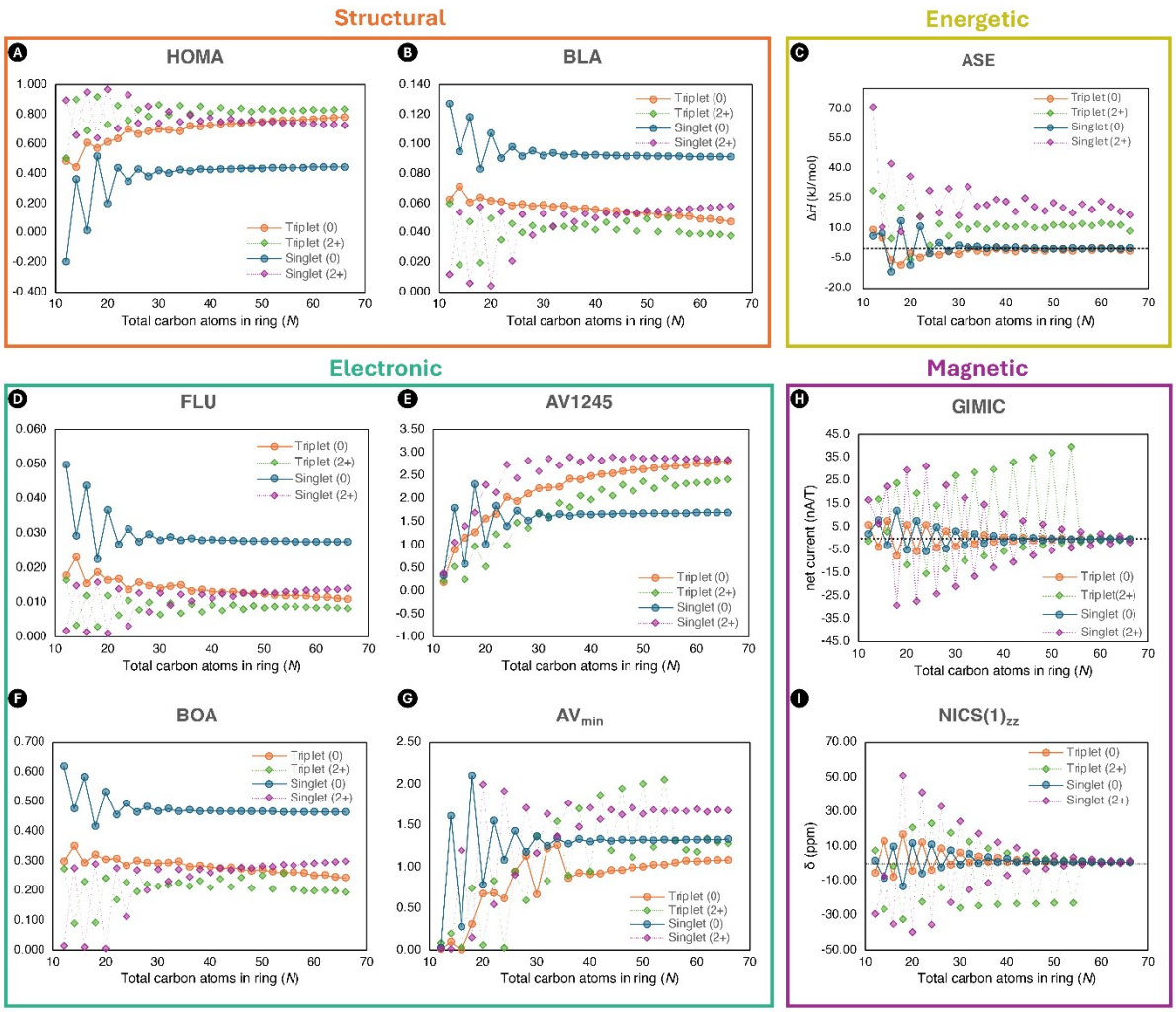

Figure S21: The evolution of selected aromaticity descriptors rooted in distinct criteria structural (A,B), energetic (C), electronic (D-G), and magnetic (H,I) of the neutral and charged [*N*]annulenes in the singlet and triplet states (*N* = 12-66) computed using the B3LYP/6-31G(d) level of theory.

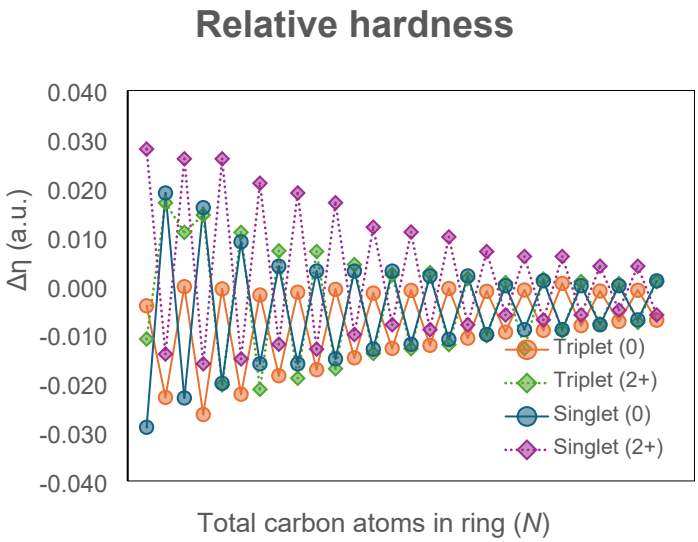

Figure S22: The relative hardness of the neutral and charged [N]annulenes (*N* = 12-66) computed with the B3LYP/6-31G(d) level of theory.

Spin density

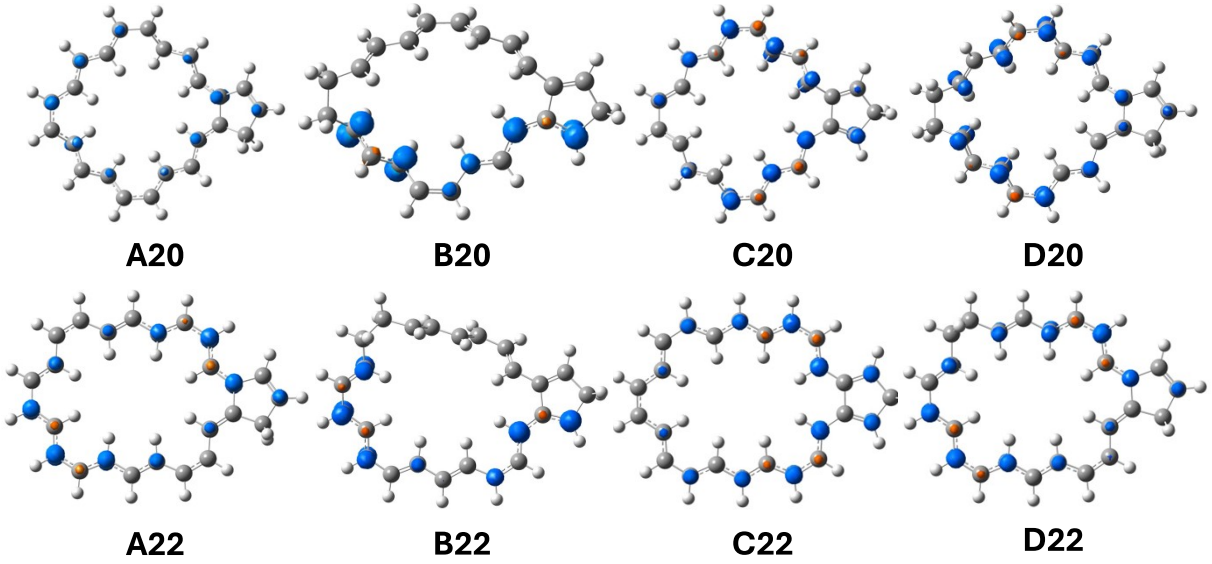

Figure S23: The spin densities of the structures employed in the ISE_{II} method. The [20]- and [22]annulenes are presented as examples to illustrate the spin density locations within the molecule (isovalue: 0.015). All structures are triplet neutral species (B3LYP/6-31G(d)).

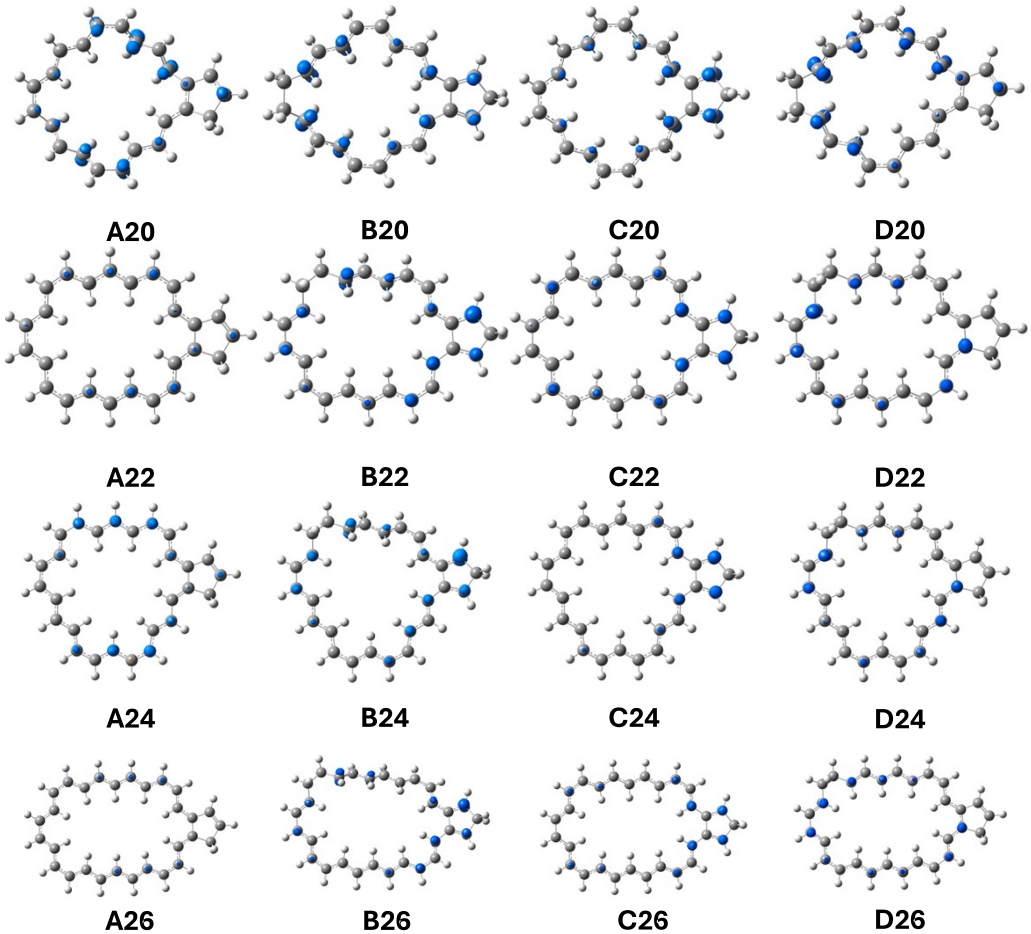

Figure S24: The spin densities of the structures employed in the ISE_{II} method for the [20]-, [22]-, [24]-, and [26]annulenes are presented to illustrate their respective locations within the molecule (isovalue: 0.015). All structures are triplet dicationic species (B3LYP/6-31G(d)).

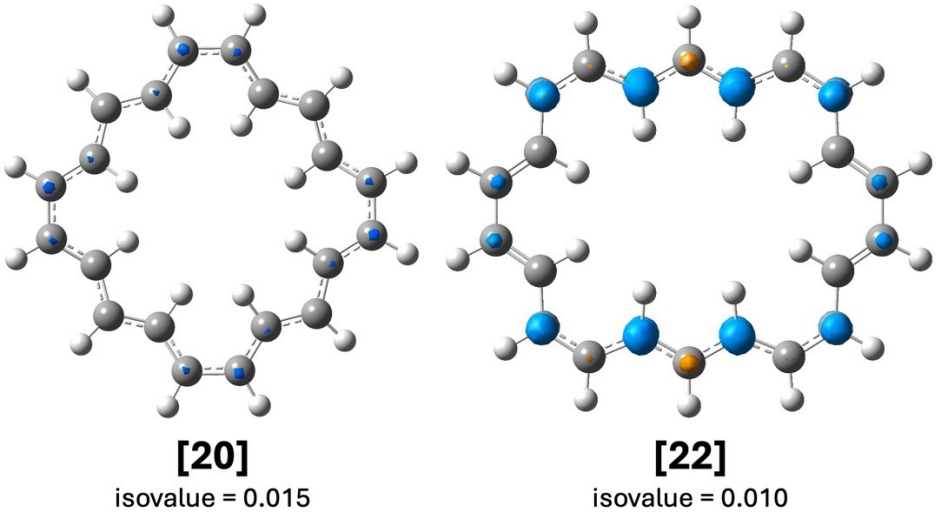

Figure S25: The spin density of the neutral triplet [20]- and [22]annulenes (B3LYP/6-31G(d)).

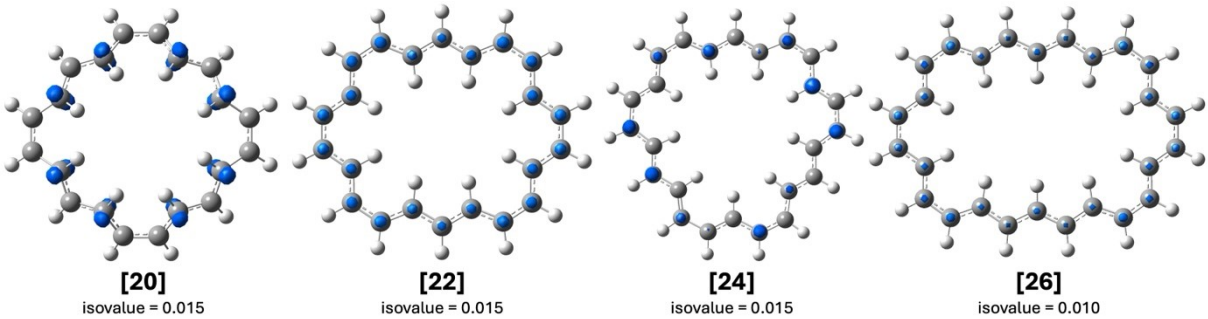

Figure S26: The spin density of the triplet dicationic [20]-, [22]-, [24]-, and [26]annulenes (B3LYP/6-31G(d)).

$EDDB_{norm}$ results

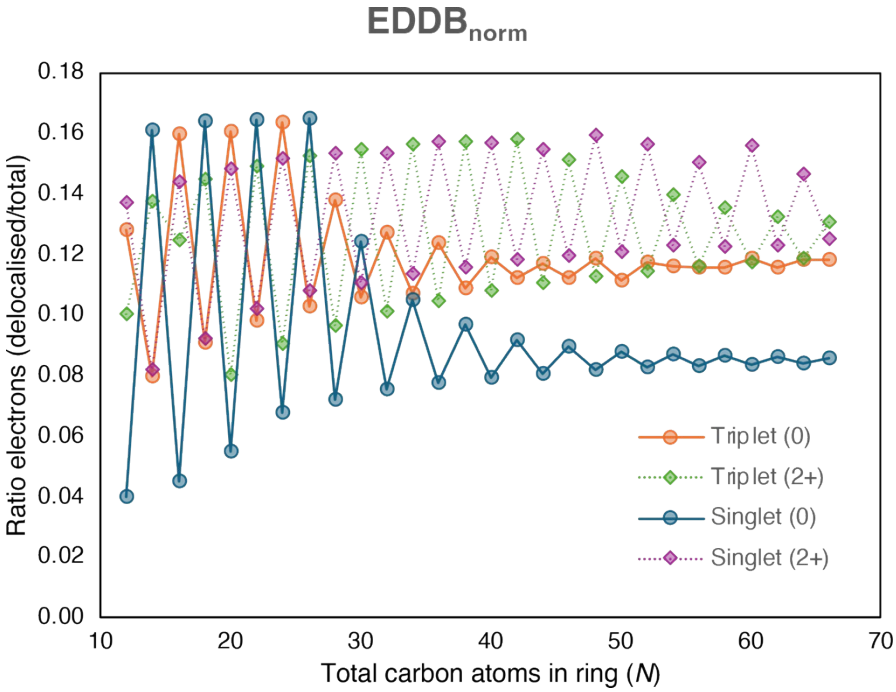

Figure S27: The evolution of $EDDB_{norm}$ index of the neutral and charged [*N*]annulenes in the singlet and triplet states (*N*=12-66). $EDDB_{norm}$ is the ratio of the delocalised electrons and the total amount of electrons in the system (B3LYP/6-31G(d)).

Table S13: The $EDDB_{norm}$ values, corresponding to the ratio of the total amount of delocalised electrons and the total amount of electrons in the system (delocalised/total).

	$EDDB_{norm}$ (delocalised/total)			
N	**Triplet (0)**	**Triplet (2+)**	**Singlet (0)**	**Singlet (2+)**
12	0.1280	0.1001	0.0400	0.1370
14	0.0799	0.1374	0.1610	0.0821
16	0.1597	0.1248	0.0453	0.1438
18	0.0907	0.1448	0.1639	0.0922
20	0.1606	0.0800	0.0551	0.1483
22	0.0981	0.1492	0.1643	0.1020
24	0.1637	0.0904	0.0677	0.1515
26	0.1028	0.1524	0.1649	0.1079
28	0.1381	0.0964	0.0722	0.1531
30	0.1058	0.1548	0.1241	0.1107
32	0.1274	0.1011	0.0753	0.1535
34	0.1072	0.1563	0.1050	0.1135
36	0.1236	0.1048	0.0776	0.1571
38	0.1089	0.1572	0.0967	0.1158
40	0.1191	0.1081	0.0794	0.1567
42	0.1123	0.1582	0.0918	0.1183
44	0.1172	0.1104	0.0808	0.1547
46	0.1123	0.1510	0.0894	0.1196
48	0.1187	0.1129	0.0818	0.1595
50	0.1115	0.1456	0.0881	0.1208
52	0.1172	0.1146	0.0826	0.1561
54	0.1159	0.1396	0.0871	0.1228
56	0.1158	0.1160	0.0832	0.1502
58	0.1158	0.1356	0.0866	0.1227
60	0.1188	0.1175	0.0837	0.1560
62	0.1156	0.1324	0.0862	0.1231
64	0.1182	0.1185	0.0841	0.1465
66	0.1184	0.1305	0.0859	0.1249

EDDB visualisation

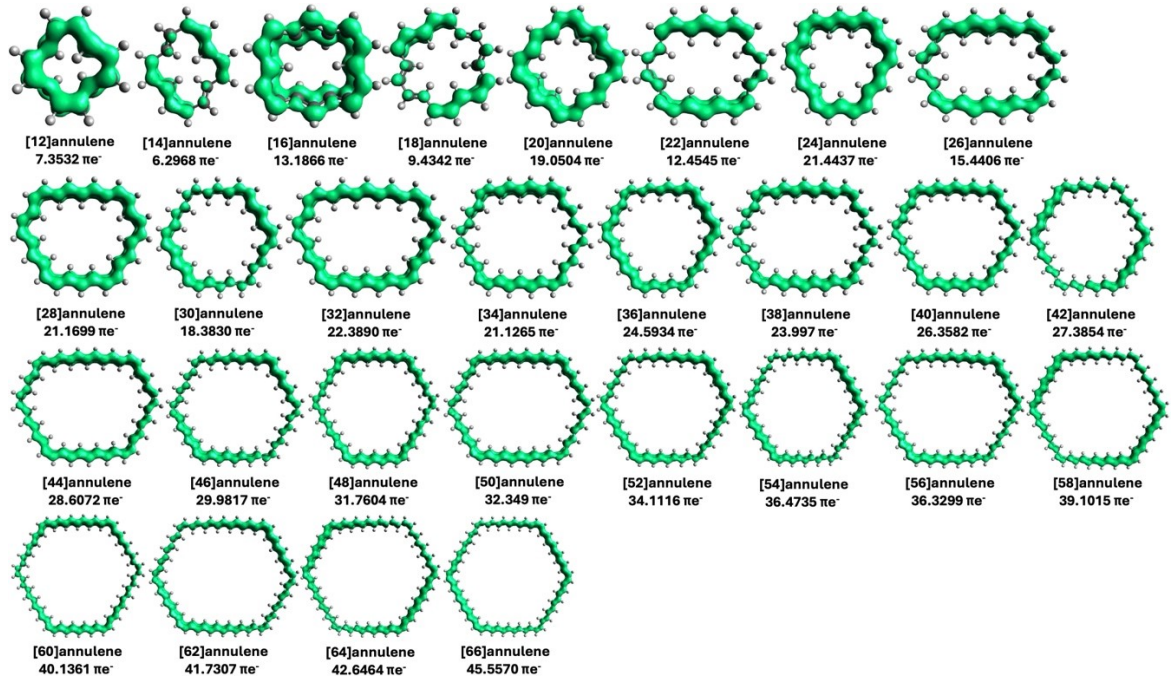

Figure S28: Visualisation of the electron density of delocalised π-electrons of the neutral triplet [*N*]annulenes determined by the EDDB software (B3LYP/6-31G(d)). Figures were generated with the Avogadro program (isovalue: 0.015).

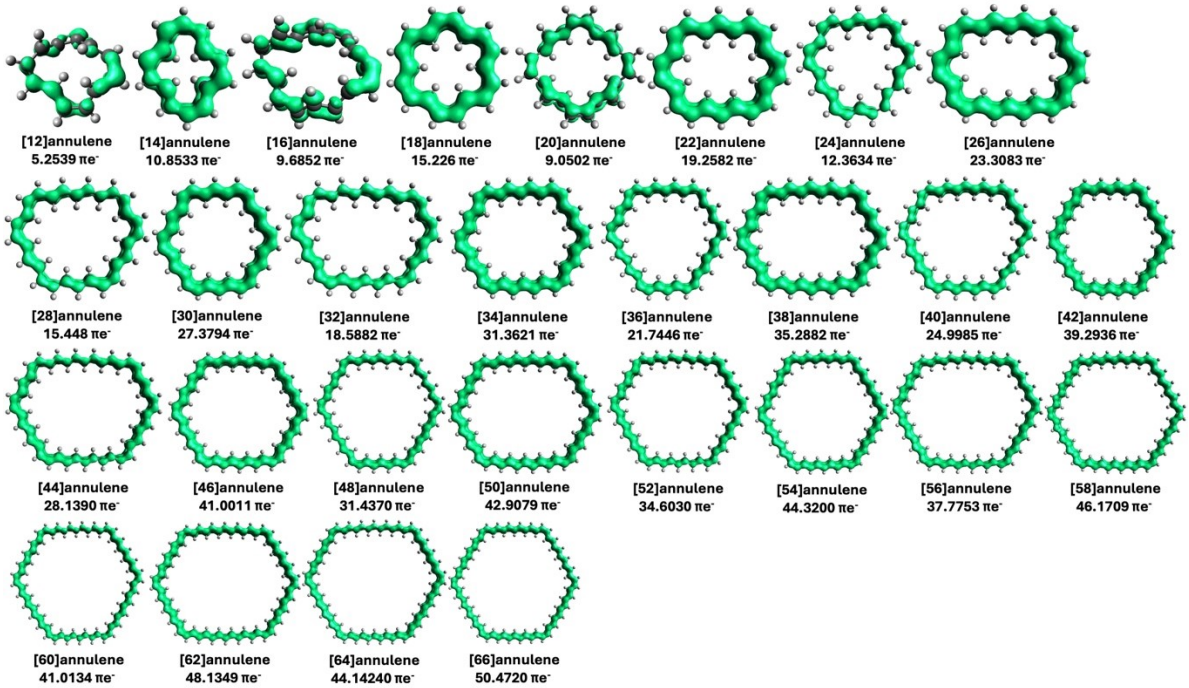

Figure S29: Visualisation of the electron density of delocalised π-electrons of the triplet dicationic [*N*]annulenes determined by the EDDB software (B3LYP/6-31G(d)). Figures were generated with the Avogadro program (isovalue: 0.015).

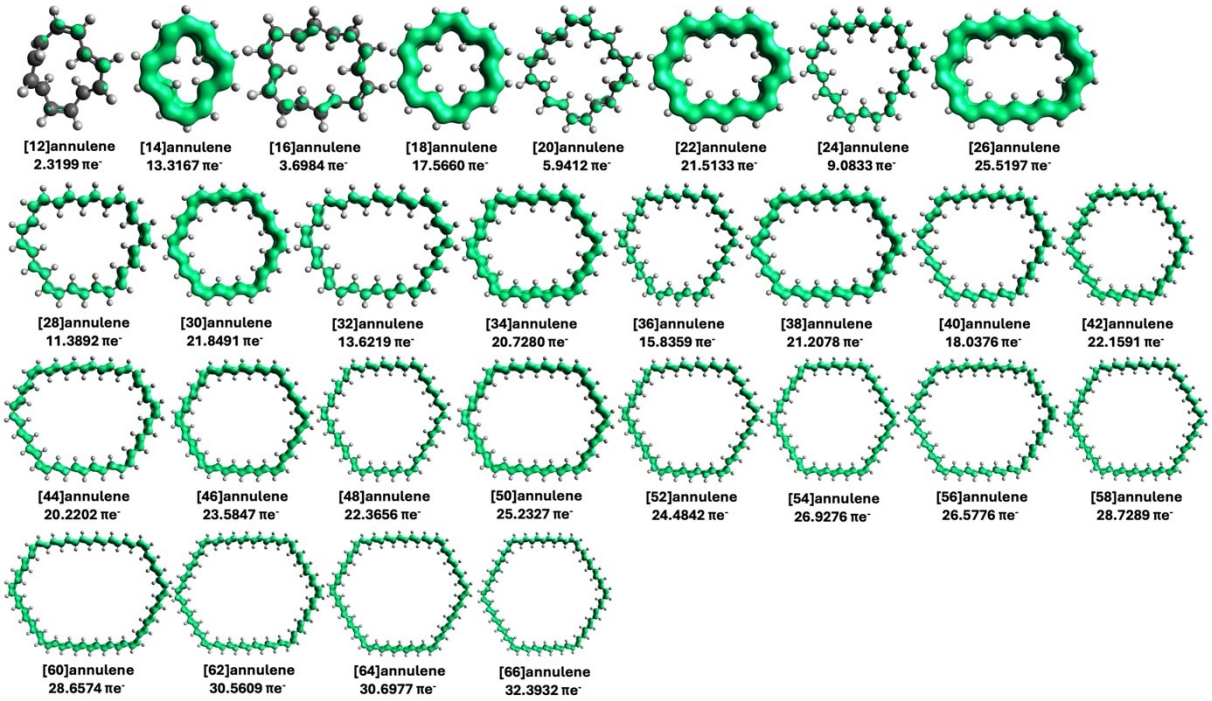

Figure S30: Visualisation of the electron density of delocalised π-electrons of the neutral singlet [*N*]annulenes determined by the EDDB software (B3LYP/6-31G(d)). Figures were generated with the Avogadro program (isovalue: 0.015).

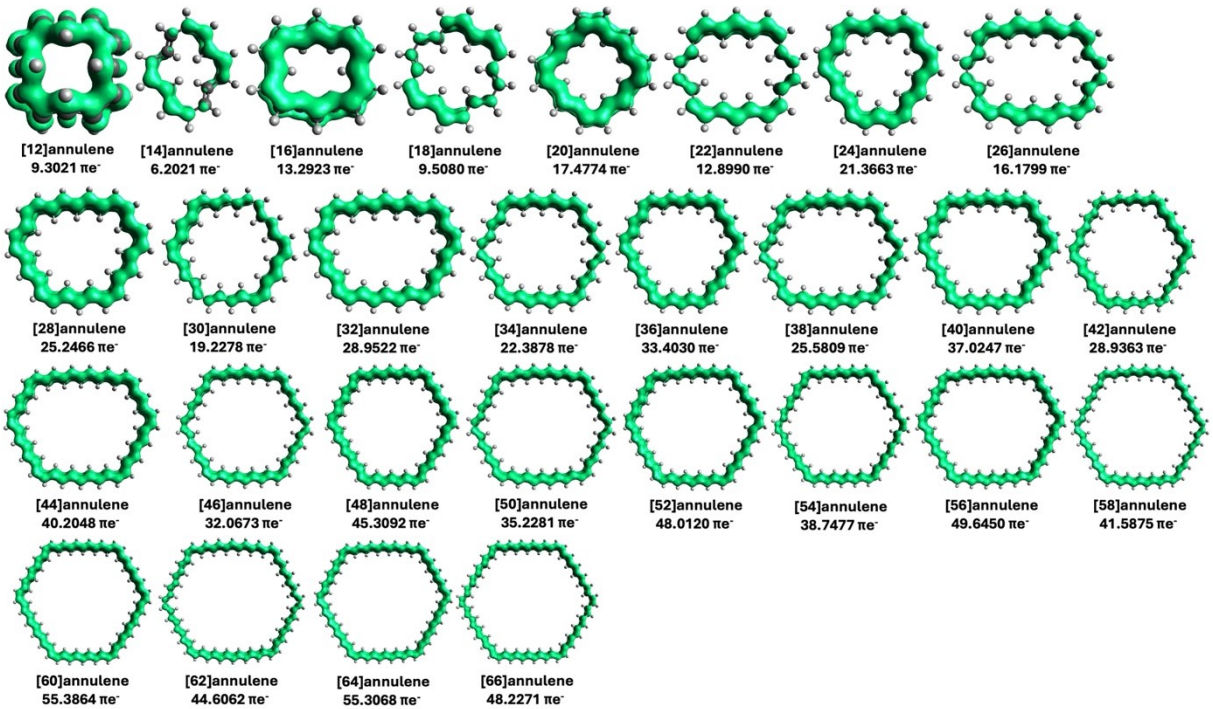

Figure S31: Visualisation of the electron density of delocalised π-electrons of the singlet dicationic [*N*]annulenes determined by the EDDB software (B3LYP/6-31G(d)). Figures were generated with the Avogadro program (isovalue: 0.015).

Aromatic stabilisation energy results of the [*N*]annulenes

Table S14: The aromatic stabilisation energy for the neutral triplet annulenes (UB3LYP/6-31G(d)). The EE and ZPVE of the **B** and **D** geometries were obtained from the supporting information of ref. [26].

Triplet (0)	$A_{Triplet}$	$B_{singlet}$	$C_{Triplet}$	$D_{Singlet}$	ASE
N	EE+ZPVE (Hartree)	EE+ZPVE (Hartree)	EE+ZPVE (Hartree)	EE+ZPVE (Hartree)	(**C**+**D**)-(**A**+**B**) (kJ/mol)
12	-579.578429	-581.00744	-579.567969	-581.0124	14.44
14	-657.00881	-658.195294	-657.00698	-658.199063	-5.09
16	-734.365018	-735.86909	-734.355442	-735.87761	2.77
18	-811.777827	-812.962504	-811.774288	-812.972397	-16.68
20	-889.130864	-890.70503	-889.118353	-890.71528	5.94
22	-966.535757	-967.712696	-966.528091	-967.724267	-10.25
24	-1043.920368	-1045.5518	-1043.904319	-1045.56548	6.22
26	-1121.290506	-1122.462569	-1121.280299	-1122.474671	-4.98
28	-1198.671841	-1199.836657	-1198.65641	-1199.849834	5.92
30	-1276.043573	-1277.211923	-1276.033154	-1277.224258	-5.03
32	-1353.422861	-1354.58551	-1353.407637	-1354.598925	4.75
34	-1430.795684	-1431.96073	-1430.784031	-1431.973484	-2.89
36	-1508.173444	-1509.335025	-1508.159325	-1509.348374	2.02
38	-1585.547131	-1586.7095	-1585.534459	-1586.722525	-0.93
40	-1662.923896	-1664.083788	-1662.909676	-1664.097243	2.01
42	-1740.297674	-1741.458114	-1740.285072	-1741.47136	-1.69
44	-1817.674172	-1818.832465	-1817.659809	-1818.84602	2.12
46	-1895.04826	-1896.206834	-1895.035065	-1896.220233	-0.54
48	-1972.423971	-1973.581144	-1972.410172	-1973.59475	0.51
50	-2049.798588	-2050.955485	-2049.784925	-2050.968995	0.40
52	-2127.17397	-2128.32979	-2127.159976	-2128.343472	0.82
54	-2204.548428	-2205.704138	-2204.535056	-2205.717716	-0.54
56	-2281.923866	-2283.078476	-2281.909684	-2283.092193	1.22
58	-2359.298393	-2360.452793	-2359.284704	-2360.466449	0.09
60	-2436.673414	-2437.827096	-2436.659649	-2437.840871	-0.03
62	-2514.04824	-2515.201456	-2514.034299	-2515.215158	0.63
64	-2591.423156	-2592.575758	-2591.409209	-2592.589529	0.46
66	-2668.797769	-2669.95006	-2668.784125	-2669.963798	-0.25

Table S15: The aromatic stabilisation energy for the triplet dicationic annulenes (UB3LYP/6-31G(d)). The EE and ZPVE of the **B** and **D** geometries were obtained from the supporting information of ref. [26].

Triplet (2+)	$\mathbf{A}_{\text{triplet charged}}$	$\mathbf{B}_{\text{singlet neutral}}$	$\mathbf{C}_{\text{triplet charged}}$	$\mathbf{D}_{\text{singlet neutral}}$	ASE
N	EE+ZPVE (Hartree)	EE+ZPVE (Hartree)	EE+ZPVE (Hartree)	EE+ZPVE (Hartree)	(**C**+**D**)-(**A**+**B**) (kJ/mol)
12	-578.961141	-581.00744	-578.956286	-581.0124	-0.28
14	-656.430638	-658.195294	-656.413916	-658.199063	34.01
16	-733.796551	-735.86909	-733.78762	-735.87761	1.08
18	-811.239436	-812.962504	-811.217566	-812.972397	31.45
20	-888.589043	-890.70503	-888.587297	-890.71528	-22.33
22	-966.024068	-967.712696	-966.00252	-967.724267	26.19
24	-1043.402317	-1045.5518	-1043.394813	-1045.56548	-16.22
26	-1120.79995	-1122.462569	-1120.778344	-1122.474671	24.95
28	-1198.177655	-1199.836657	-1198.167506	-1199.849834	-7.95
30	-1275.572515	-1277.211923	-1275.55126	-1277.224258	23.42
32	-1352.947377	-1354.58551	-1352.935401	-1354.598925	-3.78
34	-1430.339376	-1431.96073	-1430.318266	-1431.973484	21.94
36	-1507.714653	-1509.335025	-1507.701532	-1509.348374	-0.60
38	-1585.103023	-1586.7095	-1585.081995	-1586.722525	21.01
40	-1662.47823	-1664.083788	-1662.464067	-1664.097243	1.86
42	-1739.864973	-1741.458114	-1739.844113	-1741.47136	19.99
44	-1817.239417	-1818.832465	-1817.22446	-1818.84602	3.68
46	-1894.624571	-1896.206834	-1894.603981	-1896.220233	18.88
48	-1971.999439	-1973.581144	-1971.983751	-1973.59475	5.47
50	-2049.382425	-2050.955485	-2049.362265	-2050.968995	17.46
52	-2126.75734	-2128.32979	-2126.741453	-2128.343472	5.79
54	-2204.13932	-2205.704138	-2204.119721	-2205.717716	15.81
56	-2281.514272	-2283.078476	-2281.498037	-2283.092193	6.61
58	-2358.895168	-2360.452793	-2358.875916	-2360.466449	14.69
60	-2436.270315	-2437.827096	-2436.253873	-2437.840871	7.00
62	-2513.65021	-2515.201456	-2513.631214	-2515.215158	13.90
64	-2591.025588	-2592.575758	-2591.008855	-2592.589529	7.78
66	-2668.404665	-2669.95006	-2668.386027	-2669.963798	12.86

Table S16: The aromatic stabilisation energy for the closed-shell dicationic annulenes (B3LYP/6-31G(d)). The EE and ZPVE of the **B** and **D** geometries were obtained from the supporting information of ref. [26].

Singlet (2+)	$\mathbf{A}_{\text{Singlet Charged}}$	$\mathbf{B}_{\text{Singlet Neutral}}$	$\mathbf{C}_{\text{Singlet Charged}}$	$\mathbf{D}_{\text{Singlet Neutral}}$	**ASE**
N	EE+ZPVE (Hartree)	EE+ZPVE (Hartree)	EE+ZPVE (Hartree)	EE+ZPVE (Hartree)	(**C**+**D**)-(**A**+**B**) (kJ/mol)
12	-578.999126	-581.00744	-578.967908	-581.0124	68.94
14	-656.439729	-658.195294	-656.438707	-658.199063	-7.21
16	-733.82673	-735.86909	-733.801399	-735.87761	44.14
18	-811.243405	-812.962504	-811.238155	-812.972397	-12.19
20	-888.622917	-890.70503	-888.598198	-890.71528	37.99
22	-966.028137	-967.712696	-966.018012	-967.724267	-3.80
24	-1043.431801	-1045.5518	-1043.404962	-1045.56548	34.55
26	-1120.803803	-1122.462569	-1120.790546	-1122.474671	3.03
28	-1198.202894	-1199.836657	-1198.175781	-1199.849834	36.59
30	-1275.575697	-1277.211923	-1275.563011	-1277.224258	0.92
32	-1352.969278	-1354.58551	-1352.942141	-1354.598925	36.03
34	-1430.342262	-1431.96073	-1430.327638	-1431.973484	4.91
36	-1507.733788	-1509.335025	-1507.708868	-1509.348374	30.38
38	-1585.105631	-1586.7095	-1585.089479	-1586.722525	8.21
40	-1662.494895	-1664.083788	-1662.469957	-1664.097243	30.15
42	-1739.86706	-1741.458114	-1739.851516	-1741.47136	6.03
44	-1817.253978	-1818.832465	-1817.229091	-1818.84602	29.75
46	-1894.626402	-1896.206834	-1894.609772	-1896.220233	8.48
48	-1972.011999	-1973.581144	-1971.98857	-1973.59475	25.79
50	-2049.384226	-2050.955485	-2049.366701	-2050.968995	10.54
52	-2126.768437	-2128.32979	-2126.74509	-2128.343472	25.38
54	-2204.14097	-2205.704138	-2204.124109	-2205.717716	8.62
56	-2281.523793	-2283.078476	-2281.500602	-2283.092193	24.87
58	-2358.896714	-2360.452793	-2358.879193	-2360.466449	10.15
60	-2436.278578	-2437.827096	-2436.256662	-2437.840871	21.37
62	-2513.651569	-2515.201456	-2513.633514	-2515.215158	11.43
64	-2591.032476	-2592.575758	-2591.010737	-2592.589529	20.92
66	-2668.405692	-2669.95006	-2668.388349	-2669.963798	9.46

Table S17: The aromatic stabilisation energy for the closed-shell neutral annulenes (B3LYP/6-31G(d)). The geometries were optimised without any constraints and do not contain imaginary frequencies.

Singlet (0)	A	B	C	D	ASE
N	EE+ZPEC (Hartree)	EE+ZPEC (Hartree)	EE+ZPEC (Hartree)	EE+ZPEC (Hartree)	(C+D)-(A+B) (kJ/mol)
12	-579.614483	-580.832116	-579.607647	-580.833682	13.84
14	-657.050448	-658.224014	-657.035656	-658.228362	27.42
16	-734.379855	-735.580202	-734.381804	-735.589802	-30.32
18	-811.815412	-812.977433	-811.791917	-812.984442	43.28
20	-889.141833	-890.332792	-889.139935	-890.338317	-9.52
22	-966.564865	-967.726611	-966.542652	-967.735346	35.39
24	-1043.928241	-1045.10232	-1043.918573	-1045.114366	-6.24
26	-1121.313332	-1122.476755	-1121.293135	-1122.488476	22.25
28	-1198.67932	-1199.85126	-1198.668172	-1199.863887	-3.88
30	-1276.06124	-1277.226069	-1276.043092	-1277.23819	15.82
32	-1353.42961	-1354.600132	-1353.417439	-1354.613137	-2.19
34	-1430.809335	-1431.974913	-1430.792322	-1431.987464	11.71
36	-1508.179594	-1509.34932	-1508.167006	-1509.362312	-1.06
38	-1585.557651	-1586.723741	-1585.541384	-1586.736606	8.93
40	-1662.929068	-1664.098116	-1662.915969	-1664.111295	-0.21
42	-1740.306043	-1741.472521	-1740.290318	-1741.485529	7.13
44	-1817.678324	-1818.846886	-1817.664858	-1818.860205	0.39
46	-1895.05458	-1896.221279	-1895.039225	-1896.234466	5.69
48	-1972.427403	-1973.595647	-1972.413706	-1973.609006	0.89
50	-2049.803176	-2050.970006	-2049.788012	-2050.983328	4.84
52	-2127.176395	-2128.344361	-2127.162493	-2128.357802	1.21
54	-2204.551766	-2205.718751	-2204.536865	-2205.732101	4.07
56	-2281.925304	-2283.093061	-2281.911245	-2283.106567	1.45
58	-2359.3004	-2360.467441	-2359.285609	-2360.480894	3.51
60	-2436.674146	-2437.841748	-2436.659971	-2437.855307	1.62
62	-2514.049038	-2515.215836	-2514.034324	-2515.229627	2.42
64	-2591.422913	-2592.59018	-2591.408702	-2592.60401	1.00
66	-2668.79767	-2669.964559	-2668.783051	-2669.978314	2.27

Table S18: The aromatic stabilisation energy for the neutral triplet annulenes (UB3LYP/6-31G(d)). The geometries were optimised without any constraints and do not contain imaginary frequencies.

Triplet (0)	A	B	C	D	ASE
N	EE+ZPVE (Hartree)	EE+ZPVE (Hartree)	EE+ZPVE (Hartree)	EE+ZPVE (Hartree)	(**C**+**D**)-(**A**+**B**) (kJ/mol)
12	-579.578429	-580.776098	-579.567969	-580.770706	41.62
14	-657.00881	-658.172843	-657.00698	-658.193134	-48.47
16	-734.365018	-735.545986	-734.355442	-735.551356	11.04
18	-811.777827	-812.945767	-811.774288	-812.965758	-43.19
20	-889.130864	-890.296798	-889.118353	-890.314729	-14.23
22	-966.535757	-967.698792	-966.528091	-967.72113	-38.52
24	-1043.920368	-1045.076695	-1043.904319	-1045.097297	-11.95
26	-1121.290506	-1122.451049	-1121.280299	-1122.474562	-34.93
28	-1198.671841	-1199.828408	-1198.65641	-1199.850285	-16.92
30	-1276.043573	-1277.205369	-1276.033154	-1277.226636	-28.48
32	-1353.422861	-1354.579673	-1353.407637	-1354.599111	-11.06
34	-1430.795684	-1431.956179	-1430.784031	-1431.978169	-27.14
36	-1508.173444	-1509.332323	-1508.159325	-1509.349782	-8.77
38	-1585.547131	-1586.706752	-1585.534459	-1586.72922	-25.72
40	-1662.923896	-1664.082667	-1662.909676	-1664.10101	-10.82
42	-1740.297674	-1741.458487	-1740.285072	-1741.476006	-12.91
44	-1817.674172	-1818.833812	-1817.659809	-1818.854818	-17.44
46	-1895.04826	-1896.208506	-1895.035065	-1896.229905	-21.54
48	-1972.423971	-1973.584012	-1972.410172	-1973.601556	-9.83
50	-2049.798588	-2050.958401	-2049.784925	-2050.980103	-21.11
52	-2127.17397	-2128.333795	-2127.159976	-2128.349243	-3.82
54	-2204.548428	-2205.709135	-2204.535056	-2205.72986	-19.31
56	-2281.923866	-2283.083489	-2281.909684	-2283.09946	-4.70
58	-2359.298393	-2360.458756	-2359.284704	-2360.477138	-12.32
60	-2436.673414	-2437.833935	-2436.659649	-2437.849182	-3.89
62	-2514.04824	-2515.205873	-2514.034299	-2515.227206	-19.41
64	-2591.423156	-2592.583424	-2591.409209	-2592.601952	-12.03
66	-2668.797769	-2669.955372	-2668.784125	-2669.973997	-13.08

Table S19: The aromatic stabilisation energy for the triplet dicationic annulenes (UB3LYP/6-31G(d)). The geometries were optimised without any constraints and do not contain imaginary frequencies.

Triplet (2+)	**A**	**B**	**C**	**D**	**ASE**
N	EE+ZPVE (Hartree)	EE+ZPVE (Hartree)	EE+ZPVE (Hartree)	EE+ZPVE (Hartree)	(**C**+**D**)-(**A**+**B**) (kJ/mol)
12	-578.961141	-580.195674	-578.956286	-580.173449	71.10
14	-656.430638	-657.606266	-656.413916	-657.610113	33.80
16	-733.796551	-734.995608	-733.78762	-734.993641	28.61
18	-811.239436	-812.401869	-811.217566	-812.405957	46.69
20	-888.589043	-889.782212	-888.587297	-889.784944	-2.59
22	-966.024068	-967.182997	-966.00252	-967.19169	33.75
24	-1043.402317	-1044.569747	-1043.394813	-1044.584606	-19.31
26	-1120.79995	-1121.958394	-1120.778344	-1121.968872	29.22
28	-1198.177655	-1199.343495	-1198.167506	-1199.358465	-12.66
30	-1275.572515	-1276.729515	-1275.55126	-1276.743791	18.32
32	-1352.947377	-1354.112309	-1352.935401	-1354.12468	-1.04
34	-1430.339376	-1431.494225	-1430.318266	-1431.511195	10.87
36	-1507.714653	-1508.875212	-1507.701532	-1508.891784	-9.06
38	-1585.103023	-1586.258635	-1585.081995	-1586.27534	11.35
40	-1662.47823	-1663.638857	-1662.464067	-1663.654857	-4.82
42	-1739.864973	-1741.018127	-1739.844113	-1741.036103	7.57
44	-1817.239417	-1818.400149	-1817.22446	-1818.418577	-9.11
46	-1894.624571	-1895.778951	-1894.603981	-1895.798613	2.44
48	-1971.999439	-1973.157509	-1971.983751	-1973.175418	-5.83
50	-2049.382425	-2050.538034	-2049.362265	-2050.557003	3.13
52	-2126.75734	-2127.916175	-2126.741453	-2127.933703	-4.31
54	-2204.13932	-2205.29378	-2204.119721	-2205.315135	-4.61
56	-2281.514272	-2282.673525	-2281.498037	-2282.690516	-1.98
58	-2358.895168	-2360.050895	-2358.875916	-2360.068997	3.02
60	-2436.270315	-2437.428145	-2436.253873	-2437.446913	-6.11
62	-2513.65021	-2514.806305	-2513.631214	-2514.824501	2.10
64	-2591.025588	-2592.183973	-2591.008855	-2592.202098	-3.65
66	-2668.404665	-2669.557972	-2668.386027	-2669.576957	-0.91

Table S20: The aromatic stabilisation energy for the closed-shell dicationic annulenes (B3LYP/6-31G(d)). The geometries were optimised without any constraints and do not contain imaginary frequencies.

Singlet (2+)	**A**	**B**	**C**	**D**	**ASE**
N	EE+ZPVE (Hartree)	EE+ZPVE (Hartree)	EE+ZPVE (Hartree)	EE+ZPVE (Hartree)	(**C**+**D**)-(**A**+**B**) (kJ/mol)
12	-578.999126	-580.191222	-578.967908	-580.186556	94.21
14	-656.439729	-657.596371	-656.438707	-657.626213	-75.67
16	-733.82673	-734.984833	-733.801399	-735.007741	6.36
18	-811.243405	-812.397026	-811.238155	-812.436596	-90.11
20	-888.622917	-889.764018	-888.598198	-889.800317	-30.40
22	-966.028137	-967.176849	-966.018012	-967.217715	-80.71
24	-1043.431801	-1044.564375	-1043.404962	-1044.602959	-30.84
26	-1120.803803	-1121.950471	-1120.790546	-1121.991121	-71.92
28	-1198.202894	-1199.335379	-1198.175781	-1199.374983	-32.80
30	-1275.575697	-1276.723137	-1275.563011	-1276.761288	-66.86
32	-1352.969278	-1354.10257	-1352.942141	-1354.142211	-32.83
34	-1430.342262	-1431.488459	-1430.327638	-1431.526747	-62.13
36	-1507.733788	-1508.869585	-1507.708868	-1508.907055	-32.95
38	-1585.105631	-1586.25126	-1585.089479	-1586.289265	-57.38
40	-1662.494895	-1663.631356	-1662.469957	-1663.668899	-33.09
42	-1739.86706	-1741.014078	-1739.851516	-1741.04984	-53.08
44	-1817.253978	-1818.394021	-1817.229091	-1818.428658	-25.60
46	-1894.626402	-1895.773123	-1894.609772	-1895.808784	-49.97
48	-1972.011999	-1973.151623	-1971.98857	-1973.186862	-31.01
50	-2049.384226	-2050.530879	-2049.366701	-2050.566231	-46.80
52	-2126.768437	-2127.908852	-2126.74509	-2127.943977	-30.92
54	-2204.14097	-2205.289008	-2204.124109	-2205.322522	-43.72
56	-2281.523793	-2282.665137	-2281.500602	-2282.699963	-30.55
58	-2358.896714	-2360.044738	-2358.879193	-2360.078064	-41.50
60	-2436.278578	-2437.421866	-2436.256662	-2437.454977	-29.39
62	-2513.651569	-2514.797387	-2513.633514	-2514.832773	-45.50
64	-2591.032476	-2592.176544	-2591.010737	-2592.209478	-29.39
66	-2668.405692	-2669.555128	-2668.388349	-2669.586685	-37.32

Table S21: The aromatic stabilisation energy for the neutral triplet annulenes (UB3LYP/6-31G(d)). The geometries were optimised using the IOp(2/15=4,2/16=2) keyword ensuring planarity. As a result, some structures may have one or more imaginary frequencies.

Triplet (0)	**A**	**B**	**C**	**D**	**ASE**
N	EE+ZPVE (Hartree)	EE+ZPVE (Hartree)	EE+ZPVE (Hartree)	EE+ZPVE (Hartree)	(**C**+**D**)-(**A**+**B**) (kJ/mol)
12	-579.541757	-580.651286	-579.527115	-580.714512	-127.56
14	-656.996285	-658.142024	-656.995884	-658.173127	-80.61
16	-734.351551	-735.477717	-734.336181	-735.519662	-69.77
18	-811.778417	-812.932159	-811.774556	-812.951422	-40.44
20	-889.128052	-890.251333	-889.112987	-890.295453	-76.28
22	-966.53574	-967.685899	-966.528096	-967.708554	-39.41
24	-1043.920284	-1045.06388	-1043.904308	-1045.08415	-11.27
26	-1121.290514	-1122.441528	-1121.281034	-1122.461795	-28.32
28	-1198.671771	-1199.81542	-1198.656361	-1199.836806	-15.69
30	-1276.043528	-1277.192903	-1276.033154	-1277.213477	-26.78
32	-1353.422861	-1354.566465	-1353.407718	-1354.58856	-18.25
34	-1430.79569	-1431.943566	-1430.784031	-1431.964801	-25.14
36	-1508.173439	-1509.319659	-1508.159436	-1509.339764	-16.02
38	-1585.547108	-1586.693957	-1585.53454	-1586.715641	-23.93
40	-1662.92391	-1664.069848	-1662.909824	-1664.090534	-17.33
42	-1740.297704	-1741.445564	-1740.285226	-1741.46573	-20.18
44	-1817.674195	-1818.819803	-1817.659982	-1818.840941	-18.18
46	-1895.048282	-1896.195413	-1895.035226	-1896.216035	-19.86
48	-1972.423978	-1973.57089	-1972.41033	-1973.590829	-16.52
50	-2049.798604	-2050.945104	-2049.785096	-2050.966091	-19.64
52	-2127.173991	-2128.320478	-2127.160161	-2128.340863	-17.21
54	-2204.548456	-2205.6958	-2204.535237	-2205.71576	-17.70
56	-2281.923886	-2283.07004	-2281.90987	-2283.09078	-17.65
58	-2359.298422	-2360.445259	-2359.284877	-2360.465604	-17.85
60	-2436.673678	-2437.819488	-2436.659505	-2437.840542	-18.07
62	-2514.048266	-2515.194674	-2514.034451	-2515.215355	-18.03
64	-2591.423118	-2592.569778	-2591.409363	-2592.590033	-17.07
66	-2668.79778	-2669.944823	-2668.784275	-2669.964787	-16.96

Table S22: The aromatic stabilisation energy for the triplet dicationic annulenes (UB3LYP/6-31G(d)). The geometries were optimised using the IOp(2/15=4,2/16=2) keyword ensuring planarity. As a result, some structures may have one or more imaginary frequencies.

Triplet (2+)	A	B	C	D	ASE
N	EE+ZPVE (Hartree)	EE+ZPVE (Hartree)	EE+ZPVE (Hartree)	EE+ZPVE (Hartree)	(**C**+**D**)-(**A**+**B**) (kJ/mol)
12	-578.904307	-580.107851	-578.915913	-580.105202	-23.52
14	-656.415691	-657.589072	-656.398929	-657.587134	49.10
16	-733.764071	-734.954052	-733.769845	-734.957379	-23.89
18	-811.239402	-812.394822	-811.217729	-812.405913	27.78
20	-888.581005	-889.761008	-888.579954	-889.766899	-12.71
22	-966.024069	-967.17656	-966.002618	-967.183607	37.82
24	-1043.40288	-1044.562402	-1043.394795	-1044.575901	-14.21
26	-1120.800854	-1121.948794	-1120.779489	-1121.962511	20.08
28	-1198.178059	-1199.335007	-1198.167468	-1199.348715	-8.18
30	-1275.572478	-1276.719466	-1275.55126	-1276.733708	18.32
32	-1352.947397	-1354.102816	-1352.935414	-1354.116785	-5.21
34	-1430.339358	-1431.486138	-1430.318264	-1431.500468	17.76
36	-1507.714677	-1508.866602	-1507.701533	-1508.88415	-11.56
38	-1585.10299	-1586.24964	-1585.08201	-1586.264049	17.25
40	-1662.478269	-1663.629545	-1662.464091	-1663.64649	-7.26
42	-1739.864993	-1741.009336	-1739.844136	-1741.02684	8.80
44	-1817.239446	-1818.390156	-1817.224486	-1818.406664	-4.06
46	-1894.624584	-1895.769472	-1894.604004	-1895.786475	9.39
48	-1971.999165	-1973.147712	-1971.983744	-1973.166547	-8.96
50	-2049.382431	-2050.527911	-2049.362286	-2050.54454	9.23
52	-2126.757375	-2127.905845	-2126.741477	-2127.923995	-5.91
54	-2204.139308	-2205.283786	-2204.119762	-2205.302398	2.45
56	-2281.514314	-2282.662779	-2281.498041	-2282.68035	-3.41
58	-2358.895128	-2360.0404	-2358.875983	-2360.05842	2.95
60	-2436.270223	-2437.418645	-2436.253603	-2437.43578	-1.35
62	-2513.650231	-2514.796058	-2513.631313	-2514.813592	3.63
64	-2591.02562	-2592.172905	-2591.008984	-2592.191458	-5.03
66	-2668.404694	-2669.549747	-2668.386176	-2669.568725	-1.21

Table S23: The aromatic stabilisation energy for the closed-shell dicationic annulenes (B3LYP/6-31G(d)). The geometries were optimised using the IOp(2/15=4,2/16=2) keyword ensuring planarity. As a result, some structures may have one or more imaginary frequencies.

Singlet (2+)	**A**	**B**	**C**	**D**	**ASE**
N	EE+ZPVE (Hartree)	EE+ZPVE (Hartree)	EE+ZPVE (Hartree)	EE+ZPVE (Hartree)	(**C**+**D**)-(**A**+**B**) (kJ/mol)
12	-578.9533	-580.096629	-578.929144	-580.127468	-17.55
14	-656.422207	-657.569341	-656.425132	-657.610689	-116.24
16	-733.807737	-734.942009	-733.781787	-734.974665	-17.61
18	-811.243404	-812.383855	-811.238376	-812.422095	-87.20
20	-888.616221	-889.748175	-888.590973	-889.781087	-20.12
22	-966.028139	-967.163632	-966.018011	-967.209204	-93.06
24	-1043.431783	-1044.558164	-1043.404962	-1044.593738	-22.98
26	-1120.805258	-1121.942519	-1120.793007	-1121.983459	-75.32
28	-1198.202857	-1199.32833	-1198.175741	-1199.364808	-24.58
30	-1275.575657	-1276.710489	-1275.563012	-1276.751127	-73.50
32	-1352.969274	-1354.094564	-1352.942155	-1354.131239	-25.09
34	-1430.342275	-1431.47556	-1430.327638	-1431.515935	-67.58
36	-1507.733782	-1508.861607	-1507.708872	-1508.895824	-24.44
38	-1585.105641	-1586.238102	-1585.089481	-1586.277863	-61.96
40	-1662.494895	-1663.622789	-1662.469958	-1663.6572	-24.87
42	-1739.867063	-1741.001038	-1739.851538	-1741.03805	-56.41
44	-1817.253968	-1818.382131	-1817.229109	-1818.416501	-24.97
46	-1894.626401	-1895.759925	-1894.609856	-1895.796605	-52.86
48	-1972.011999	-1973.142025	-1971.988653	-1973.174455	-23.85
50	-2049.384239	-2050.517492	-2049.366813	-2050.553724	-49.38
52	-2126.768449	-2127.898807	-2126.745193	-2127.931284	-24.21
54	-2204.140983	-2205.275607	-2204.124247	-2205.309773	-45.76
56	-2281.523794	-2282.654687	-2281.500723	-2282.68703	-24.34
58	-2358.896691	-2360.031225	-2358.879334	-2360.065102	-43.37
60	-2436.278329	-2437.409731	-2436.255426	-2437.441911	-24.36
62	-2513.651561	-2514.786093	-2513.633651	-2514.819609	-40.97
64	-2591.032479	-2592.165453	-2591.010866	-2592.196187	-23.95
66	-2668.40577	-2669.541422	-2668.388488	-2669.573372	-38.51

Table S24: The aromatic stabilisation energy for the closed-shell neutral annulenes (CAM-B3LYP/6-31G(d)). The geometries were optimised without any constraints and do not contain imaginary frequencies.

Singlet (0)	A	B	C	D	ASE
N	EE+ZPEC (Hartree)	EE+ZPEC (Hartree)	EE+ZPEC (Hartree)	EE+ZPEC (Hartree)	(C+D)-(A+B) (kJ/mol)
12	-579.257294	-580.469237	-579.25118	-580.472907	6.42
14	-656.632584	-657.816259	-656.626662	-657.819321	7.51
16	-733.921953	-735.126293	-733.922698	-735.12997	-11.61
18	-811.289824	-812.469522	-811.280526	-812.473618	13.66
20	-888.577797	-889.775301	-888.579043	-889.77722	-8.31
22	-965.938462	-967.117584	-965.929353	-967.122537	10.91
24	-1043.260963	-1044.4418	-1043.25409	-1044.449673	-2.63
26	-1120.58689	-1121.766069	-1120.578177	-1121.773662	2.94
28	-1197.91005	-1199.089959	-1197.90227	-1199.098193	-1.19
30	-1275.235178	-1276.414251	-1275.226684	-1276.422209	1.41
32	-1352.558545	-1353.737736	-1352.550265	-1353.745812	0.54
34	-1429.883147	-1431.061972	-1429.874585	-1431.070172	0.95
36	-1507.207028	-1508.385794	-1507.198543	-1508.394155	0.33
38	-1584.531036	-1585.709649	-1584.522409	-1585.718028	0.65
40	-1661.854836	-1663.033444	-1661.846293	-1663.041937	0.13
42	-1739.178842	-1740.357215	-1739.170166	-1740.365736	0.41
44	-1816.502662	-1817.680932	-1816.493991	-1817.689652	-0.13
46	-1893.826571	-1895.004698	-1893.817816	-1895.013426	0.07
48	-1971.150404	-1972.328469	-1971.141646	-1972.33726	-0.09
50	-2048.474251	-2049.652275	-2048.465449	-2049.661074	0.01
52	-2125.798071	-2126.976037	-2125.789249	-2126.984886	-0.07
54	-2203.121897	-2204.299817	-2203.113038	-2204.308661	0.04
56	-2280.445699	-2281.623586	-2280.436831	-2281.632473	-0.05
58	-2357.769501	-2358.94735	-2357.760606	-2358.95624	0.01
60	-2435.093294	-2436.271119	-2435.084392	-2436.280036	-0.04
62	-2512.417077	-2513.594968	-2512.408154	-2513.603797	0.25
64	-2589.740862	-2590.918613	-2589.731918	-2590.927567	-0.03
66	-2667.064635	-2668.242378	-2667.055695	-2668.251314	0.01

Table S25: The aromatic stabilisation energy for the closed-shell dicationic annulenes (CAM-B3LYP/6-31G(d)). The geometries were optimised without any constraints and do not contain imaginary frequencies.

Singlet (2+)	A	B	C	D	ASE
N	EE+ZPEC (Hartree)	EE+ZPEC (Hartree)	EE+ZPEC (Hartree)	EE+ZPEC (Hartree)	(C+D)-(A+B) (kJ/mol)
12	-578.624345	-579.82439	-578.595726	-579.81355	103.60
14	-656.01975	-657.182186	-656.013545	-657.201131	-33.45
16	-733.347435	-734.516186	-733.32659	-734.542223	-13.63
18	-810.719552	-811.872684	-810.708595	-811.900498	-44.26
20	-888.038878	-889.203216	-888.019221	-889.220341	6.65
22	-965.400207	-966.545948	-965.385378	-966.589882	-76.42
24	-1042.743742	-1043.886608	-1042.723359	-1043.92508	-47.49
26	-1120.074338	-1121.225982	-1120.058345	-1121.263007	-55.22
28	-1197.411436	-1198.554022	-1197.390662	-1198.594246	-51.07
30	-1274.741257	-1275.890629	-1274.725937	-1275.928165	-58.33
32	-1352.074955	-1353.217551	-1352.053693	-1353.258602	-51.96
34	-1429.40457	-1430.552177	-1429.387316	-1430.590924	-56.43
36	-1506.736308	-1507.885203	-1506.718576	-1507.920678	-46.58
38	-1584.064731	-1585.211483	-1584.046013	-1585.250721	-53.88
40	-1661.394893	-1662.543505	-1661.376445	-1662.579719	-46.64
42	-1738.722864	-1739.874888	-1738.706366	-1739.908612	-45.23
44	-1816.05157	-1817.200177	-1816.032444	-1817.23669	-45.65
46	-1893.379118	-1894.530628	-1893.361671	-1894.564833	-44.00
48	-1970.706868	-1971.860181	-1970.690097	-1971.892074	-39.70
50	-2048.033934	-2049.184746	-2048.015663	-2049.219625	-43.60
52	-2125.361033	-2126.514286	-2125.343643	-2126.546453	-38.80
54	-2202.68768	-2203.843042	-2202.67131	-2203.873244	-36.32
56	-2280.014217	-2281.167054	-2279.996219	-2281.199765	-38.63
58	-2357.340529	-2358.495808	-2357.323516	-2358.526143	-34.98
60	-2434.666586	-2435.819678	-2434.64803	-2435.852217	-36.71
62	-2511.992588	-2513.147541	-2511.975002	-2513.178264	-34.49
64	-2589.318336	-2590.474884	-2589.301604	-2590.503928	-32.33
66	-2666.644098	-2667.802159	-2666.628013	-2667.829614	-29.85

Table S26: The aromatic stabilisation energy for the neutral triplet annulenes (UCAM-B3LYP/6-31G(d)). The geometries were optimised without any constraints and do not contain imaginary frequencies.

Triplet (0)	A	B	C	D	ASE
N	EE+ZPEC (Hartree)	EE+ZPEC (Hartree)	EE+ZPEC (Hartree)	EE+ZPEC (Hartree)	(C+D)-(A+B) (kJ/mol)
12	-579.214462	-580.417422	-579.209328	-580.443968	-56.22
14	-656.600181	-657.765764	-656.596127	-657.782368	-32.95
16	-733.89842	-735.083739	-733.896026	-735.09935	-34.70
18	-811.266452	-812.43746	-811.261788	-812.451587	-24.85
20	-888.562903	-889.742891	-888.557886	-889.751974	-10.68
22	-965.922908	-967.090428	-965.915804	-967.109962	-32.63
24	-1043.251103	-1044.41849	-1043.242726	-1044.436368	-24.94
26	-1120.576652	-1121.745854	-1120.568631	-1121.763068	-24.14
28	-1197.903326	-1199.069681	-1197.894479	-1199.088967	-27.41
30	-1275.228839	-1276.39683	-1275.220762	-1276.414926	-26.30
32	-1352.554867	-1353.720392	-1352.545478	-1353.740616	-28.45
34	-1429.880236	-1431.047071	-1429.871472	-1431.066168	-27.13
36	-1507.205671	-1508.373188	-1507.196903	-1508.391394	-24.78
38	-1584.531085	-1585.696979	-1584.52183	-1585.716952	-28.14
40	-1661.856247	-1663.022915	-1661.847101	-1663.041996	-26.08
42	-1739.181238	-1740.34851	-1739.172355	-1740.36709	-25.46
44	-1816.506573	-1817.672195	-1816.497099	-1817.692298	-27.91
46	-1893.831489	-1894.99792	-1893.822252	-1895.017275	-26.56
48	-1971.156405	-1972.323069	-1971.147336	-1972.34215	-26.29
50	-2048.481522	-2049.646894	-2048.472021	-2049.667274	-28.56
52	-2125.806359	-2126.972252	-2125.797046	-2126.992085	-27.62
54	-2203.131155	-2204.297338	-2203.122066	-2204.316951	-27.63
56	-2280.456192	-2281.621239	-2280.446678	-2281.641892	-29.25
58	-2357.781006	-2358.946409	-2357.771656	-2358.966738	-28.83
60	-2435.105926	-2436.270311	-2435.096251	-2436.2916	-30.49
62	-2512.430715	-2513.59693	-2512.421198	-2513.616421	-26.19
64	-2589.755455	-2590.917222	-2589.746092	-2590.941147	-38.23
66	-2667.080204	-2668.245246	-2667.070989	-2668.265909	-30.06

Table S27: The aromatic stabilisation energy for the triplet dicationic annulenes (UCAM-B3LYP/6-31G(d)). The geometries were optimised without any constraints and do not contain imaginary frequencies.

Triplet (2+)	A	B	C	D	ASE
N	EE+ZPEC (Hartree)	EE+ZPEC (Hartree)	EE+ZPEC (Hartree)	EE+ZPEC (Hartree)	(C+D)-(A+B) (kJ/mol)
12	-578.599567	-579.785285	-578.586951	-579.804228	-16.61
14	-656.006264	-657.187315	-655.994136	-657.190723	22.89
16	-733.323042	-734.518363	-733.316529	-734.522764	5.55
18	-810.7103	-811.879649	-810.694762	-811.891905	8.62
20	-888.014911	-889.210665	-888.011172	-889.213603	2.10
22	-965.391669	-966.562924	-965.376769	-966.567973	25.86
24	-1042.725793	-1043.899138	-1042.71588	-1043.908889	0.43
26	-1120.065536	-1121.234371	-1120.051633	-1121.246619	4.35
28	-1197.398862	-1198.571052	-1197.387031	-1198.580418	6.47
30	-1274.735012	-1275.904434	-1274.721411	-1275.916212	4.79
32	-1352.066508	-1353.237907	-1352.053332	-1353.247083	10.50
34	-1429.400245	-1430.570263	-1429.386473	-1430.581406	6.90
36	-1506.731129	-1507.900571	-1506.717985	-1507.91395	-0.62
38	-1584.062259	-1585.232685	-1584.048336	-1585.243402	8.42
40	-1661.392528	-1662.562305	-1661.378908	-1662.574769	3.04
42	-1738.722235	-1739.891459	-1738.708644	-1739.90542	-0.97
44	-1816.051603	-1817.221657	-1816.037608	-1817.233432	5.83
46	-1893.380095	-1894.55035	-1893.36671	-1894.563429	0.80
48	-1970.708745	-1971.878264	-1970.695248	-1971.89259	-2.18
50	-2048.037275	-2049.207504	-2048.023248	-2049.219894	4.30
52	-2125.365398	-2126.535071	-2125.351345	-2126.548538	1.54
54	-2202.692861	-2203.862443	-2202.679036	-2203.876725	-1.20
56	-2280.020602	-2281.190587	-2280.006335	-2281.203353	3.94
58	-2357.34767	-2358.51773	-2357.333676	-2358.531227	1.30
60	-2434.674858	-2435.845083	-2434.66043	-2435.857287	5.84
62	-2512.001661	-2513.171908	-2511.987503	-2513.184894	3.08
64	-2589.328507	-2590.498417	-2589.314461	-2590.512098	0.96
66	-2666.654062	-2667.824828	-2666.641095	-2667.839001	-3.17

Table S28: The aromatic stabilisation energy for the neutral triplet annulenes (UCAM-B3LYP/6-31G(d)). The closed-shell neutral **B** and **D** geometries were optimised using the IOp(2/15=4,2/16=2) keyword ensuring planarity.

Triplet (0)	$A_{Triplet\ neutral}$	$B_{Singlet\ neutral}$	$C_{Triplet\ neutral}$	$D_{Singlet\ neutral}$	ASE
N	EE+ZPEC (Hartree)	EE+ZPEC (Hartree)	EE+ZPEC (Hartree)	EE+ZPEC (Hartree)	(C+D)-(A+B) (kJ/mol)
12	-579.214462	-580.381995	-579.209328	-580.383566	9.35
14	-656.600181	-657.783408	-656.596127	-657.78551	5.12
16	-733.89842	-735.077439	-733.896026	-735.082073	-5.88
18	-811.266452	-812.451885	-811.261788	-812.459648	-8.14
20	-888.562903	-889.745547	-888.557886	-889.751467	-2.37
22	-965.922908	-967.101288	-965.915804	-967.110106	-4.50
24	-1043.251103	-1044.42571	-1043.242726	-1044.435	-2.40
26	-1120.576652	-1121.750119	-1120.568631	-1121.759299	-3.04
28	-1197.903326	-1199.073855	-1197.894479	-1199.083238	-1.41
30	-1275.228839	-1276.398572	-1275.220762	-1276.407681	-2.71
32	-1352.554867	-1353.721738	-1352.545478	-1353.731217	-0.24
34	-1429.880236	-1431.046404	-1429.871472	-1431.055643	-1.25
36	-1507.205671	-1508.370181	-1507.196903	-1508.379594	-1.69
38	-1584.531085	-1585.694133	-1584.52183	-1585.703441	-0.14
40	-1661.856247	-1663.017886	-1661.847101	-1663.027325	-0.77
42	-1739.181238	-1740.341643	-1739.172355	-1740.351121	-1.56
44	-1816.506573	-1817.665498	-1816.497099	-1817.674965	0.02
46	-1893.831489	-1894.989268	-1893.822252	-1894.998775	-0.71
48	-1971.156405	-1972.313014	-1971.147336	-1972.322578	-1.30
50	-2048.481522	-2049.636824	-2048.472021	-2049.646352	-0.07
52	-2125.806359	-2126.960565	-2125.797046	-2126.970147	-0.71
54	-2203.131155	-2204.284323	-2203.122066	-2204.293923	-1.34
56	-2280.456192	-2281.608116	-2280.446678	-2281.617705	-0.20
58	-2357.781006	-2358.931857	-2357.771656	-2358.941465	-0.68
60	-2435.105926	-2436.255619	-2435.096251	-2436.265226	0.18
62	-2512.430715	-2513.579372	-2512.421198	-2513.588987	-0.26
64	-2589.755455	-2590.903094	-2589.746092	-2590.912738	-0.74
66	-2667.080204	-2668.226818	-2667.070989	-2668.236479	-1.17

Table S29: The aromatic stabilisation energy for the triplet dicationic annulenes (UCAM-B3LYP/6-31G(d)). The closed-shell neutral **B** and **D** geometries were optimised using the IOp(2/15=4,2/16=2) keyword ensuring planarity.

Triplet (2+)	$A_{Triplet\ charged}$	$B_{Singlet\ neutral}$	$C_{Triplet\ charged}$	$D_{Singlet\ neutral}$	ASE
N	EE+ZPEC (Hartree)	EE+ZPEC (Hartree)	EE+ZPEC (Hartree)	EE+ZPEC (Hartree)	(C+D)-(A+B) (kJ/mol)
12	-578.599567	-580.381995	-578.586951	-580.383566	29.00
14	-656.006264	-657.783408	-655.994136	-657.78551	26.32
16	-733.323042	-735.077439	-733.316529	-735.082073	4.93
18	-810.7103	-812.451885	-810.694762	-812.459648	20.41
20	-888.014911	-889.745547	-888.011172	-889.751467	-5.73
22	-965.391669	-967.101288	-965.376769	-967.110106	15.97
24	-1042.725793	-1044.42571	-1042.71588	-1044.435	1.64
26	-1120.065536	-1121.750119	-1120.051633	-1121.759299	12.40
28	-1197.398862	-1199.073855	-1197.387031	-1199.083238	6.43
30	-1274.735012	-1276.398572	-1274.721411	-1276.407681	11.79
32	-1352.066508	-1353.721738	-1352.053332	-1353.731217	9.71
34	-1429.400245	-1431.046404	-1429.386473	-1431.055643	11.90
36	-1506.731129	-1508.370181	-1506.717985	-1508.379594	9.80
38	-1584.062259	-1585.694133	-1584.048336	-1585.703441	12.12
40	-1661.392528	-1663.017886	-1661.378908	-1663.027325	10.98
42	-1738.722235	-1740.341643	-1738.708644	-1740.351121	10.80
44	-1816.051603	-1817.665498	-1816.037608	-1817.674965	11.89
46	-1893.380095	-1894.989268	-1893.36671	-1894.998775	10.18
48	-1970.708745	-1972.313014	-1970.695248	-1972.322578	10.33
50	-2048.037275	-2049.636824	-2048.023248	-2049.646352	11.81
52	-2125.365398	-2126.960565	-2125.351345	-2126.970147	11.74
54	-2202.692861	-2204.284323	-2202.679036	-2204.293923	11.09
56	-2280.020602	-2281.608116	-2280.006335	-2281.617705	12.28
58	-2357.34767	-2358.931857	-2357.333676	-2358.941465	11.52
60	-2434.674858	-2436.255619	-2434.66043	-2436.265226	12.66
62	-2512.001661	-2513.579372	-2511.987503	-2513.588987	11.93
64	-2589.328507	-2590.903094	-2589.314461	-2590.912738	11.56
66	-2666.654062	-2668.226818	-2666.641095	-2668.236479	8.68

Table S30: The aromatic stabilisation energy for the closed-shell dicationic annulenes (CAM-B3LYP/6-31G(d)). The closed-shell neutral **B** and **D** geometries were optimised using the IOp(2/15=4,2/16=2) keyword ensuring planarity.

Singlet (2+)	$A_{Singlet\ charged}$	$B_{Singlet\ neutral}$	$C_{Singlet\ charged}$	$D_{Singlet\ neutral}$	ASE
N	EE+ZPEC (Hartree)	EE+ZPEC (Hartree)	EE+ZPEC (Hartree)	EE+ZPEC (Hartree)	(C+D)-(A+B) (kJ/mol)
12	-578.624345	-580.381995	-578.595726	-580.383566	71.01
14	-656.01975	-657.783408	-656.013545	-657.78551	10.77
16	-733.347435	-735.077439	-733.32659	-735.082073	42.56
18	-810.719552	-812.451885	-810.708595	-812.459648	8.39
20	-888.038878	-889.745547	-888.019221	-889.751467	36.07
22	-965.400207	-967.101288	-965.385378	-967.110106	15.78
24	-1042.743742	-1044.42571	-1042.723359	-1044.435	29.12
26	-1120.074338	-1121.750119	-1120.058345	-1121.759299	17.89
28	-1197.411436	-1199.073855	-1197.390662	-1199.083238	29.91
30	-1274.741257	-1276.398572	-1274.725937	-1276.407681	16.31
32	-1352.074955	-1353.721738	-1352.053693	-1353.731217	30.94
34	-1429.40457	-1431.046404	-1429.387316	-1431.055643	21.04
36	-1506.736308	-1508.370181	-1506.718576	-1508.379594	21.84
38	-1584.064731	-1585.694133	-1584.046013	-1585.703441	24.71
40	-1661.394893	-1663.017886	-1661.376445	-1663.027325	23.65
42	-1738.722864	-1740.341643	-1738.706366	-1740.351121	18.43
44	-1816.05157	-1817.665498	-1816.032444	-1817.674965	25.36
46	-1893.379118	-1894.989268	-1893.361671	-1894.998775	20.85
48	-1970.706868	-1972.313014	-1970.690097	-1972.322578	18.92
50	-2048.033934	-2049.636824	-2048.015663	-2049.646352	22.95
52	-2125.361033	-2126.960565	-2125.343643	-2126.970147	20.50
54	-2202.68768	-2204.284323	-2202.67131	-2204.293923	17.77
56	-2280.014217	-2281.608116	-2279.996219	-2281.617705	22.08
58	-2357.340529	-2358.931857	-2357.323516	-2358.941465	19.44
60	-2434.666586	-2436.255619	-2434.64803	-2436.265226	23.50
62	-2511.992588	-2513.579372	-2511.975002	-2513.588987	20.93
64	-2589.318336	-2590.903094	-2589.301604	-2590.912738	18.61
66	-2666.644098	-2668.226818	-2666.628013	-2668.236479	16.87

Table S31: The aromatic stabilisation energy for the closed-shell neutral annulenes (CAM-B3LYP/6-31G(d)). The geometries were optimised using the IOp(2/15=4,2/16=2) keyword ensuring planarity. As a result, some structures may have one or more imaginary frequencies.

Singlet (0)	A	B	C	D	ASE
N	EE+ZPEC (Hartree)	EE+ZPEC (Hartree)	EE+ZPEC (Hartree)	EE+ZPEC (Hartree)	(C+D)-(A+B) (kJ/mol)
12	-579.184459	-580.381995	-579.190851	-580.383566	-20.91
14	-656.617439	-657.783408	-656.60434	-657.78551	28.87
16	-733.894614	-735.077439	-733.89396	-735.082073	-10.45
18	-811.290257	-812.451885	-811.277601	-812.459648	12.85
20	-888.568999	-889.745547	-888.565037	-889.751467	-5.14
22	-965.938895	-967.101288	-965.927714	-967.110106	6.20
24	-1043.260949	-1044.42571	-1043.252684	-1044.435	-2.69
26	-1120.587249	-1121.750119	-1120.576982	-1121.759299	2.85
28	-1197.910126	-1199.073855	-1197.901228	-1199.083238	-1.27
30	-1275.235361	-1276.398572	-1275.225767	-1276.407681	1.27
32	-1352.558865	-1353.721738	-1352.549429	-1353.731217	-0.11
34	-1429.883508	-1431.046404	-1429.873834	-1431.055643	1.14
36	-1507.207191	-1508.370181	-1507.197788	-1508.379594	-0.03
38	-1584.531395	-1585.694133	-1584.521733	-1585.703441	0.93
40	-1661.855167	-1663.017886	-1661.845622	-1663.027325	0.28
42	-1739.179126	-1740.341643	-1739.16947	-1740.351121	0.47
44	-1816.502991	-1817.665498	-1816.493371	-1817.674965	0.40
46	-1893.82687	-1894.989268	-1893.817179	-1894.998775	0.48
48	-1971.150684	-1972.313014	-1971.140998	-1972.322578	0.32
50	-2048.474565	-2049.636824	-2048.464833	-2049.646352	0.54
52	-2125.798362	-2126.960565	-2125.788643	-2126.970147	0.36
54	-2203.122168	-2204.284323	-2203.112436	-2204.293923	0.35
56	-2280.445988	-2281.608116	-2280.436236	-2281.617705	0.43
58	-2357.769772	-2358.931857	-2357.760014	-2358.941465	0.39
60	-2435.093592	-2436.255619	-2435.083804	-2436.265226	0.48
62	-2512.417347	-2513.579372	-2512.407568	-2513.588987	0.43
64	-2589.741119	-2590.903094	-2589.731336	-2590.912738	0.36
66	-2667.064884	-2668.226818	-2667.055094	-2668.236479	0.34

Table S32: The aromatic stabilisation energy for the closed-shell dicationic annulenes (CAM-B3LYP/6-31G(d)). The geometries were optimised using the IOp(2/15=4,2/16=2) keyword ensuring planarity. As a result, some structures may have one or more imaginary frequencies.

Singlet (2+)	A	B	C	D	ASE
N	EE+ZPEC (Hartree)	EE+ZPEC (Hartree)	EE+ZPEC (Hartree)	EE+ZPEC (Hartree)	(C+D)-(A+B) (kJ/mol)
12	-578.574667	-579.706439	-578.55217	-579.751012	-57.96
14	-655.997815	-657.135759	-655.997228	-657.182633	-121.53
16	-733.326729	-734.449857	-733.303873	-734.497438	-64.92
18	-810.718429	-811.858189	-810.709079	-811.893282	-67.59
20	-888.030945	-889.152661	-888.010577	-889.201582	-74.97
22	-965.400476	-966.534088	-965.38566	-966.580935	-84.10
24	-1042.743749	-1043.874739	-1042.723381	-1043.915495	-53.53
26	-1120.074343	-1121.213711	-1120.058427	-1121.253034	-61.46
28	-1197.411428	-1198.541436	-1197.390815	-1198.583637	-56.68
30	-1274.74126	-1275.878088	-1274.725936	-1275.917471	-63.17
32	-1352.074945	-1353.204431	-1352.053936	-1353.24714	-56.97
34	-1429.40457	-1430.539384	-1429.387433	-1430.579504	-60.34
36	-1506.736306	-1507.872314	-1506.718684	-1507.908958	-49.94
38	-1584.064732	-1585.198405	-1584.046154	-1585.238665	-56.93
40	-1661.39489	-1662.530326	-1661.376561	-1662.567496	-49.47
42	-1738.722864	-1739.861388	-1738.706476	-1739.896196	-48.36
44	-1816.051569	-1817.186752	-1816.032541	-1817.223987	-47.80
46	-1893.379118	-1894.516967	-1893.361747	-1894.552031	-46.45
48	-1970.70688	-1971.84646	-1970.690138	-1971.87913	-41.82
50	-2048.033933	-2049.171442	-2048.015698	-2049.206457	-44.06
52	-2125.361034	-2126.500414	-2125.343642	-2126.53321	-40.44
54	-2202.687679	-2203.828951	-2202.671308	-2203.859881	-38.22
56	-2280.014218	-2281.153562	-2279.996191	-2281.18625	-38.49
58	-2357.340534	-2358.481615	-2357.323478	-2358.51255	-36.44
60	-2434.666586	-2435.806059	-2434.647949	-2435.83847	-36.16
62	-2511.992589	-2513.133677	-2511.974914	-2513.164453	-34.40
64	-2589.318337	-2590.460985	-2589.301496	-2590.490082	-32.18
66	-2666.644085	-2667.788033	-2666.627887	-2667.8157	-30.11

Table S33: The aromatic stabilisation energy for the neutral triplet annulenes (UCAM-B3LYP/6-31G(d)). The geometries were optimised using the IOp(2/15=4,2/16=2) keyword ensuring planarity. As a result, some structures may have one or more imaginary frequencies.

Triplet (0)	A	B	C	D	ASE
N	EE+ZPEC (Hartree)	EE+ZPEC (Hartree)	EE+ZPEC (Hartree)	EE+ZPEC (Hartree)	(C+D)-(A+B) (kJ/mol)
12	-579.170093	-580.300612	-579.163501	-580.350786	-114.42
14	-656.583855	-657.730732	-656.582097	-657.759778	-71.64
16	-733.880073	-735.003423	-733.873679	-735.057324	-124.73
18	-811.266698	-812.422764	-811.262288	-812.439464	-32.27
20	-888.554432	-889.673923	-888.550411	-889.733152	-144.95
22	-965.922922	-967.076311	-965.916203	-967.096992	-36.66
24	-1043.251103	-1044.404306	-1043.242876	-1044.423045	-27.60
26	-1120.57666	-1121.731902	-1120.569024	-1121.750024	-27.53
28	-1197.903326	-1199.055411	-1197.894655	-1199.075295	-29.44
30	-1275.22883	-1276.382862	-1275.220932	-1276.401487	-28.16
32	-1352.554867	-1353.705978	-1352.545727	-1353.726676	-30.35
34	-1429.880235	-1431.032956	-1429.871659	-1431.052541	-28.90
36	-1507.205671	-1508.359036	-1507.1971	-1508.377623	-26.30
38	-1584.5311	-1585.682863	-1584.522027	-1585.703129	-29.39
40	-1661.856247	-1663.008682	-1661.847307	-1663.028084	-27.47
42	-1739.181271	-1740.334346	-1739.172539	-1740.353105	-26.33
44	-1816.506573	-1817.658308	-1816.497309	-1817.67824	-28.01
46	-1893.831489	-1894.983771	-1893.822423	-1895.003191	-27.18
48	-1971.156402	-1972.309169	-1971.147492	-1972.327983	-26.00
50	-2048.481494	-2049.633434	-2048.472184	-2049.653081	-27.14
52	-2125.805562	-2126.958727	-2125.797209	-2126.977831	-28.23
54	-2203.131226	-2204.283916	-2203.1222	-2204.302693	-25.60
56	-2280.456194	-2281.608572	-2280.446833	-2281.62758	-25.33
58	-2357.780998	-2358.933708	-2357.771784	-2358.952382	-24.84
60	-2435.105925	-2436.258259	-2435.096411	-2436.277204	-24.76
62	-2512.430715	-2513.583361	-2512.42132	-2513.60199	-24.24
64	-2589.755432	-2590.90837	-2589.746205	-2590.926714	-23.94
66	-2667.079854	-2668.233342	-2667.071087	-2668.251456	-24.54

Table S34: The aromatic stabilisation energy for the triplet dicationic annulenes (UCAM-B3LYP/6-31G(d)). The geometries were optimised using the IOp(2/15=4,2/16=2) keyword ensuring planarity. As a result, some structures may have one or more imaginary frequencies.

Triplet (2+)	A	B	C	D	ASE
N	EE+ZPEC (Hartree)	EE+ZPEC (Hartree)	EE+ZPEC (Hartree)	EE+ZPEC (Hartree)	(C+D)-(A+B) (kJ/mol)
12	-578.532306	-579.736043	-578.540344	-579.729511	-3.95
14	-655.989086	-657.168141	-655.976565	-657.16551	39.78
16	-733.291457	-734.482834	-733.293397	-734.48215	-3.30
18	-810.710965	-811.874037	-810.694299	-811.885013	14.94
20	-888.005426	-889.188929	-888.002425	-889.190338	4.18
22	-965.392065	-966.55425	-965.37689	-966.559266	26.67
24	-1042.726395	-1043.889859	-1042.716065	-1043.899766	1.11
26	-1120.065452	-1121.224818	-1120.051858	-1121.237054	3.57
28	-1197.399285	-1198.560745	-1197.387222	-1198.570336	6.49
30	-1274.735029	-1275.894059	-1274.721693	-1275.905877	3.99
32	-1352.066542	-1353.22679	-1352.053512	-1353.236224	9.44
34	-1429.400092	-1430.559195	-1429.386732	-1430.570349	5.79
36	-1506.730979	-1507.889234	-1506.718245	-1507.902607	-1.68
38	-1584.062251	-1585.221055	-1584.048555	-1585.231744	7.89
40	-1661.392395	-1662.55048	-1661.379152	-1662.562913	2.13
42	-1738.722064	-1739.879404	-1738.70909	-1739.893167	-2.07
44	-1816.051465	-1817.209383	-1816.037886	-1817.221147	4.77
46	-1893.380533	-1894.537937	-1893.367217	-1894.550807	1.17
48	-1970.708735	-1971.865684	-1970.695803	-1971.879783	-3.06
50	-2048.036976	-2049.194754	-2048.023807	-2049.206951	2.55
52	-2125.365124	-2126.522199	-2125.351893	-2126.535428	0.01
54	-2202.69274	-2203.849436	-2202.679857	-2203.863493	-3.08
56	-2280.020306	-2281.17746	-2280.00682	-2281.190028	2.41
58	-2357.347088	-2358.504487	-2357.334642	-2358.517781	-2.23
60	-2434.674147	-2435.831716	-2434.660844	-2435.843778	3.26
62	-2512.000875	-2513.158587	-2511.988641	-2513.171283	-1.21
64	-2589.327586	-2590.485004	-2589.31461	-2590.498366	-1.01
66	-2666.654038	-2667.811307	-2666.641968	-2667.825185	-4.75

GIMIC results

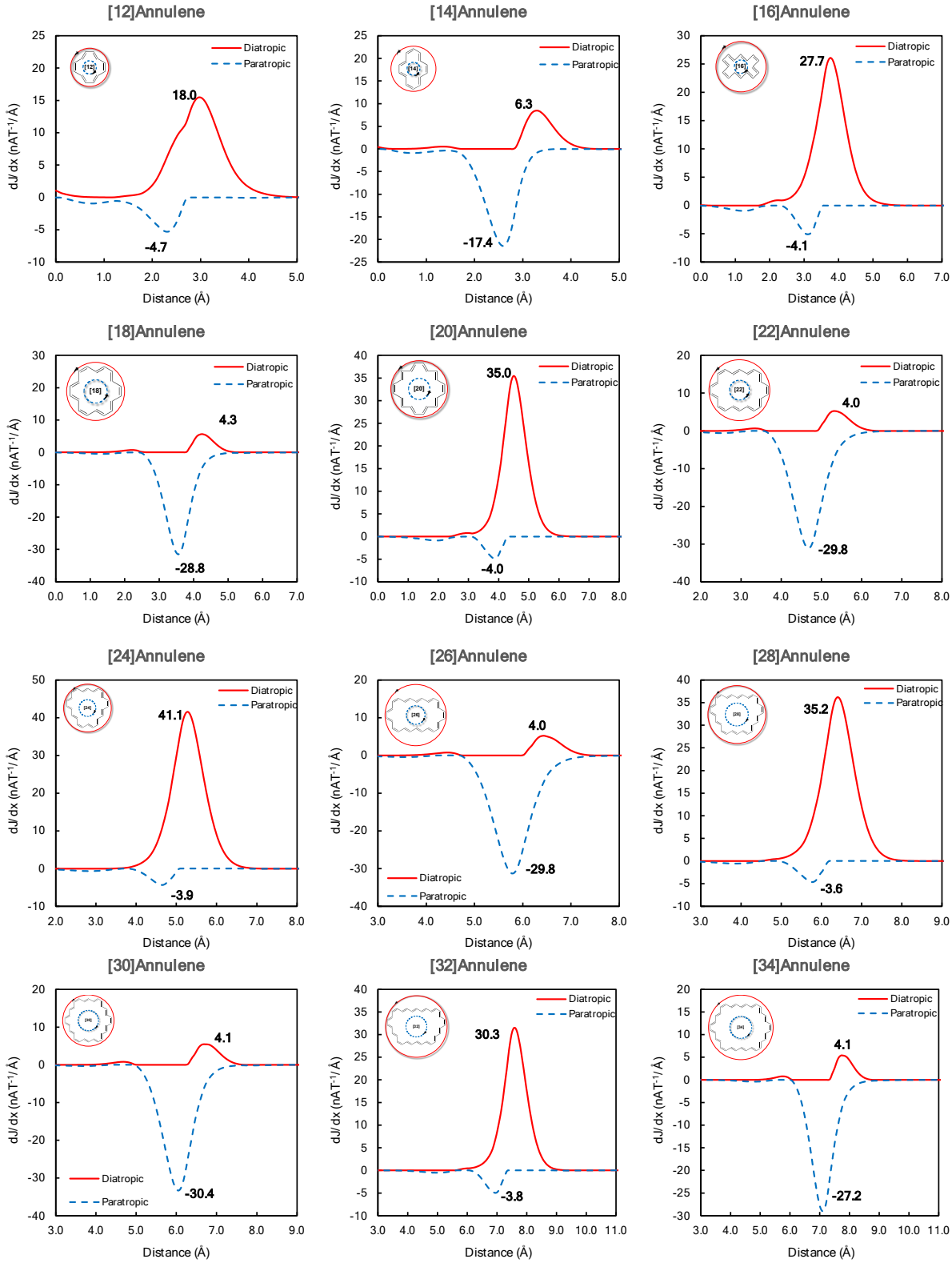

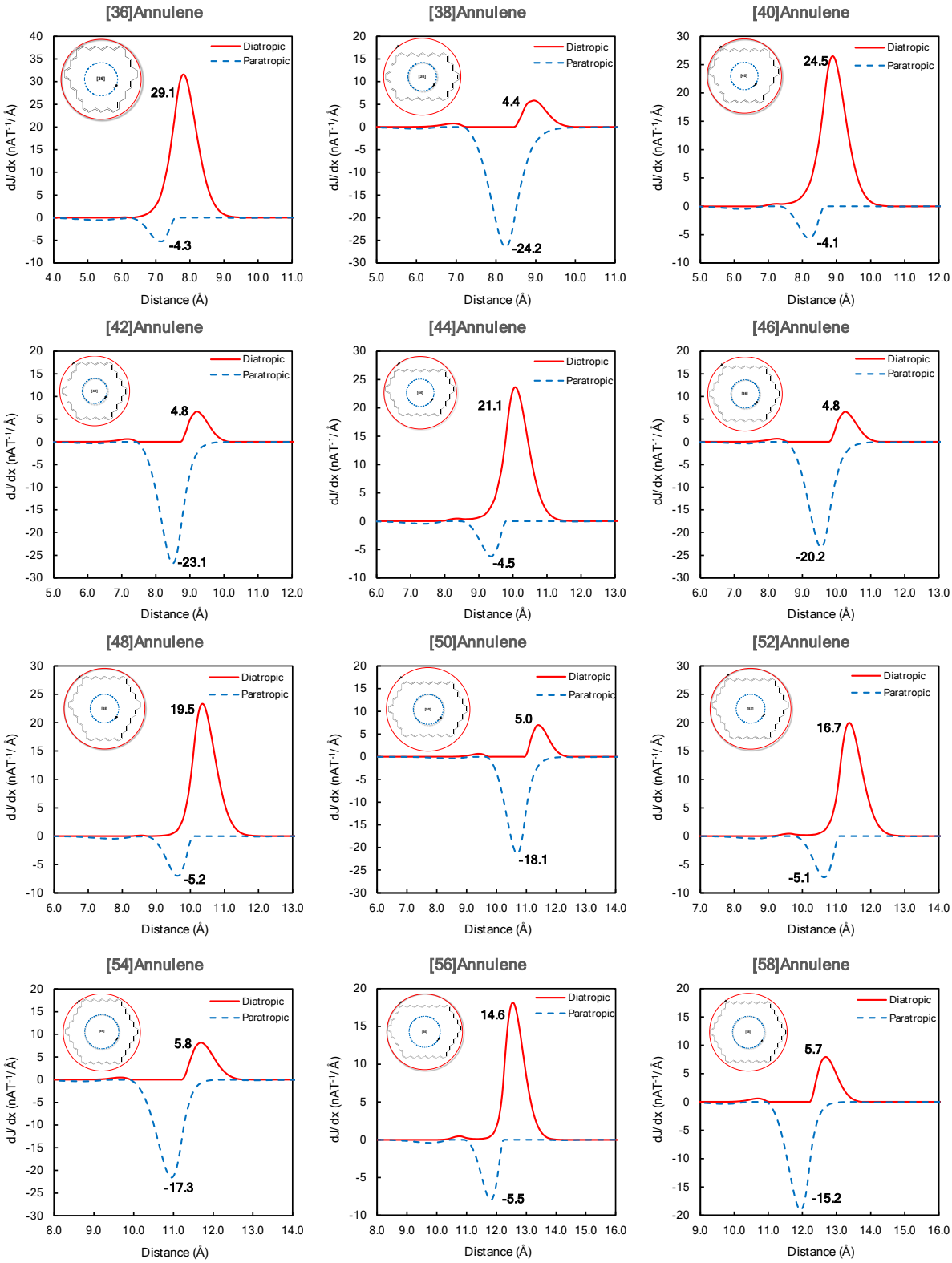
[36]Annulene
Diatropic
Paratropic
29.1
-4.3
dJ/ dx (nAT-1/ Å)
Distance (Å)
[38]Annulene
4.4
-24.2
[40]Annulene
24.5
-4.1
[42]Annulene
4.8
-23.1
[44]Annulene
21.1
-4.5
[46]Annulene
4.8
-20.2
[48]Annulene
19.5
-5.2
[50]Annulene
5.0
-18.1
[52]Annulene
16.7
-5.1
[54]Annulene
5.8
-17.3
[56]Annulene
14.6
-5.5
[58]Annulene
5.7
-15.2

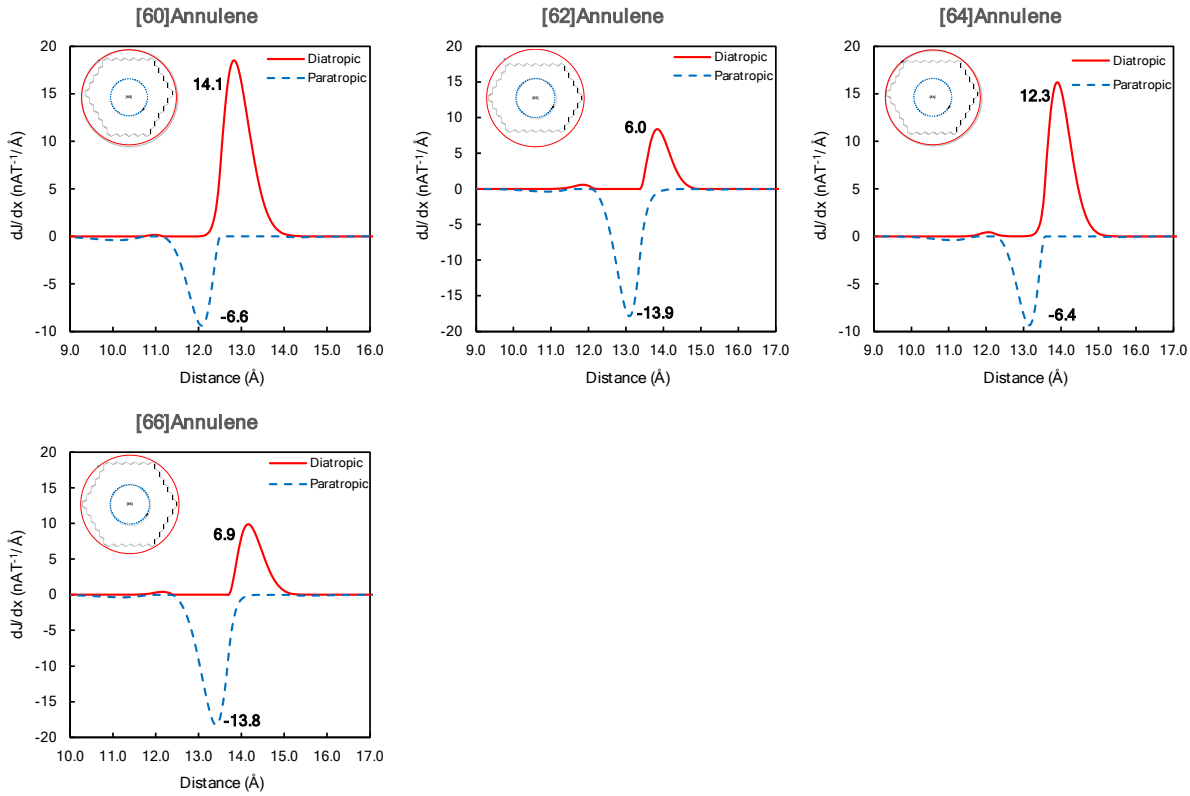

Figure S32: Profiles of current strength for the neutral triplet [*N*]annulenes through a plane situated halfway between two consecutive atoms and extending from the center of the molecule to a region where the current density vanishes planes. The numerical integration of the ring current strength was conducted using the GIMIC programme at the B3LYP/6-31G(d) level of theory. The positive and negative values represent the sum of the diatropic and paratropic contributions, which is determined through the subdivided slices of the integration plane.

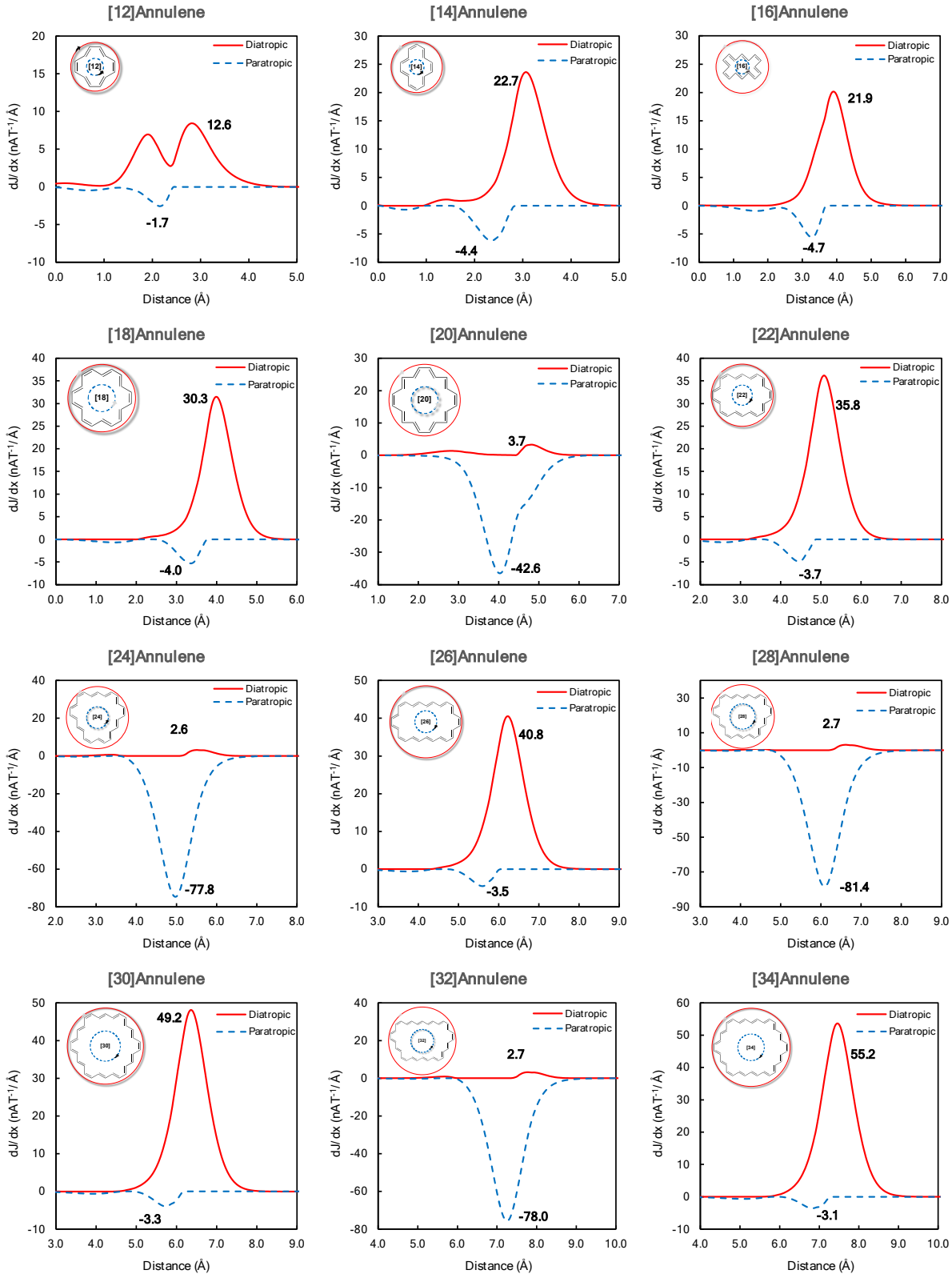
[12]Annulene
Diatropic
Paratropic
12.6
-1.7
dJ/ dx (nAT-1/ Å)
Distance (Å)
[14]Annulene
22.7
-4.4
[16]Annulene
21.9
-4.7
[18]Annulene
30.3
-4.0
[20]Annulene
3.7
-42.6
[22]Annulene
35.8
-3.7
[24]Annulene
2.6
-77.8
[26]Annulene
40.8
-3.5
[28]Annulene
2.7
-81.4
[30]Annulene
49.2
-3.3
[32]Annulene
2.7
-78.0
[34]Annulene
55.2
-3.1

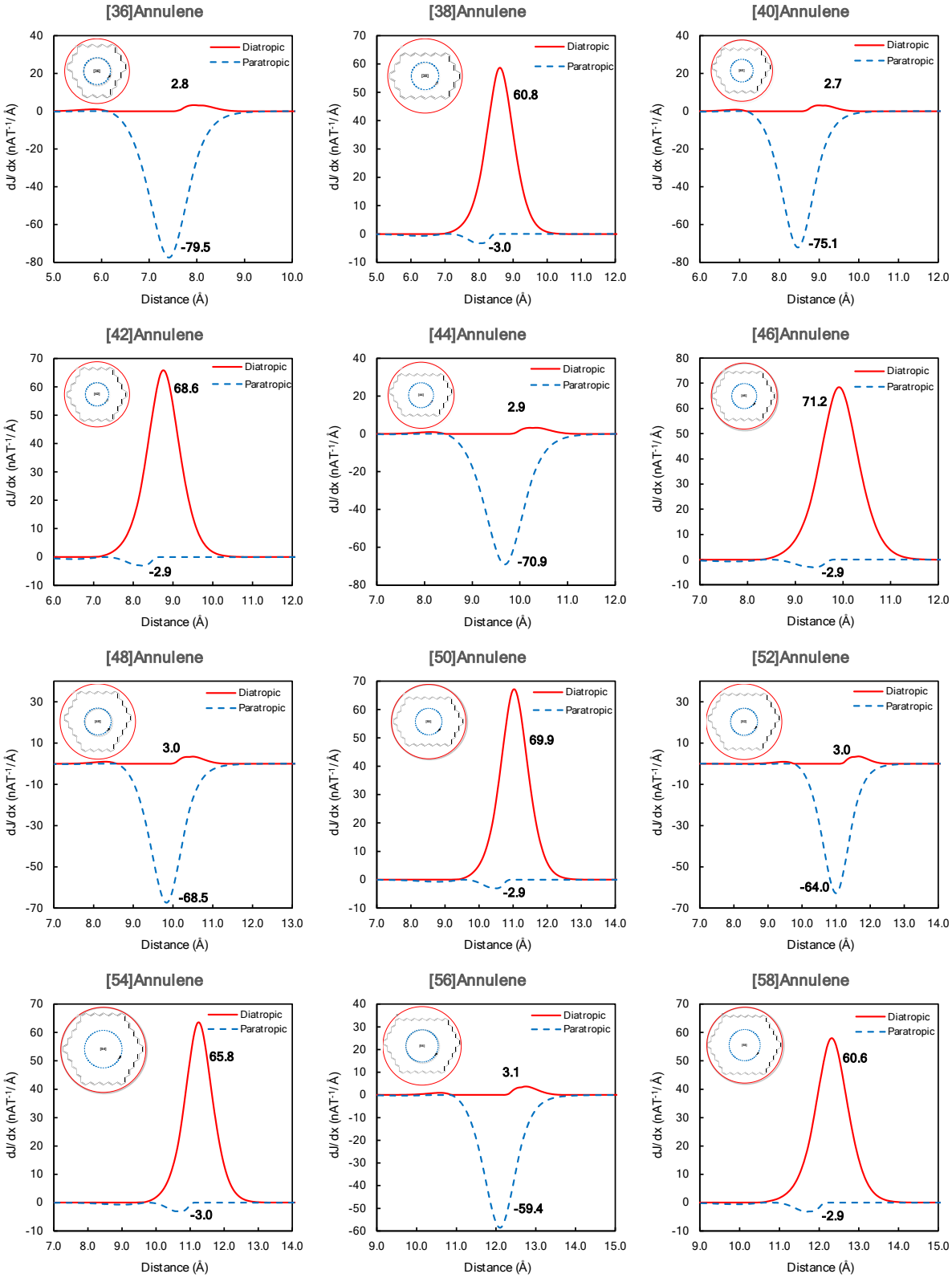
[36]Annulene
Diatropic
Paratropic
2.8
-79.5
dJ/ dx (nAT-1/ Å)
Distance (Å)
[38]Annulene
Diatropic
Paratropic
60.8
-3.0
dJ/ dx (nAT-1/ Å)
Distance (Å)
[40]Annulene
Diatropic
Paratropic
2.7
-75.1
dJ/ dx (nAT-1/ Å)
Distance (Å)
[42]Annulene
Diatropic
Paratropic
68.6
-2.9
dJ/ dx (nAT-1/ Å)
Distance (Å)
[44]Annulene
Diatropic
Paratropic
2.9
-70.9
dJ/ dx (nAT-1/ Å)
Distance (Å)
[46]Annulene
Diatropic
Paratropic
71.2
-2.9
dJ/ dx (nAT-1/ Å)
Distance (Å)
[48]Annulene
Diatropic
Paratropic
3.0
-68.5
dJ/ dx (nAT-1/ Å)
Distance (Å)
[50]Annulene
Diatropic
Paratropic
69.9
-2.9
dJ/ dx (nAT-1/ Å)
Distance (Å)
[52]Annulene
Diatropic
Paratropic
3.0
-64.0
dJ/ dx (nAT-1/ Å)
Distance (Å)
[54]Annulene
Diatropic
Paratropic
65.8
-3.0
dJ/ dx (nAT-1/ Å)
Distance (Å)
[56]Annulene
Diatropic
Paratropic
3.1
-59.4
dJ/ dx (nAT-1/ Å)
Distance (Å)
[58]Annulene
Diatropic
Paratropic
60.6
-2.9
dJ/ dx (nAT-1/ Å)
Distance (Å)

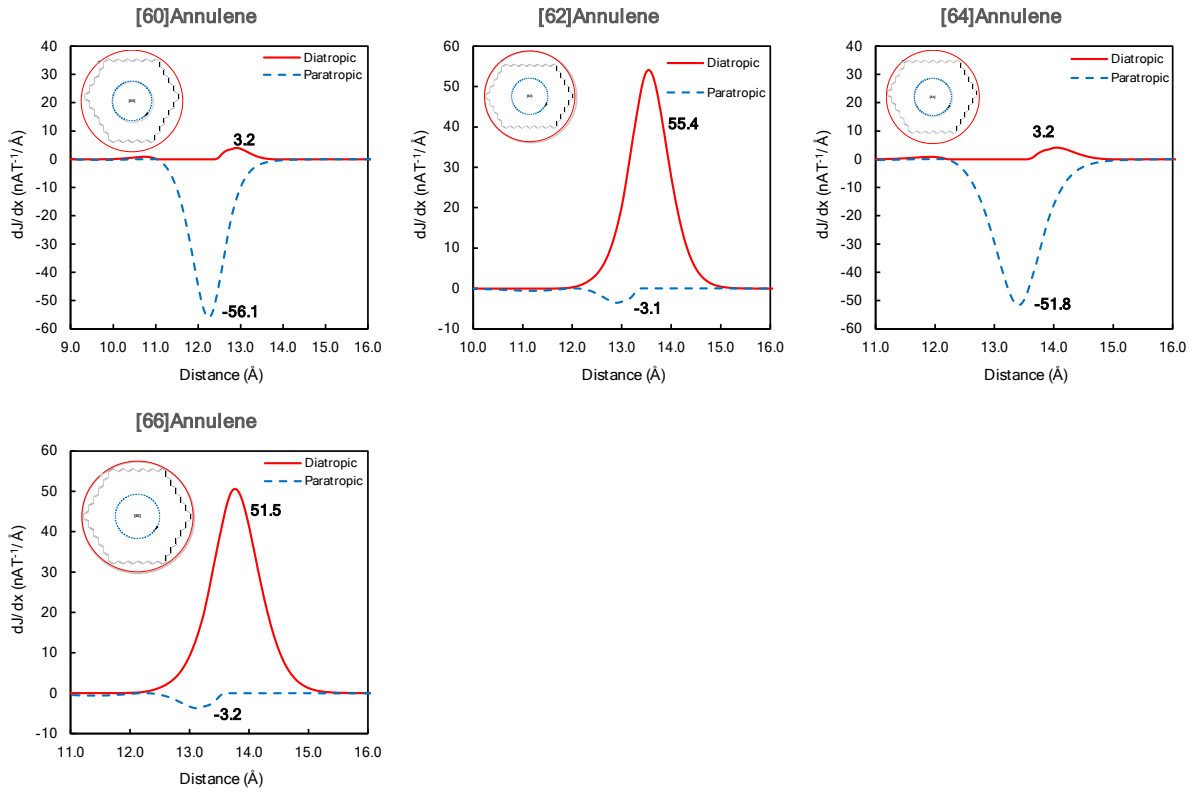

Figure S33: Profiles of current strength for the neutral triplet dicationic [*N*]annulenes through a plane situated halfway between two consecutive atoms and extending from the center of the molecule to a region where the current density vanishes planes. The numerical integration of the ring current strength was conducted using the GIMIC programme at the B3LYP/6-31G(d) level of theory. The positive and negative values represent the sum of the diatropic and paratropic contributions, which is determined through the subdivided slices of the integration plane.

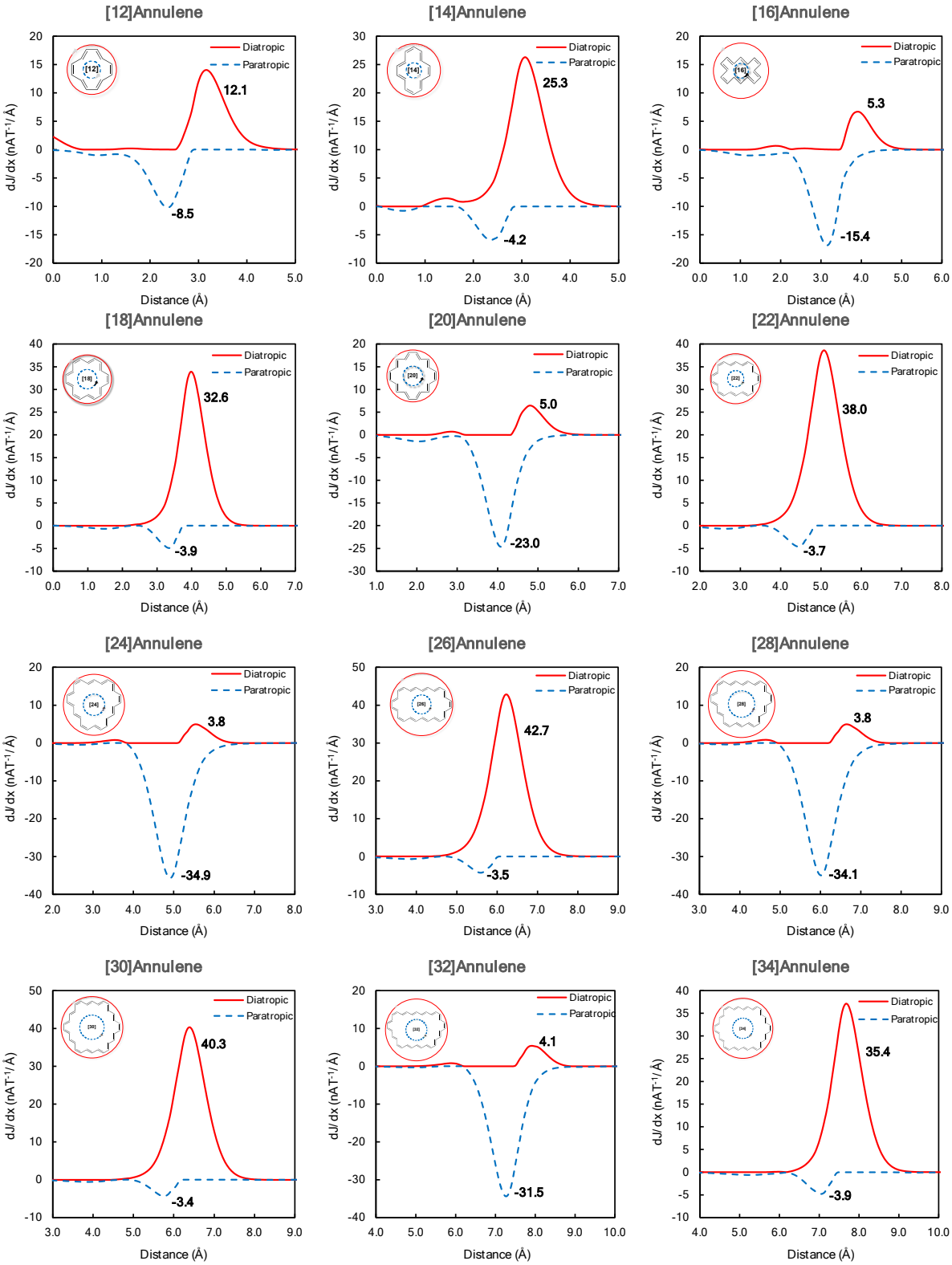
[12]Annulene
Diatropic
Paratropic
12.1
-8.5
dJ/ dx (nAT⁻¹/ Å)
Distance (Å)
[14]Annulene
25.3
-4.2
[16]Annulene
5.3
-15.4
[18]Annulene
32.6
-3.9
[20]Annulene
5.0
-23.0
[22]Annulene
38.0
-3.7
[24]Annulene
3.8
-34.9
[26]Annulene
42.7
-3.5
[28]Annulene
3.8
-34.1
[30]Annulene
40.3
-3.4
[32]Annulene
4.1
-31.5
[34]Annulene
35.4
-3.9

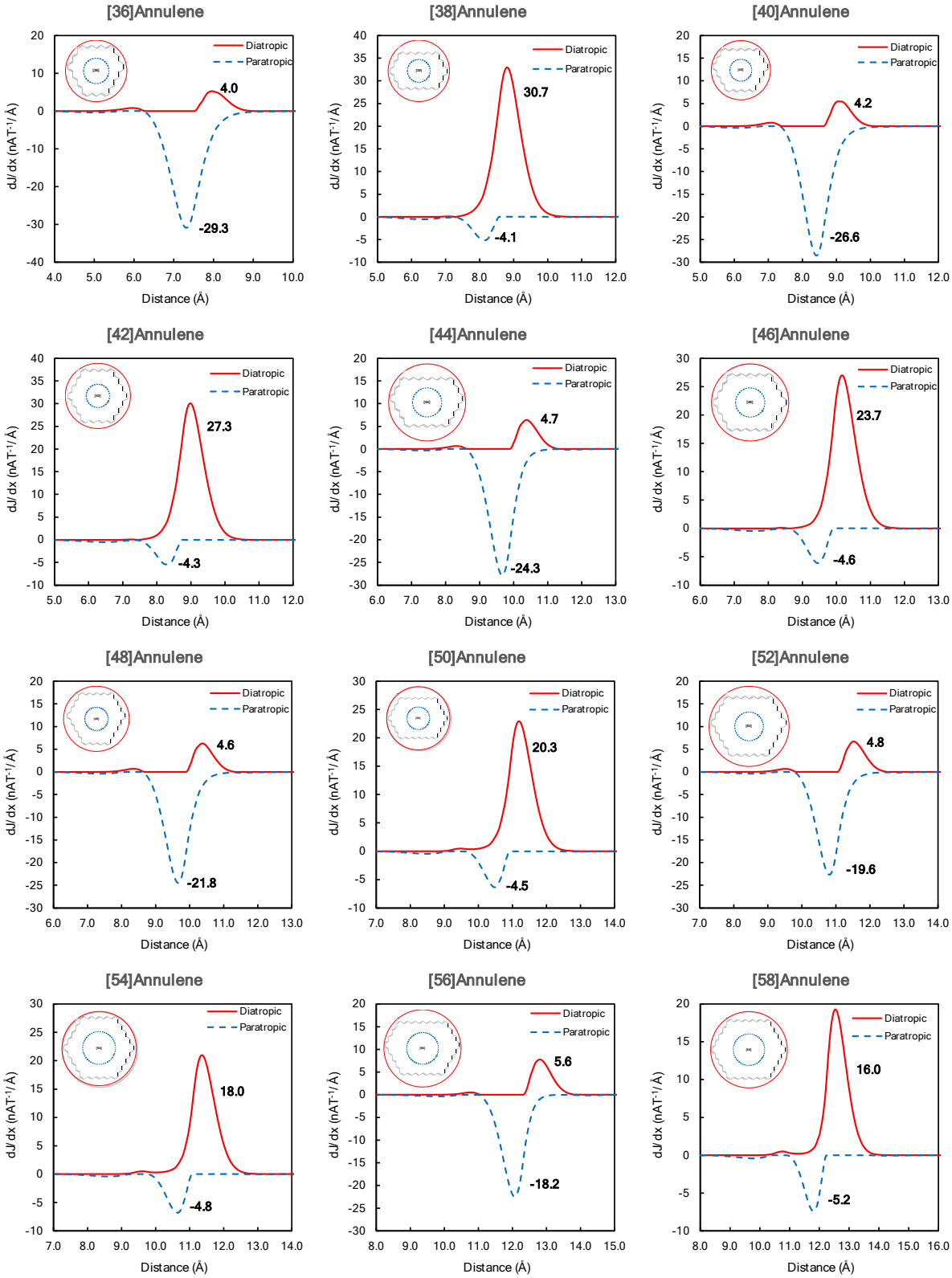
[36]Annulene
Diatropic
Paratropic
4.0
-29.3
dJ/dx (nAT⁻¹/Å)
Distance (Å)
[38]Annulene
30.7
-4.1
[40]Annulene
4.2
-26.6
[42]Annulene
27.3
-4.3
[44]Annulene
4.7
-24.3
[46]Annulene
23.7
-4.6
[48]Annulene
4.6
-21.8
[50]Annulene
20.3
-4.5
[52]Annulene
4.8
-19.6
[54]Annulene
18.0
-4.8
[56]Annulene
5.6
-18.2
[58]Annulene
16.0
-5.2

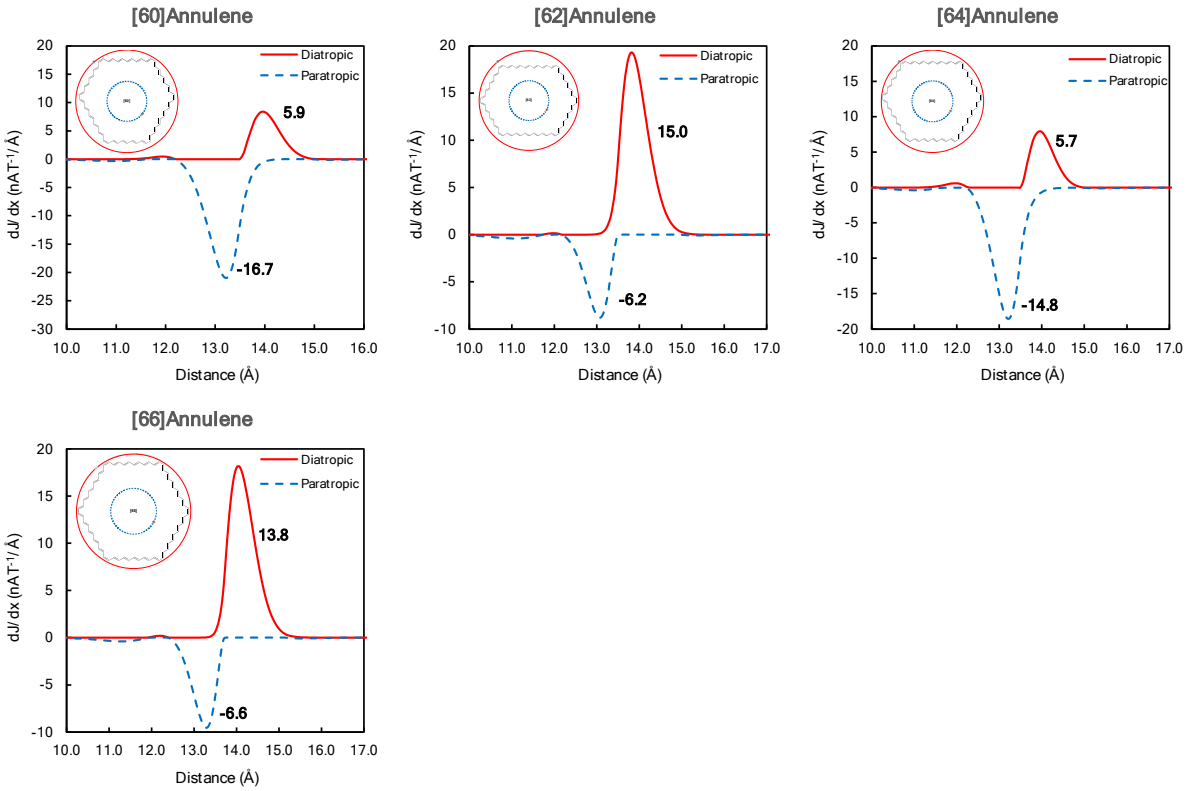

Figure S34: Profiles of current strength for the neutral singlet [*N*]annulenes through a plane situated halfway between two consecutive atoms and extending from the center of the molecule to a region where the current density vanishes planes. The numerical integration of the ring current strength was conducted using the GIMIC programme at the B3LYP/6-31G(d) level of theory. The positive and negative values represent the sum of the diatropic and paratropic contributions, which is determined through the subdivided slices of the integration plane.

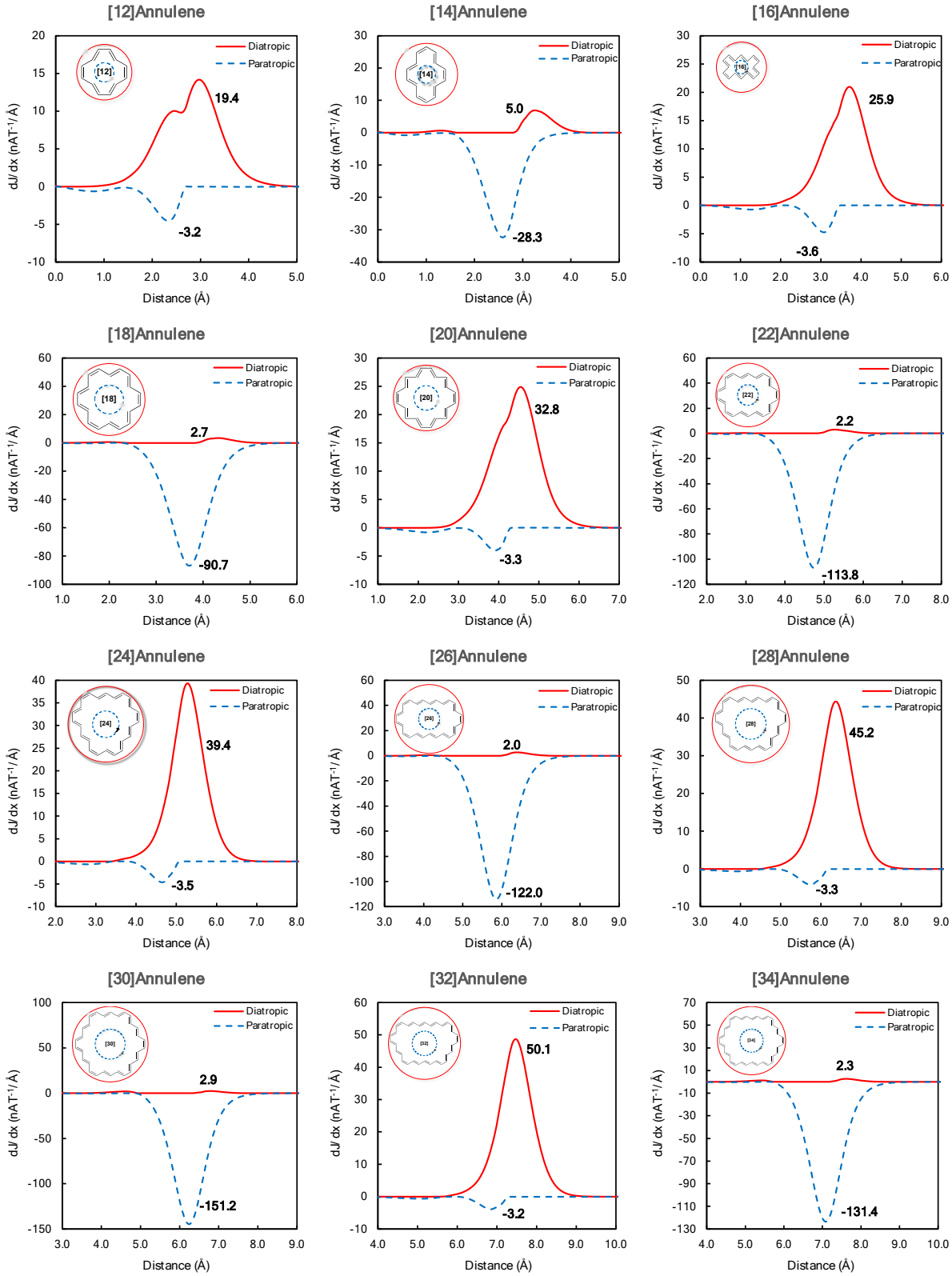
[12]Annulene
Diatropic
Paratropic
19.4
-3.2
dJ/ dx (nAT-1/ Å)
Distance (Å)
[14]Annulene
5.0
-28.3
[16]Annulene
25.9
-3.6
[18]Annulene
2.7
-90.7
[20]Annulene
32.8
-3.3
[22]Annulene
2.2
-113.8
[24]Annulene
39.4
-3.5
[26]Annulene
2.0
-122.0
[28]Annulene
45.2
-3.3
[30]Annulene
2.9
-151.2
[32]Annulene
50.1
-3.2
[34]Annulene
2.3
-131.4

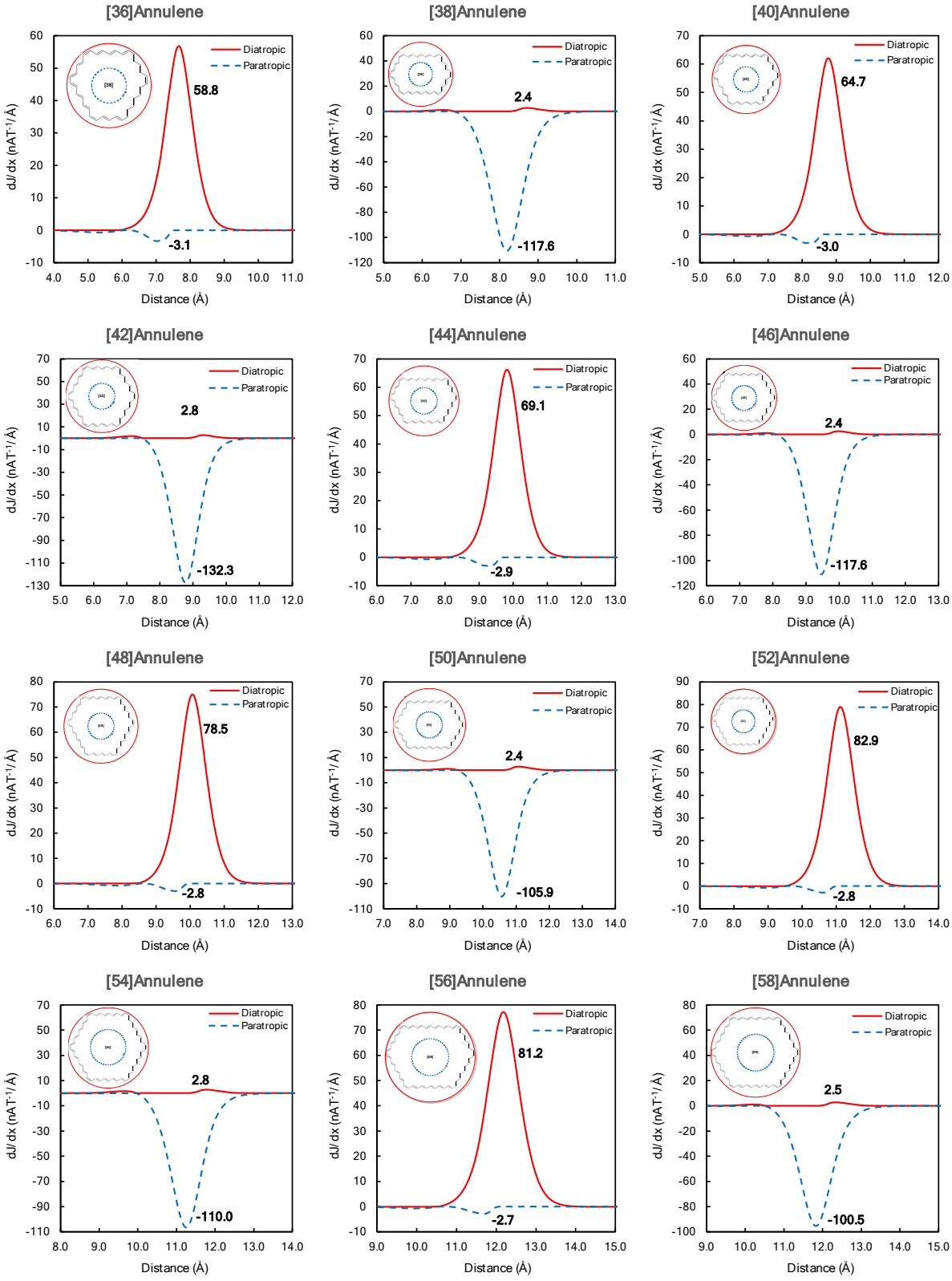
[36]Annulene
Diatropic
Paratropic
58.8
-3.1
dJ/ dx (nAT-1/ Å)
Distance (Å)
[38]Annulene
2.4
-117.6
[40]Annulene
64.7
-3.0
[42]Annulene
2.8
-132.3
dJ/dx (nAT-1/ Å)
[44]Annulene
69.1
-2.9
[46]Annulene
2.4
-117.6
[48]Annulene
78.5
-2.8
[50]Annulene
2.4
-105.9
[52]Annulene
82.9
-2.8
[54]Annulene
2.8
-110.0
[56]Annulene
81.2
-2.7
[58]Annulene
2.5
-100.5

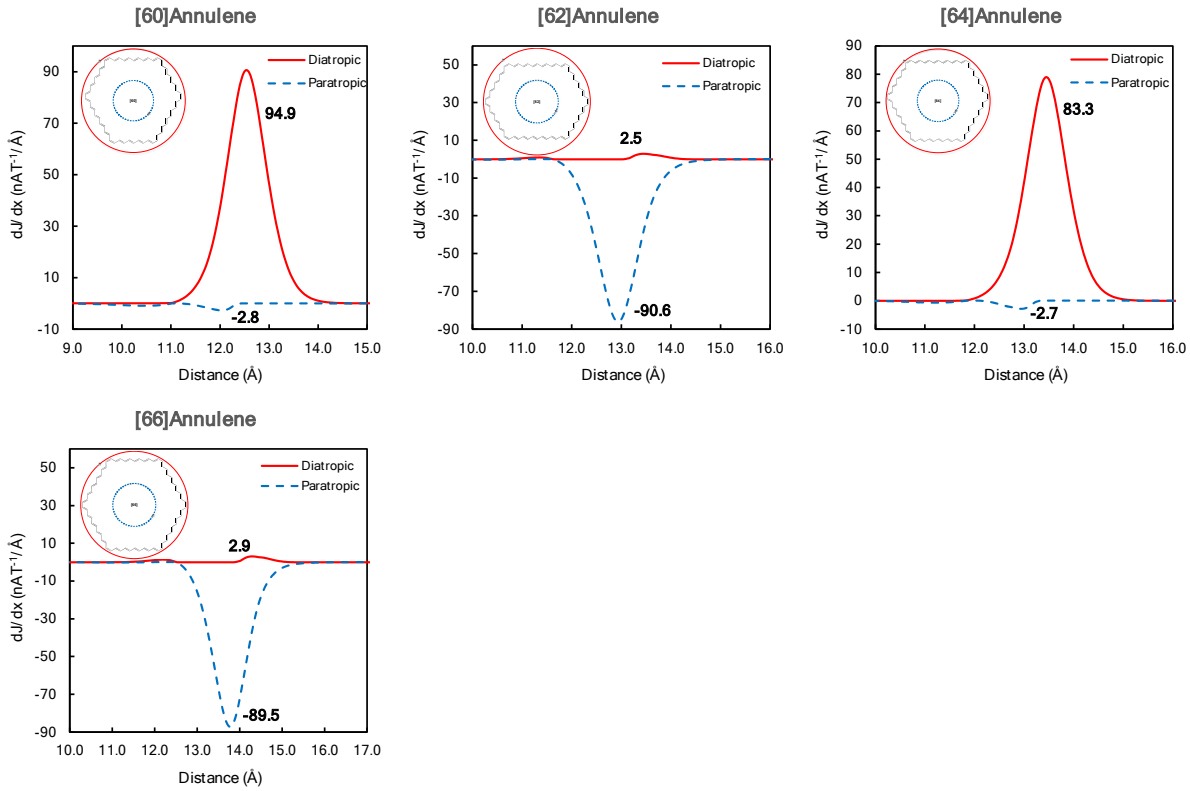

Figure S35: Profiles of current strength for the singlet dicationic [*N*]annulenes through a plane situated halfway between two consecutive atoms and extending from the center of the molecule to a region where the current density vanishes planes. The numerical integration of the ring current strength was conducted using the GIMIC programme at the B3LYP/6-31G(d) level of theory. The positive and negative values represent the sum of the diatropic and paratropic contributions, which is determined through the subdivided slices of the integration plane.

Correlation Analysis

A

B3LYP	Structural		Electronic				Magnetic		Reactivity	Energetic
R^2	HOMA	BLA	FLU	BOA	AV1245	AV_{min}	GIMIC	$NICS(1)_{zz}$	Δη	ASE
HOMA	1.00									
BLA	0.77	1.00								
FLU	0.94	0.90	1.00							
BOA	0.73	0.99	0.87	1.00						
AV1245	0.27	0.05	0.13	0.04	1.00					
AV_{min}	0.29	0.11	0.17	0.09	0.86	1.00				
GIMIC	0.06	0.15	0.07	0.15	0.02	0.15	1.00			
$NICS(1)_{zz}$	0.10	0.19	0.12	0.20	0.04	0.19	0.89	1.00		
Δη	0.36	0.48	0.42	0.51	0.05	0.20	0.36	0.47	1.00	
ASE	0.27	0.47	0.35	0.50	0.03	0.16	0.24	0.34	0.76	1.00

B

CAM-B3LYP	Structural		Electronic				Magnetic		Reactivity	Energetic
R^2	HOMA	BLA	FLU	BOA	AV1245	AV_{min}	GIMIC	$NICS(1)_{zz}$	Δη	ASE
HOMA	1.00									
BLA	0.91	1.00								
FLU	0.98	0.96	1.00							
BOA	0.87	1.00	0.94	1.00						
AV1245	0.22	0.08	0.14	0.05	1.00					
AV_{min}	0.04	0.00	0.01	0.00	0.49	1.00				
GIMIC	0.09	0.09	0.09	0.09	0.00	0.15	1.00			
$NICS(1)_{zz}$	0.11	0.12	0.11	0.13	0.00	0.13	0.89	1.00		
Δη	0.22	0.23	0.22	0.23	0.05	0.11	0.31	0.42	1.00	
ASE	0.25	0.34	0.29	0.35	0.02	0.05	0.10	0.17	0.45	1.00

Figure S36: Correlation coefficients (R^2) between the aromaticity indices rooted in distinct criteria employed in the analysis of the [*N*]annulenes (n = 112) computed with (A) B3LYP and (B) CAM-B3LYP. R^2 values exceeding 0.60 are indicated in green, results below 0.40 are identified in red, and outcomes between both are marked by orange colouring.

Neutral

B3LYP

	Structural		Electronic					Magnetic		Reactivity	Energetic
R^2	HOMA	BLA	FLU	BOA	AV1245	AV_{min}		GIMIC	NICS(1)$_{zz}$	Δη	ASE
HOMA	1.00										
BLA	0.78	1.00									
FLU	0.95	0.91	1.00								
BOA	0.73	0.99	0.88	1.00							
AV1245	0.50	0.25	0.37	0.24	1.00						
AV_{min}	0.42	0.24	0.33	0.24	0.85	1.00					
GIMIC	0.21	0.34	0.27	0.35	0.14	0.25	1.00				
NICS(1)$_{zz}$	0.29	0.46	0.37	0.48	0.19	0.32	0.92	1.00			
Δη	0.51	0.46	0.52	0.46	0.49	0.65	0.63	0.70	1.00		
ASE	0.21	0.32	0.28	0.34	0.29	0.47	0.42	0.56	0.56	1.00	

Charged

	Structural		Electronic					Magnetic		Reactivity	Energetic
R^2	HOMA	BLA	FLU	BOA	AV1245	AV_{min}		GIMIC	NICS(1)$_{zz}$	Δη	ASE
HOMA	1.00										
BLA	0.60	1.00									
FLU	0.85	0.85	1.00								
BOA	0.52	0.98	0.81	1.00							
AV1245	0.40	0.03	0.11	0.01	1.00						
AV_{min}	0.63	0.24	0.35	0.16	0.87	1.00					
GIMIC	0.28	0.69	0.46	0.67	0.01	0.16	1.00				
NICS(1)$_{zz}$	0.38	0.80	0.62	0.79	0.01	0.18	0.89	1.00			
Δη	0.25	0.68	0.51	0.74	0.00	0.07	0.49	0.61	1.00		
ASE	0.30	0.63	0.53	0.69	0.00	0.13	0.39	0.52	0.88	1.00	

CAM-B3LYP

	Structural		Electronic					Magnetic		Reactivity	Energetic
R^2	HOMA	BLA	FLU	BOA	AV1245	AV_{min}		GIMIC	NICS(1)$_{zz}$	Δη	ASE
HOMA	1.00										
BLA	0.91	1.00									
FLU	0.97	0.98	1.00								
BOA	0.88	1.00	0.96	1.00							
AV1245	0.70	0.51	0.58	0.48	1.00						
AV_{min}	0.00	0.04	0.01	0.06	0.16	1.00					
GIMIC	0.00	0.00	0.00	0.00	0.00	0.04	1.00				
NICS(1)$_{zz}$	0.02	0.01	0.02	0.01	0.04	0.13	0.88	1.00			
Δη	0.12	0.05	0.09	0.04	0.19	0.19	0.45	0.62	1.00		
ASE	0.01	0.02	0.01	0.02	0.00	0.13	0.39	0.38	0.17	1.00	

	Structural		Electronic					Magnetic		Reactivity	Energetic
R^2	HOMA	BLA	FLU	BOA	AV1245	AV_{min}		GIMIC	NICS(1)$_{zz}$	Δη	ASE
HOMA	1.00										
BLA	0.68	1.00									
FLU	0.89	0.87	1.00								
BOA	0.61	0.99	0.84	1.00							
AV1245	0.00	0.14	0.08	0.20	1.00						
AV_{min}	0.09	0.02	0.00	0.04	0.73	1.00					
GIMIC	0.39	0.21	0.43	0.19	0.00	0.18	1.00				
NICS(1)$_{zz}$	0.51	0.38	0.57	0.36	0.01	0.14	0.89	1.00			
Δη	0.13	0.23	0.19	0.23	0.00	0.04	0.34	0.46	1.00		
ASE	0.07	0.21	0.12	0.23	0.00	0.01	0.06	0.18	0.50	1.00	

Figure S37: Correlation coefficients (R^2) between the aromaticity indices rooted in distinct criteria employed in the analysis of neutral and charged [*N*]annulenes (n = 112) computed with (A) B3LYP and (B) CAM-B3LYP. R^2 values exceeding 0.60 are indicated in green, results below 0.40 are identified in red, and outcomes between both are marked by orange colouring.

Hückel

B3LYP

	Structural		Electronic					Magnetic		Reactivity	Energetic
R^2	HOMA	BLA	FLU	BOA	AV1245	AV_{min}		GIMIC	NICS(1)$_{zz}$	Δη	ASE
HOMA	1.00										
BLA	0.81	1.00									
FLU	0.97	0.90	1.00								
BOA	0.77	0.99	0.87	1.00							
AV1245	0.46	0.25	0.36	0.22	1.00						
AV_{min}	0.45	0.29	0.38	0.27	0.89	1.00					
GIMIC	0.03	0.09	0.04	0.10	0.04	0.20	1.00				
NICS(1)$_{zz}$	0.06	0.12	0.07	0.13	0.07	0.28	0.88	1.00			
Δη	0.49	0.65	0.58	0.68	0.07	0.21	0.34	0.45	1.00		
ASE	0.37	0.65	0.50	0.69	0.03	0.13	0.24	0.35	0.79	1.00	

Baird

	Structural		Electronic					Magnetic		Reactivity	Energetic
R^2	HOMA	BLA	FLU	BOA	AV1245	AV_{min}		GIMIC	NICS(1)$_{zz}$	Δη	ASE
HOMA	1.00										
BLA	0.58	1.00									
FLU	0.83	0.87	1.00								
BOA	0.54	0.99	0.84	1.00							
AV1245	0.28	0.00	0.04	0.01	1.00						
AV_{min}	0.47	0.07	0.19	0.05	0.85	1.00					
GIMIC	0.15	0.32	0.23	0.30	0.03	0.19	1.00				
NICS(1)$_{zz}$	0.21	0.44	0.34	0.42	0.03	0.19	0.90	1.00			
Δη	0.42	0.59	0.57	0.58	0.01	0.12	0.54	0.69	1.00		
ASE	0.38	0.64	0.54	0.64	0.01	0.12	0.39	0.52	0.70	1.00	

CAM-B3LYP

	Structural		Electronic					Magnetic		Reactivity	Energetic
R^2	HOMA	BLA	FLU	BOA	AV1245	AV_{min}		GIMIC	NICS(1)$_{zz}$	Δη	ASE
HOMA	1.00										
BLA	0.91	1.00									
FLU	0.99	0.96	1.00								
BOA	0.88	1.00	0.94	1.00							
AV1245	0.51	0.30	0.44	0.25	1.00						
AV_{min}	0.17	0.06	0.12	0.04	0.56	1.00					
GIMIC	0.05	0.10	0.06	0.11	0.00	0.14	1.00				
NICS(1)$_{zz}$	0.08	0.13	0.09	0.14	0.00	0.15	0.94	1.00			
Δη	0.55	0.58	0.57	0.59	0.14	0.13	0.44	0.46	1.00		
ASE	0.67	0.82	0.75	0.84	0.17	0.02	0.08	0.20	0.62	1.00	

	Structural		Electronic					Magnetic		Reactivity	Energetic
R^2	HOMA	BLA	FLU	BOA	AV1245	AV_{min}		GIMIC	NICS(1)$_{zz}$	Δη	ASE
HOMA	1.00										
BLA	0.73	1.00									
FLU	0.91	0.87	1.00								
BOA	0.64	0.99	0.83	1.00							
AV1245	0.13	0.00	0.01	0.02	1.00						
AV_{min}	0.38	0.06	0.23	0.02	0.50	1.00					
GIMIC	0.16	0.07	0.22	0.06	0.00	0.31	1.00				
NICS(1)$_{zz}$	0.25	0.19	0.34	0.18	0.00	0.23	0.88	1.00			
Δη	0.14	0.17	0.22	0.18	0.00	0.05	0.29	0.44	1.00		
ASE	0.18	0.46	0.39	0.52	0.12	0.03	0.18	0.25	0.17	1.00	

Figure S38: Correlation coefficients (R^2) between the aromaticity indices rooted in distinct criteria employed in the analysis of Hückel and Baird [*N*]annulenes (n = 112) computed with (A) B3LYP and (B) CAM-B3LYP. R^2 values exceeding 0.60 are indicated in green, results below 0.40 are identified in red, and outcomes between both are marked by orange colouring.

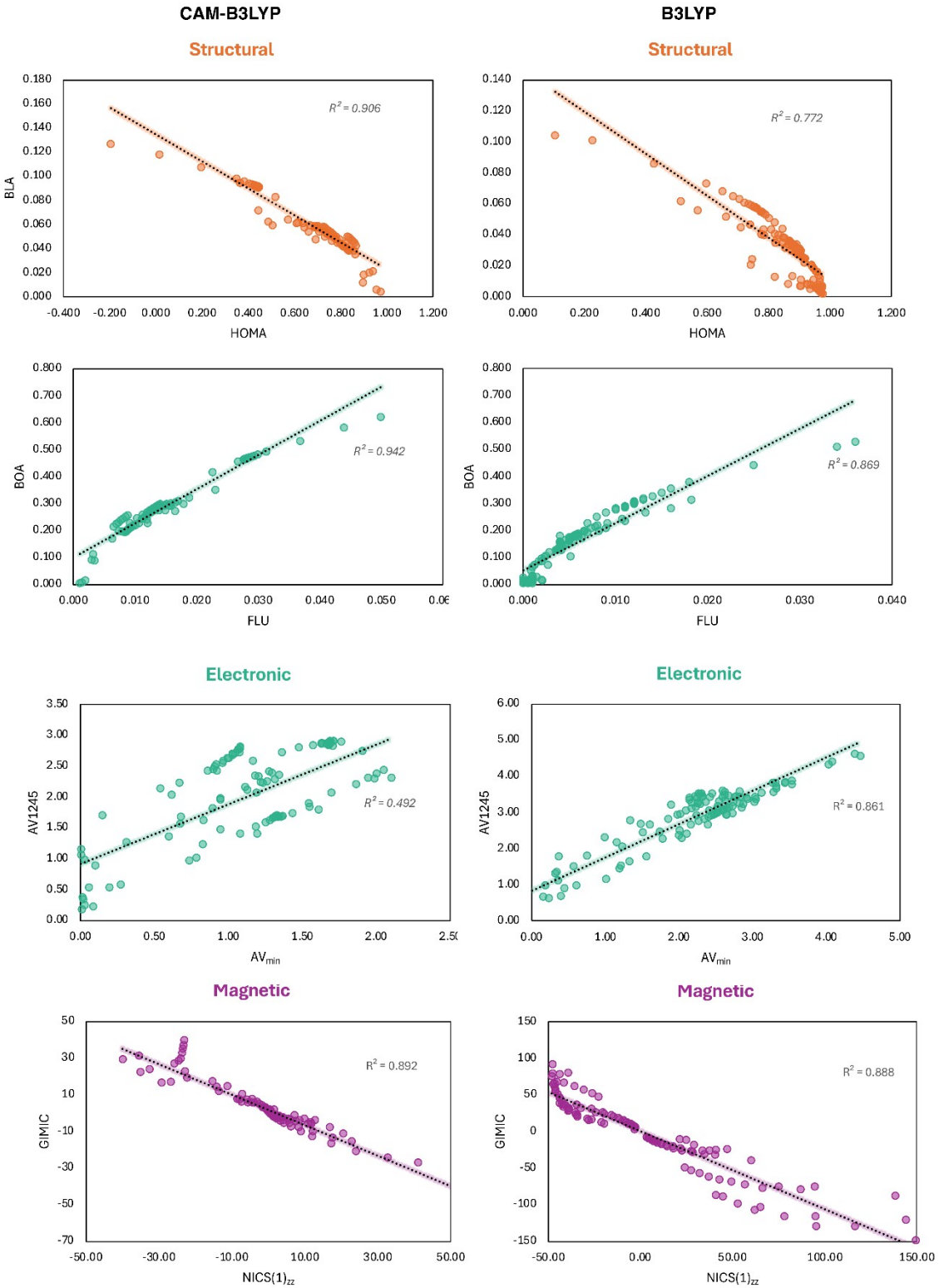

Figure S39: The correlation plots between selected aromaticity indices rooted in the same criteria of the neutral and charged [N]annulenes in the singlet and triplet states (*N* = 12-66) computed with B3LYP and CAM-B3LYP (112 systems).

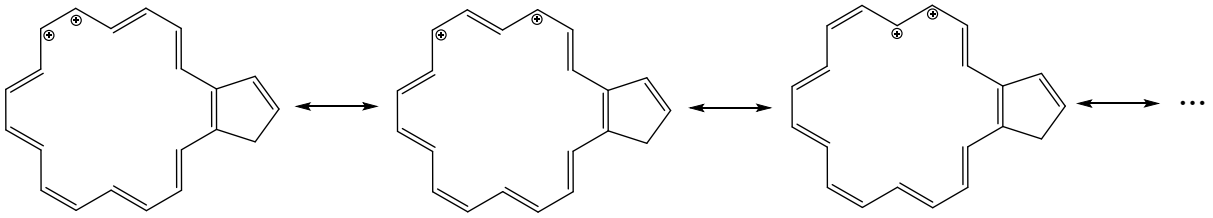

Figure S40: Several resonance structures for the charged species of [18] annulene.

References

1 Kruszewski, J., Krygowski, T. Definition of aromaticity basing on the harmonic oscillator model. *Tetrahedron Lett.* **1972**, *13,* 3839–3842.
2 Matito, E., Duran, M., Solà, M. The aromatic fluctuation index (FLU): A new aromaticity index based on electron delocalization. *J. Chem. Phys.* **2005**, *122*, 014109.
3 Szatylowicz, H., Wieczorkiewicz, P.A., Krygowski, T.M. Molecular geometry as a source of electronic structure of π-electron systems and their physicochemical properties. Aromaticity: Elsevier; **2021**. p. 71-99.
4 Casademont-Reig, I., Woller, T., Contreras-García, J., Alonso, M., Torrent-Sucarrat, M., Matito, E. New electron delocalization tools to describe the aromaticity in porphyrinoids. *Phys. Chem. Chem. Phys.* **2018**, *20,* 2787–2796.
5 Casademont-Reig, I., Ramos-Cordoba, E., Torrent-Sucarrat, M., Matito, E. How do the Hückel and Baird rules fade away in annulenes? *Molecules* **2020***, 25*, 711.
6 Casademont-Reig, I. Computational study of aromaticity in porphyrinoid systems and photosensitizers from chemical bonding descriptors. PhD thesis (Universidad del País Vasco-Euskal Herriko Unibertsitatea, **2021**).
7 Matito, E. ESI-3D: electron sharing indices program for 3d molecular space partitioning; Institute of Computational Chemistry and Catalysis (IQCC). http://iqc.udg.es/eduard/ESI (2006).
8 Bader, R., Stephens, M. Fluctuation and correlation of electrons in molecular systems. *Chem. Phys. Lett.* **1974**, *26,* 445–449.
9 Poater, J., Fradera, X., Duran, M., Solà, M. The delocalization index as an electronic aromaticity criterion: application to a series of planar polycyclic aromatic hydrocarbons. *Chem. Eur. J.* **2003**, *9,* 400–406.
10 Feixas, F., Matito, E., Poater, J., Solà, M. Quantifying aromaticity with electron delocalisation measures. *Chem. Soc. Rev.* **2015,** *44,* 6434–6451.
11 Popelier PLA, Aicken F, O'Brien S. Atoms in molecules: Prentice Hall Manchester; **2000**.
12 Giambiagi, M., de Giambiagi, M. S., dos Santos Silva, C. D., de Figueiredo, A. P. Multicenter bond indices as a measure of aromaticity. *Phys. Chem. Chem. Phys.* **2000**, *2,* 3381–3392.
13 Matito, E. An electronic aromaticity index for large rings. *Phys. Chem. Chem. Phys.* **2016,** *18,* 11839–11846.
14 Bultinck, P., Ponec, R., Van Damme, S. Multicenter bond indices as a new measure of aromaticity in polycyclic aromatic hydrocarbons. *J. Phys. Org. Chem.* **2005**, *18,* 706–718.
15 Szczepanik, D. W., Andrzejak, M., Dyduch, K., Zak, E., Makowski, M., Mazur, G., Mrozek, J. A uniform approach to the description of multicenter bonding. *Phys. Chem. Chem. Phys.* **2014**, *16,* 20514–20523.
16 Szczepanik, D.W., Solà, M. The electron density of delocalized bonds (EDDBs) as a measure of local and global aromaticity. Aromaticity: Elsevier; **2021**. pp. 259–84.
17 Gershoni-Poranne, R., Stanger, A. NICS–nucleus independent chemical shift. Aromaticity: Elsevier; **2021**. pp.99–154.
18 Fliegl, H., Taubert, S., Lehtonen, O., Sundholm, D. The gauge including magnetically induced current method. *Phys. Chem. Chem. Phys.* **2011**, *13,* 20500–20518.
19 Schleyer, P. v. R., Maerker, C., Dransfeld, A., Jiao, H., van Eikema Hommes, N. J. Nucleus-independent chemical shifts: a simple and efficient aromaticity probe. *J. Am. Chem. Soc.* **1996**, *118,* 6317–6318.
20 Stanger, A. NICS–past and present. *Eur. J. Org. Chem.* **2020**, 3120-3127.
21 Gershoni-Poranne, R., Stanger, A. Magnetic criteria of aromaticity. *Chem. Soc. Rev.* **2015**, *44,* 6597–6615.
22 Ditchfield, R. Self-consistent perturbation theory of diamagnetism: I. A gauge-invariant LCAO method for NMR chemical shifts. *Mol. Phys.* **1974**, *27,* 789–807.
23 López, C.S., Faza, O.N. Overview of the computational methods to assess aromaticity. Aromaticity: Elsevier; **2021**. pp. 41-71.
24 Dimitrova, M., Sundholm, D. Current density, current-density pathways, and molecular aromaticity. Aromaticity: Elsevier; **2021**. pp. 155-194.
25 De Proft, F., Geerlings, P. Relative hardness as a measure of aromaticity. *Phys. Chem. Chem. Phys.* **2004**, *6,* 242–248.
26 Jirásek, M., Rickhaus, M., Tejerina, L., Anderson, H. L. Experimental and theoretical evidence for aromatic stabilization energy in large macrocycles. *J. Am. Chem. Soc.* **2021**, *143,* 2403–2412.